8-2013

Developing 16- and 18-Atom Ringed Macrocyclic Tetracarbene Complexes

Heather Marie Bass
hbass1@utk.edu

To the Graduate Council:

I am submitting herewith a dissertation written by Heather Marie Bass entitled "Developing 16- and 18-Atom Ringed Macrocyclic Tetracarbene Complexes." I have examined the final electronic copy of this dissertation for form and content and recommend that it be accepted in partial fulfillment of the requirements for the degree of Doctor of Philosophy, with a major in Chemistry.

David M. Jenkins, Major Professor

We have read this dissertation and recommend its acceptance:

Ziling B. Xue, Charles S. Feigerle, Claudia J. Rawn

Accepted for the Council:

Carolyn R. Hodges

Vice Provost and Dean of the Graduate School

(Original signatures are on file with official student records.)

Developing 16- and 18-Atom Ringed Macrocyclic Tetracarbene Complexes

A Dissertation Presented for the
Doctor of Philosophy Degree
The University of Tennessee, Knoxville

Heather Marie Bass
August 2013

Dedication

I dedicate my dissertation research to my mom, my dad, and my sister. Throughout my life my family has always stood behind me and pushed me on even when I have wanted to give up. They always provided more for me than I could ever hope to receive. They taught me right from wrong, pride from arrogance, and so much more. Without them, I would not be who I am today or I would not have as much success as I have received.

I would also like to dedicate my dissertation to God. Although I have no scientific proof of His existence, my existence and my success are all that I require. He is a feeling within me that keeps me going. He has been here from my beginning and will be here until my end. For that I am ever grateful.

Acknowledgements

First and foremost, I would like to acknowledge Dr. David M. Jenkins. When I first came to graduate school, I was inept in synthetic lab techniques. He took time out of his schedule to mentor me, allowing me to develop into the chemist I am today. He also allowed me to knock on his door relentlessly whenever I had a question or just to talk. I thank him for all he has done.

I would also like to acknowledge all of the people in my lab, including past and present members: S. Alan Cramer, Chris R. Murdock, Brianna C. Hughes, Preeti Chandrachud, Zheng Lu, Chi-Linh Do-Thanh, Elizabeth Jacobs, Ben Sundell, Julia L. Price, A. Scott McCullough, and Forrest Sturgill. Each one has contributed vastly to my knowledge, experiences, and memories at UT. I will always remember them and look back fondly on this period of my life due to their presence.

Abstract

Stabilizing metal-ligand multiple bonds is important for the understanding of biological intermediates, as well as, for their use in group transfer reactions. Two considerations to make when developing a ligand system to support metal-ligand multiple bonds are the strength of the ligand and the symmetry of the ligand. Herein, our group has proposed a class of four-coordinate, strong σ-donor ligands by synthesizing macrocyclic tetraimidazoliums that form tetracarbenes upon deprotonation. By examining group theory, these systems should allow for the formation of complexes with metal-ligand multiple bonds in a bent square pyramidal geometry that exhibit high oxidation states and novel spin states.

The first step in accomplishing this goal was the synthesis of a neutral, 18-atom ringed macrocyclic tetraimidazolium system. By employing a weak base deprotonation strategy, we were able to form a platinum tetracarbene complex. Unlike previous macrocyclic tetracarbene systems, our complex was rigid in solution, allowing for accessible apical positions. A major drawback to this first neutral, 18-atom ringed macrocyclic tetracarbene system was its inherent insolubility in nonpolar solvents. In order to compensate for this shortcoming, we added two borate moieties to second generation macrocyclic tetraimidazoliums, leading to dianionic ligands upon deprotonation. These three additional systems included two 16-atom ringed tetraimidazoliums and one 18-atom ringed tetraimidazolium. While results of forming metal complexes with the 16-atom ringed variants are incomplete, we were able to form metal complexes with the 18-atom ringed, borate-based tetracarbene ligand. Not only did the complexes formed by the 18-atom ringed, borate-based tetracarbene ligand have enhanced solubility in solvents such as toluene, but preliminary results suggest they may stabilize metal-ligand multiple bonds.

Table of Contents

List of Tables

List of Figures

List of Schemes

Introduction

Stabilizing metal-ligand multiple bonds is important since many biological and chemical processes go through reactive intermediates that contain metal-ligand multiple bonds,[1] such as the activation of dioxygen to produce methanol in monooxygenase reactions.[1a] By isolating these reactive intermediates, we are able to gain a better understanding of how these reactions proceed and ultimately manipulate them for enhancing chemical processes, such as group transfer reactions.[2] Two important aspects of stabilizing metal-ligand multiple bonds are the ligand donor strength and symmetry of the auxiliary ligand bound to the metal center.[1c] Figure I.1 highlights a few examples of metal-ligand multiple bonds isolated by ligands of various donor strengths and various symmetries. By examining the spin states and location of the electrons in the energy orbital diagrams from Figure I.1, it can be concluded that Smith's Fe(IV) nitride[3] is more stable than Que's Fe(IV) oxo[4] and Hillhouse's Ni(II) imide[5] due to the fact that it has four paired electrons in non-bonding orbitals and a large HOMO-LUMO gap due to the ligand donor strength of Smith's auxiliary ligand. The inherent change in stability and reactivity is due to the fact that as ligand donor strength increases, the energy gap between the non-bonding and anti-bonding orbitals increases concurrently. Although Hillhouse uses a strong ligand, the d-count of his complex is such that electrons must occupy the anti-bonding orbitals.

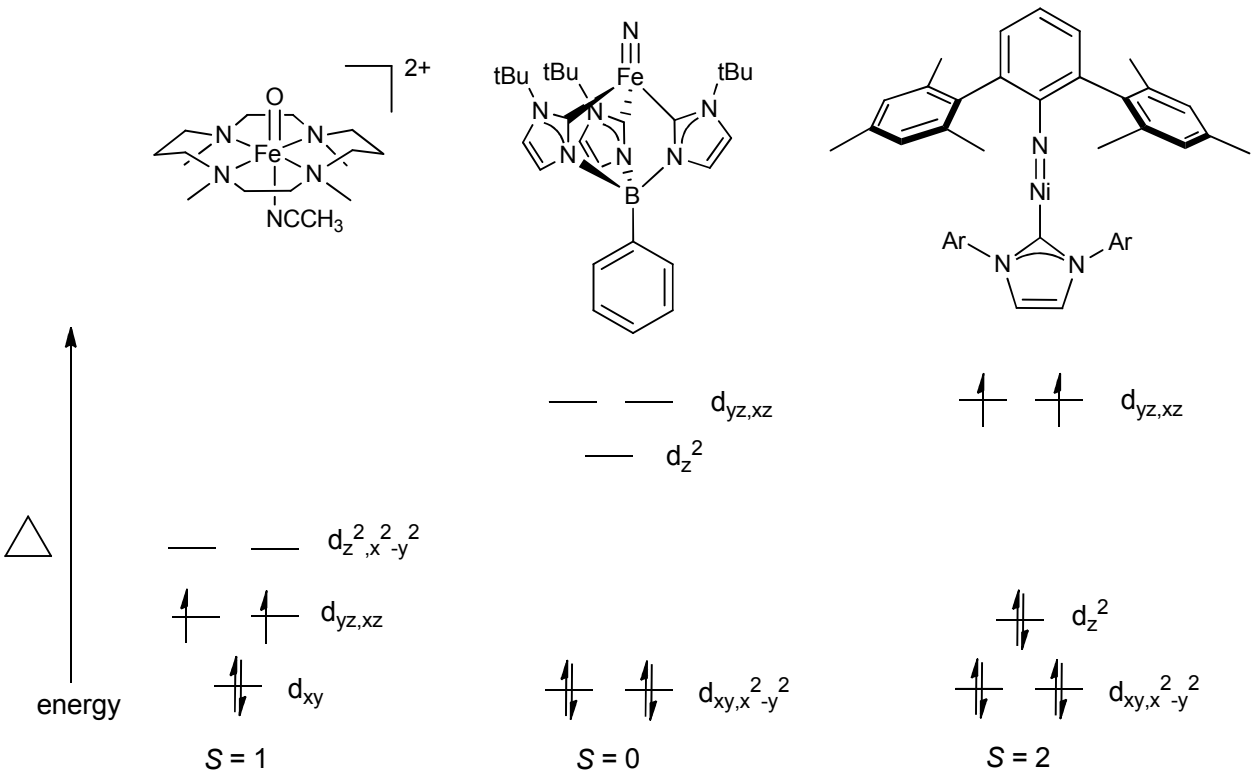

Figure I.1. Energy splitting diagrams of previously synthesized metal-ligand multiple bonds in various geometries and with various strength ligands.

A more comparative example of the difference of a weak donor and a strong donor stabilizing metal-ligand multiple bonds entails looking at systems in the same geometry with an identical d-count. Figure I.2 shows the difference between a weak donor ligand and a strong donor ligand both in a bent square pyramidal geometry with a d^4 electron count.[6] In the case of the weak donor ligand with π-bonding, the complex is a more reactive, high-spin complex where $S = 2$; however, for the strong donor ligand with π-bonding, the complex is a less reactive, low-spin complex with $S = 0$. Since both pairs of electrons for the strong donor ligand are in non-bonding orbitals and the anti-bonding orbitals are unoccupied, this complex is more stable. If an

electron is promoted into the anti-boding orbital of the strong donor ligand, however, it will be more destabilized and hence more reactive since it is of a higher energy than its weak donor counterpart. Due to this apparent stability using stronger donor ligands and enhanced reactivity upon electron promotion, our group is focused on using strong σ-donating systems in order to stabilize high-valent complexes with metal-ligand multiple bonds.

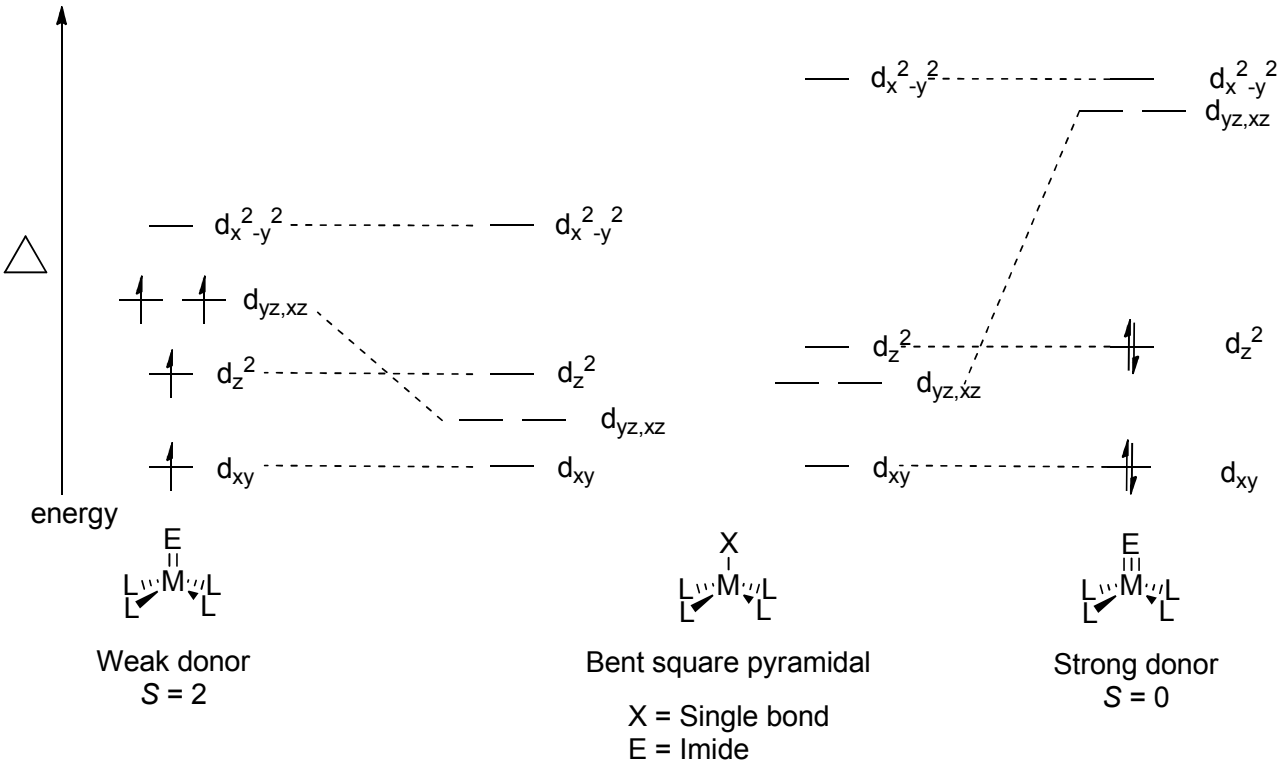

Figure I.2. Comparison of an energy splitting diagram of bent square pyramidal complexes with a strong vs. weak-field donor.

As previously stated, donor strength and symmetry of the auxiliary ligand determine the stability of metal-ligand multiple bonds. Along with synthesizing a strong σ-donating ligand, we were interested in incorporating it into a tetradentate macrocyclic system. Macrocyclic ligands have previously been shown to play a major role in catalysis and small molecule activation both in biological and synthetic systems.[7] A major reason for the success of macrocyclic ligands, especially tetradentate ligands, is that four equatorial sites in a plane about a transition metal are blocked, allowing for reactions to be mediated at the apical positions. We believed that by synthesizing a strong σ-donating, tetradentate ligand that we could take advantage of these freely accessible apical sites and synthesize complexes with novel metal-ligand multiple bonds.

Typically, phosphines have been used as strong σ-donating ligands. Since phosphines are typically sensitive to O_2,[8] there has been a push towards N-heterocyclic carbene systems due to their inherent stability in the presence of O_2.[9] For our ligand system, we decided to synthesis macrocycle tetracarbene complexes. With respect to current research on macrocyclic carbene complexes, only two research groups have thus far been able to synthesize such species (Figure I.3). The first reported macrocyclic carbene was a 16-atom ringed platinum tetracarbene complex by Hahn's group.[10] Later, Murphy's group synthesized several 24-atom ringed metal tetracarbenes. In regards to size, Hahn's complex is far more suitable for monomeric complexation, since it has a methyl-bridge between each carbene, which induces rigidity and gives 6-member rings around the metal center as seen in Figure I.4.[10] Hahn synthesized his complex using a templating reaction in which four monomeric carbenes were attached to the platinum before linking them together, thus making the tetracarbene.[10] This kind of synthesis generally pertains only to transition metals that C-H bond activate, hence this synthetic protocol is limited. As far as synthetic methodology, Murphy's approach is more applicable to a wide

range of transition metals, because he was able to prepare a free tetraimidazolium ligand before putting it on a metal center.[11] Unfortunately, Murphy's tetraimidazolium is a 24-atom ringed macrocycle, which produces saddle-shaped complexes with blocked apical positions as seen in Figure I.6.[11] Furthermore, Murphy's 24-atom ringed macrocycle formed palladium, nickel, and cobalt monomeric species, yet dimeric species were formed on silver and copper.[11] We realized a solution to the pitfalls of both of these tetracarbene metal complexation methods would be synthesizing a free tetraimidazolium ligand with a 16- or 18- atom ring.

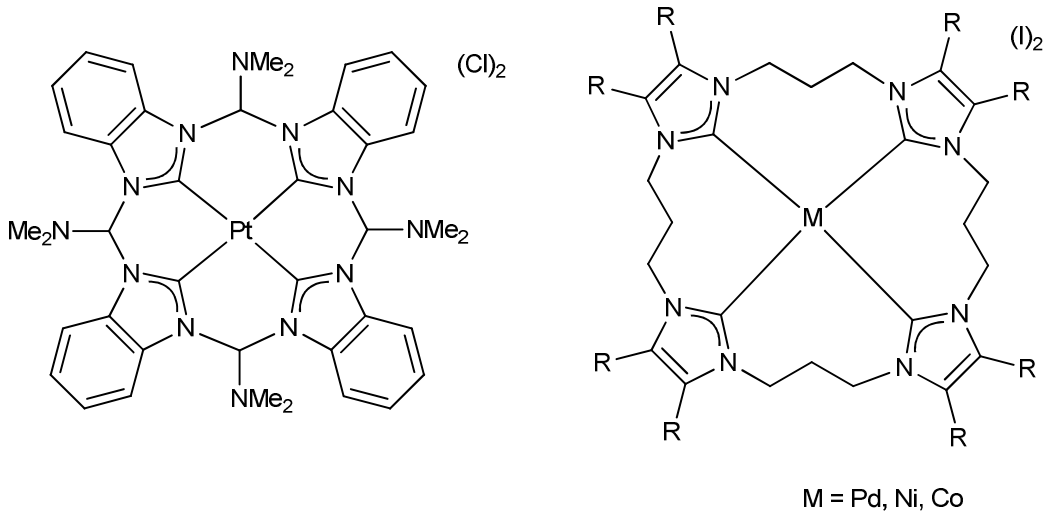

Figure I.3. Hahn's templated 16-atom ringed macrocycle (left) and Murphy's 24-atom ringed macrocycle using a tetraimidazolium (right).

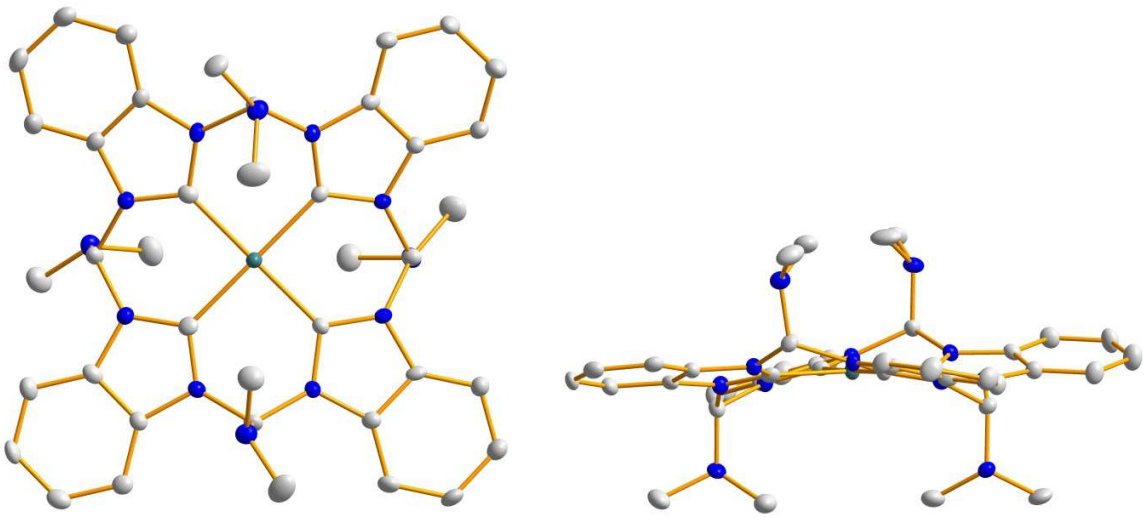

Figure I.4. Top-down (left) and side-view (right) of Hahn's 16-atom ringed macrocycle. Blue, gray, and aqua ellipsoids (50% probability) represent N, C, and Pt, respectively. Hydrogens and anions have been omitted for clarity.

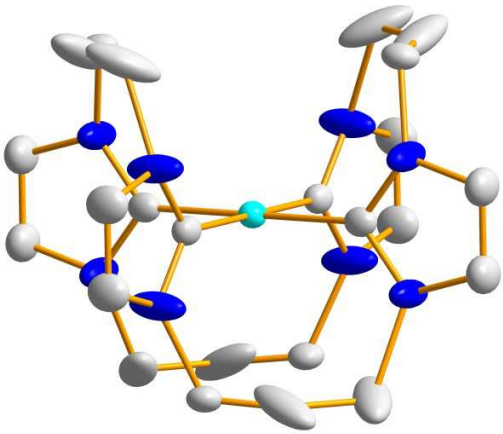

Figure I.5. Murphy's 24-atom ringed nickel complex with saddling around the metal center. Blue, gray, and teal ellipsoids (50% probability) represent N, C, and Ni, respectively. Hydrogens and anions have been omitted for clarity.

Our research goal was to synthesize 16- or 18-atom ringed tetraimidazolium precursors that could be deprotonated to form monomeric tetracarbene complexes. By synthesizing complexes of a smaller ring size than Murphy's, we believed our complexes would be more rigid and not buckled at the apical positions, allowing for access to the metal centers. The first step of this process involved the synthesis of a diimidazoles that then had to be fused together by a dielectrophile. Once the synthesis of a tetraimidazolium was complete, complexation was accomplished by using both a weak and strong base approach. From here, our research turned to making more soluble macrocyclic tetracarbenes. In order to accomplish this task, we installed borates into our macrocycles to reduce the overall charge, allowing the formation of isostructural complexes that were different electronically.

Two side projects were the investigation of catalytic reactions using one of our 18-atom ringed tetracarbene complexes and determining the bonding mode of aryl phosphines on a surface. The first project entailed screening aziridination, epoxidation, and cyclopropanation reactions using various reaction conditions. These results were then compared to our previously obtained results. For the bonding mode of aryl phosphines, we examined secondary aryl phosphines, secondary aryl phosphine oxides, and tertiary aryl phosphines using Raman. The objective was to determine which complexes bonded and which did not, and ultimately to determine their bonding mode to metal surfaces.

References

(1) (a) de Montellano, P. R., Ed. *Cytochrome P450 Structure, Mechanism, and Biochemistry*; Plenum Press: New York, 1986. (b) Lippard, S. J.; Berg, J. M. *Principles of Bioinorganic Chemistry*; University Science Books: Mill Valley, 1994. (c) Tollman, W. B., Ed. *Activation of Small Molecules: Organometallic and Biorganic Perspectives*; Wiley-VCH: Weinheim, Germany, 2006. (d) Ertl, G. *Chem. Rec.* **2001**, *1*, 33.

(2) (a) Brown, S. D.; Betley, T. A.; Peters, J. C. *J. Am. Chem. Soc.* **2003**, *125*, 322. (b) Scepaniak, J. J.; Vogel, C. S.; Khusniyarov, M. M.; Heinemann, F. W.; Meyer, K.; Smith, J. M. *Science* **2011**, *331*, 1049. (c) Mindiola, D. J.; Hillhouse, G. L. *J. Amer. Chem. Soc.* **2001,** *123*, 4623.

(3) Scepaniak, J. J.; Margarit, C. G.; Harvey, J. N.; Smith, J. M. *Inorg.Chem.* **2011**, *50*, 9508.

(4) McDonald, A. R.; Que Jr, L. *Coord. Chem. Rev.* **2013**, *257*, 414.

(5) Laskowski, C. A.; Miller, A. J. M.; Hillhouse, G. L.; Cundari, T. R. *J. Amer. Chem. Soc.* **2010**, *133*, 771.

(6) Miessler, G. L.; Tarr, D. A. *Inorganic Chemistry Third Edition*; Pearson Prentice Hall: New Jersey, 2004.

(7) (a) Shekhawat, G. S.; Verma, K. *J. of Exp. Bot.* **2010**, *61*, 2255. (b) Fantauzzi, S.; Caselli, A.; Gallo, E. *Dalton Trans.* **2009**, 5434-5443. (c) Zhang, J.-L.; Che, C.-M. *Org. Lett.* **2002**, *4*, 1911. (d) Rose, E.; Andrioletti, B.; Zrig, S.; Quelquejeu-Ethève, M. *Chem. Soc. Rev.* **2005**, 34, 573-583. (e) Hong, S.; So, H.; Yoon, H.; Cho, K.-B.; Lee, Y.-M.; Fukuzumi, S.; Nam, W. *Dalton Trans.* **2013,** *42*, 7842. (f) Van Heuvelen, K. M.; Fiedler, A. T.; Shan, X.; De Hont, R. F.; Meier, K. K.; Bominaar, E. L.; Münck, E.; Que, L. *Proc. Natl. Acad. Sci. U. S. A.* **2012,** *109*, 11933.

(8) (a) Kyba, E. P.; Davis, R. E.; Hudson, C. W.; John, A. M.; Brown, S. B.; McPhaul, M. J.; Liu, L.-K.; Glover, A. C. *J. Am. Chem. Soc.* **1981**, *103*, 3868. (b) Kyba, E. P.; Hudson, C. W.; McPhaul, M. J.; John, A. M. *J. Am. Chem. Soc.* **1977**, *99*, 8053. (c) Mizuta, T.; Okano, A.; Sasaki, T.; Nakazawa, H.; Miyoshi, K. *Inorg. Chem.* **1997**, *36*, 200.

(9) Strassner, T. *Top. Organomet. Chem.* **2007**, *22*, 125.

(10) Hahn, F. E.; Langenhahn, V.; Lügger, T.; Pape, T.; Le Van, D. *Angew. Chem., Int. Ed.* **2005**, 44, 3759.

(11) (a) McKie, R.; Murphy, J. A.; Park, S. R.; Spicer, M. D.; Zhou, S. *Angew. Chem., Int. Ed.* **2007**, 46, 6525. (b) Findlay, N. J.; Park, S. R.; Schoenebeck, F.; Cahard, E.; Zhou, S.-z.; Berlouis, L. E. A.; Spicer, M. D.; Tuttle, T.; Murphy, J. A. *J. Amer. Chem. Soc.* **2010,** *132*, 15462. (c) Park, S. R.; Findlay, N. J.; Garnier, J.; Zhou, S.; Spicer, M. D.; Murphy, J. A. *Tetrahedron* **2009**, *65*, 10756.

Chapter 1

Synthesis of an 18-Atom Ringed Tetracarbene

A version of this chapter was originally published by Heather M. Bass, S. Alan Cramer, Julia L. Price, and David M. Jenkins:

Bass, H. M.; Cramer, S. A.; Price, J. L.; Jenkins, D. M. “18-Atom-Ringed Macrocyclic Tetraimidazoliums for Preparation of Monomeric Tetracarbene Complexes.” *Organometallics* **2010**, *29*, 3235-3238.

Abstract

The 18-atom ringed macrocyclic tetraimidazolium, ($^{Me,Et}TC^{H}$)$(OTf)_4$, was formed through a two-step process and without the use of dilute solvent conditions. The tetraimidazolium was the exclusive product, as opposed to the concurrent formation of a tetraimidazolium and diimidazolium species. Due to its small ring size, this 18-atom ringed macrocyclic tetraimidazolium should favor monomeric complexation. By employing a weak base deprotonation strategy, the macrocyclic tetracarbene platinum complex, [($^{Me,Et}TC^{H}$)Pt]$(OTf)_2$, was synthesized. Although not conclusively confirmed, ESI/MS also suggested the formation of two other metal complexes, [($^{Me,Et}TC^{H}$)IrH]$(OTf)_2$ and [($^{Me,Et}TC^{H}$)RhH]$(OTf)_2$.

Introduction

The stabilization of complexes that contain metal-ligand multiple bonds, such as oxo and nitride ligands, is dependent on the symmetry and donor strength of the auxiliary ligands bound to the transition metal.[1] Recent advancements in the preparation of iron oxos and nitrides for bioinorganic models of O_2 and N_2 activation have employed neutral tetradentate weak σ-donors, such as cyclam, as the auxiliary macrocyclic ligand.[2] Current research on three-fold symmetry complexes of iron[3] and cobalt[4] has demonstrated that increasing the σ-donor strength of the

auxiliary ligands stabilizes novel imido and nitride complexes. To our knowledge, few neutral tetradentate strong σ-donor ligands have been synthesized. In fact, few macrocyclic tetradentate phosphines have been prepared and isolated, due to their difficult syntheses, instability, and sensitivity to O_2.[5] Lately, *N*-heterocyclic carbenes (NHCs) have become a more attractive alternative to phosphines for many catalytic applications.[6] In addition to strong σ-donation, NHCs exhibit other beneficial properties, in particular their resistance to degradation in the presence of O_2.[7] This chapter presents an easy to synthesize strong σ-donor macrocyclic tetra-NHC that exclusively produces monomeric transition metal complexes.

Recently synthesized tetra-*N*-heterocyclic carbene complexes include the classes of tetra-monodentate-carbenes, bis-bidentate-carbenes, and macrocyclic tetradentate-carbenes.[8] These tetracarbene complexes have found potential applications as near UV-phosphorescent emitters,[9] radiopharmaceuticals,[10] and catalyst precursors.[11] Yet, of these tetra-NHCs, only four examples of monomeric macrocyclic tetracarbene complexes have been prepared, and both synthetic approaches are somewhat limited in scope. Hahn's synthesis of the first macrocyclic tetracarbene complex requires a templating reaction on platinum.[12] In addition to requiring a tetra-isocyanide complex as a precursor to the monodentate carbene ligands, the synthesis also requires harsh reagents like phosgene. The other two examples have been prepared from a macrocyclic tetraimidazolium ligand and, although a few macrocyclic tetraimidazoliums have been synthesized,[13] only one of these species has been employed as a ligand for synthesizing tetracarbene complexes. Murphy's group was able to prepare a 24-atom ringed tetraimidazolium using 1,3-diiodopropane as the key dielectrophile for ring formation.[14] This tetracarbene ligand is so large and flexible that some metal complexes are monomeric, such as palladium,[14] nickel,[15]

and cobalt,[16] but others are dimeric, such as silver[14] and copper.[14] Since most NHC complexes are prepared from imidazoliums, this approach provides a wider-ranging scope than templating.

Results and Discussion

We have synthesized an 18-atom ringed tetraimidazolium macrocycle that should exclusively favor monomeric complexation. In comparison to Murphy's 24-atom ringed macrocycle, which suffered from saddling, our 18-atom ringed macrocycle should be more suitable for forming planar complexes that will allow for reactivity at the apical positions. This tetraimidazolium was synthesized in multi-gram quantities using a simple two-step process starting from commercially available imidazole and without the use of dilute solvent conditions (Scheme 1.1). We prepared 1,1'-methylene(bis-imidazole) (**1**) using the methods of Diez-Barra[17] and Claramunt.[18] Although previous syntheses of macrocyclic tetraimidazolium species have employed dihaloalkanes or dihaloxylenes as the key dielectrophile for ring formation,[13, 14] we were unsuccessful in our attempts at similar reactions to produce smaller-sized macrocycles with reagents such as diiodomethane and 1,2-diiodoethane. However, utilizing the stronger dielectrophile 1,2-bis-(trifoxy)ethane[19] allowed us to prepare the 18-atom ringed macrocyclic tetraimidazolium, ($^{Me,Et}TC^{H}$)$(OTf)_4$ (**2**) in greater than 15% yield and within three days. We were then able to exchange the triflates to various counteranions by mixing **2** with excess ($^{n}Bu_4N$)X (where X = Cl or I) in an acetonitrile solution to yield the appropriate halide analogue. Since anion exchange must be from a hard anion to a soft anion and vice versa, in order to get the PF_6 analogue, we used excess $TlPF_6$ with either of our halide variants in acetonitrile (Scheme 1.1/Reaction 3). By examining the C2 peak position in the ^1H NMR of each counteranion, it is noted that as the donor strength and relative electronegativity of the counteranion increases, the

C2 proton position shifts downfield due to the weakening of the C2 carbon-proton bond, which leads to deshielding of the proton. This effect can be seen in Figure 1.1 and is most significant in the chloride analogue. A compiled list of C2 values for each of the various counteranions can be seen in Table 1.1.

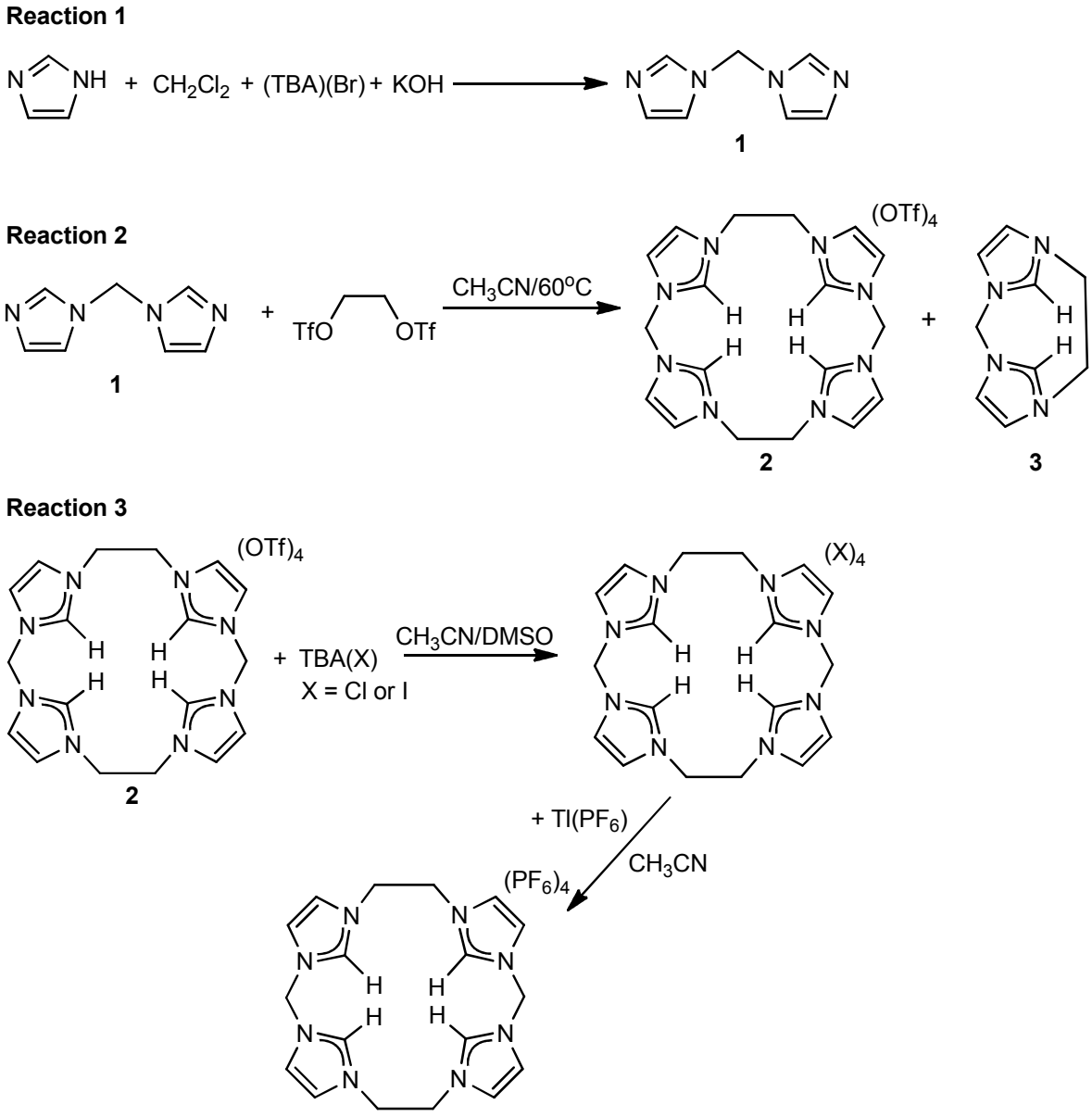

Scheme 1.1. Synthesis of diimidazole (Reaction 1) followed by the formation of ($^{Me,Et}TC^{H}$)$(OTf)_4$ (**2**) (Reaction 2). Reaction 3 shows how to make each corresponding halide analogue.

Table 1.1. ^{1}H NMR comparison in DMSO-d_6 of the C2 peak positions of the tetraimidazolium, ($^{Me,Et}TC^{H}$)(X)$_4$, based on various counteranions.

Counteranion	C2 proton peak position (ppm)
PF_6^-	8.96
OTf^-	8.98
I^-	9.15
Cl^-	9.87

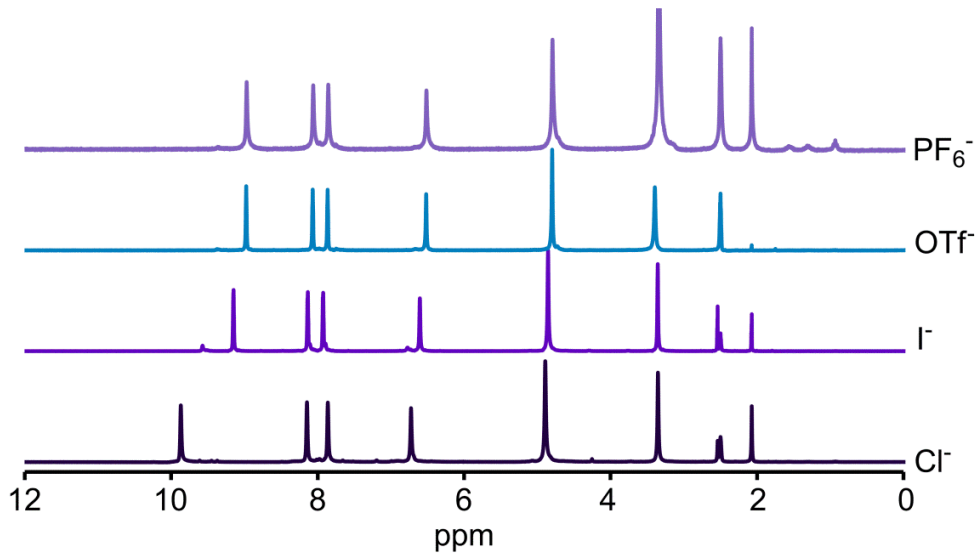

Figure 1.1. ^{1}H NMR in DMSO-d_6 of ($^{Me,Et}TC^{H}$)(X)$_4$ with various counteranions.

One challenge in the synthesis of ($^{Me,Et}TC^{H}$)$(OTf)_4$ is distinguishing between the di-imidazolium species (**3**) shown in Scheme 1.1 and the desired macrocyclic species (**2**) since they are often synthesized concurrently.[13b, 14] ^{1}H and ^{13}C NMR for the white solid formed were consistent with imidazolium formation, and although this evidence was not sufficient to distinguish between **2** and **3**,[20] high resolution ESI/MS conclusively confirmed the formation of **2**, as opposed to **3**. The ESI/MS spectrum exhibited peaks at 167.1 and 799.1 *m*/*z* (Figure 1.2) that are associated with $[(^{Me,Et}TC^{H})(OTf)]^{3+}$ and $[(^{Me,Et}TC^{H})(OTf)_3]^{+}$, respectively, and are unique to **2**. In addition, the peak at 325.1 *m*/*z* exhibited isotopomers that were ½ of a mass unit apart, which is consistent with $[(^{Me,Et}TC^{H})(OTf)_2]^{2+}$ from **2** and not with the 1+ ion of **3**-OTf. The ratio of the isotopomers at 325.1 *m*/*z* is consistent with only **2** and not a mixture of **2** and **3**. Furthermore, the peak at 88.1 *m*/*z* showed ¼ of a mass unit splitting, which is consistent with $[(^{Me,Et}TC^{H})]^{4+}$ and not with the 2+ ion of **3**-2OTf. Combined, these data demonstrate that only the macrocyclic 18-atom ring, **2**, was isolated from the reaction.

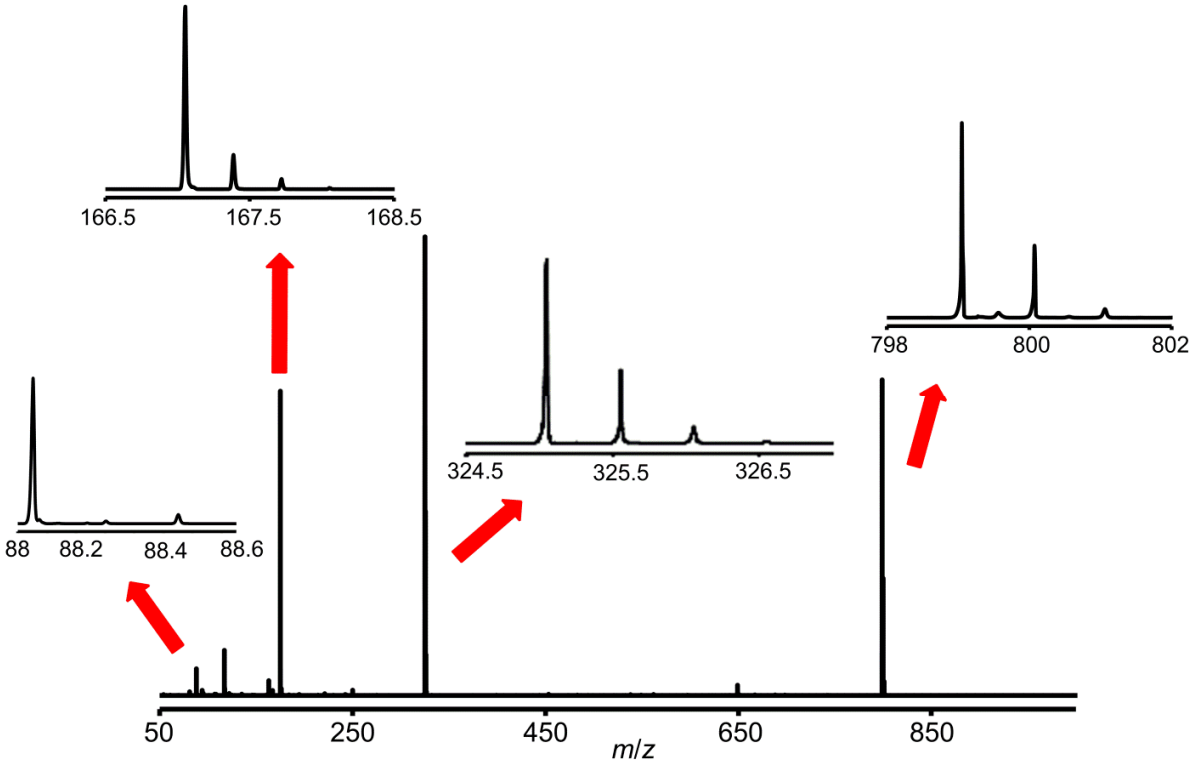

Figure 1.2. An example electrospray ionization mass spectrum (ESI/MS) measured for an acetonitrile solution of **2**. The insets show highlights for the $[(^{Me,Et}TC^{H})]^{4+}$, $[(^{Me,Et}TC^{H})(OTf)]^{3+}$, $[(^{Me,Et}TC^{H})(OTf)_2]^{2+}$, and $[(^{Me,Et}TC^{H})(OTf)_3]^{+}$ ions at 88.1, 167.1, 325.1, and 799.1 *m*/*z*, respectively.

Further evidence that we formed only **2** and not **3** was the single crystal X-ray structure we obtained of **2** as seen in Figure 1.3. Alongside the high resolution ESI/MS evidence, the X-ray structure corroborates that **2** is indeed a macrocycle. The crystal for ($^{Me,Et}TC^{H}$)$(OTf)_4$ was obtained via vapor diffusion of diethyl ether in a concentrated DMSO solution. In comparison to Murphy's 24-atom ringed tetraimidazlium ligand, the structure of **2** seems to be highly restricted in its mobility, suggesting that it would not saddle upon complexation as Murphy's macrocycle did, as well as, suggesting that it would exclusively form monomeric metal complexes.[14]

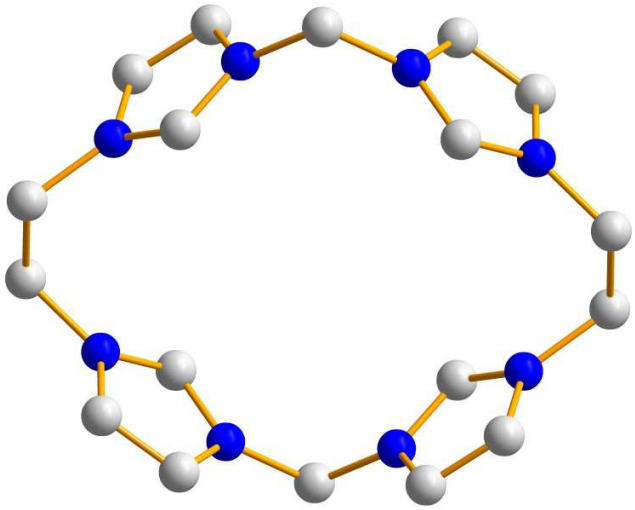

Figure 1.3. Crystal structure of ($^{Me,Et}TC^{H}$)$(OTf)_4$. Blue and grey ellipsoids (50% probability) represent N and C, respectively. Counteranions and hydrogens have been omitted for clarity.

To test the ability of **2** to form monomeric metal complexes, we synthesized a platinum complex (Scheme 1.2). Bis-bidentate platinum[9, 10] and palladium[21] carbene complexes that are similar in size to **4** have been prepared previously via *in situ* deprotonation with a weak base from the free imidazolium ligands. Thallium salts were employed in the reaction to remove any iodide ions and prevent anion confusion during purification. Spectroscopic characterization of **4** was consistent with a tetracarbene complex. The ESI/MS of **4** (Figure 1.4) shows peaks at 271.1 and 691.1 *m*/*z* that are associated with $[(^{Me,Et}TC^{H})Pt]^{2+}$ and $\{[(^{Me,Et}TC^{H})Pt](OTf)\}^{+}$, respectively. The geminal AB splitting pattern in the ^{1}H NMR of the protons on the methylene position on **4** demonstrates the rigidity of the ligand in solution (Figure 1.5),[9, 21b] which is in direct contrast to Murphy's complex.[14] The ^{13}C NMR of **4** is consistent with NHC formation with the carbene peak at 158 ppm for which platinum satellites could be observed with a ^{195}Pt-C coupling constant of 942 Hz, which is similar to Hahn's observed ^{195}Pt-C coupling constant of 902 Hz.[12]

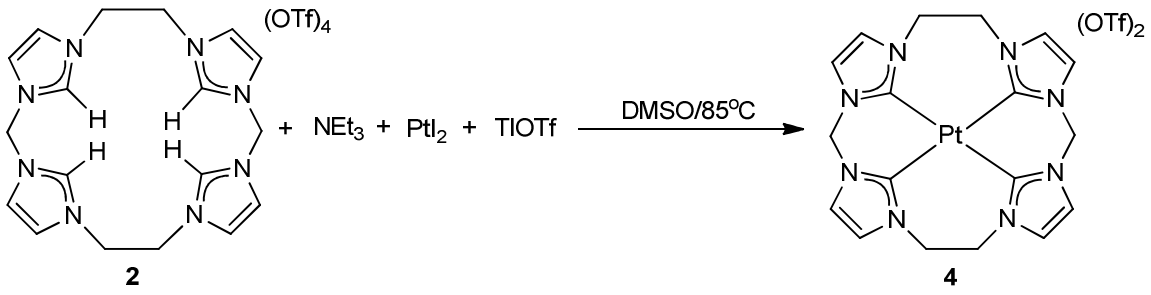

Scheme 1.2. Formation of $[(^{Me,Et}TC^{H})Pt](OTf)_2$ (**4**) from the reaction of $(^{Me,Et}TC^{H})(OTf)_4$ (**2**) with a weak base and platinum(II) iodide.

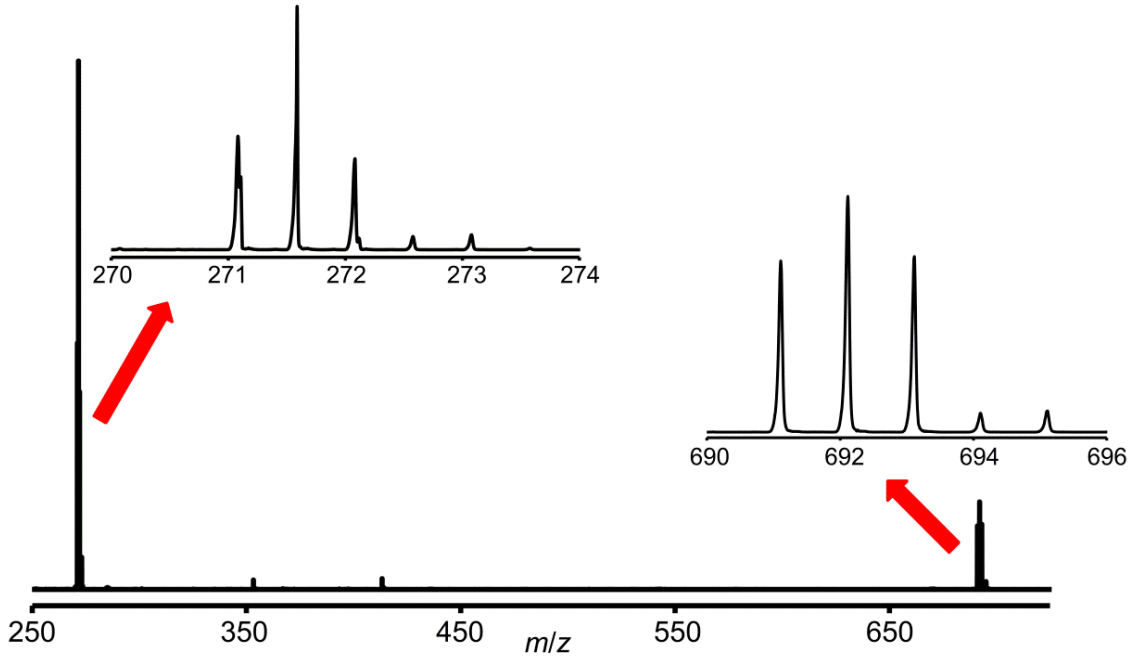

Figure 1.4. An example electrospray ionization mass spectrum measured for an acetonitrile solution of [($^{Me,Et}TC^{H}$)Pt](OTf)$_2$. The insets show highlights for the [($^{Me,Et}TC^{H}$)Pt]$^{2+}$ and {[($^{Me,Et}TC^{H}$)Pt](OTf)}$^{+}$ ions, which are seen at 271.1 and 692.1 *m*/*z*, respectively.

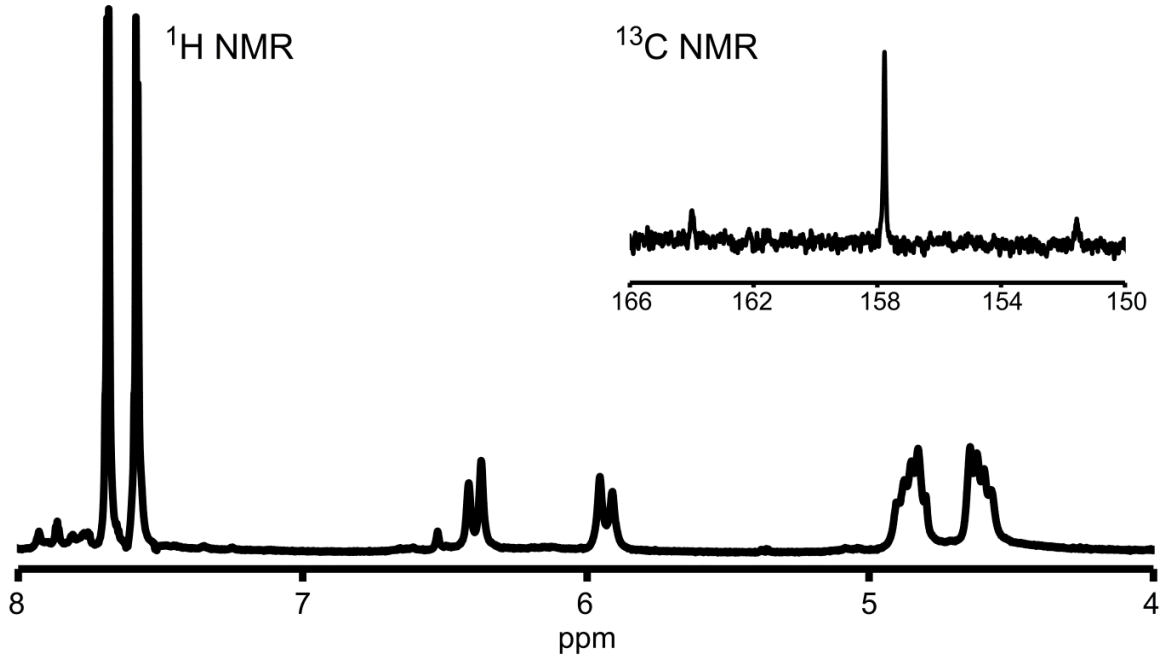

Figure 1.5. ^{1}H NMR of [(^{Me,Et}TC^{H})Pt](OTf)$_2$ in DMSO-d$_6$, exhibiting geminal AB splitting of the methylene and the ethylene positions, suggesting the rigidity of the complex in solution. The inset is a highlight of the ^{13}C NMR carbene peak featuring platinum satellites with a ^{195}Pt-C coupling constant of 942 Hz.

In addition to the synthesis of [(^{Me,Et}TC^{H})Pt](OTf)$_2$, we synthesized iridium and rhodium complexes following the same weak base approach used for the platinum complex. Unlike their platinum counterpart, both the iridium and rhodium ESI/MS exhibited metal hyrides with peaks at 271.1 and 691.1 *m*/*z* for [(^{Me,Et}TC^{H})IrH]$^{+2}$ and {[(^{Me,Et}TC^{H})IrH](OTf)}$^{+}$ and 226.0 and 601.1 *m*/*z* for [(^{Me,Et}TC^{H})RhH]$^{+2}$ and {[(^{Me,Et}TC^{H})RhH](OTf)}$^{+}$, as seen in Figure 1.5. Presumably, this anomaly arises from the fact that both rhodium and iridium prefer to be in the +3 oxidation state as opposed to +1 oxidation state, thus causing a redox reaction to occur. Although no other data

were collected for either species, the formation of a hydride was corroborated by crystal structures obtained for the phenyl variants, [($^{Me,Et}TC^{Ph}$)IrH](OTF)$_2$ and [($^{Me,Et}TC^{Ph}$)RhH](OTf)$_2$.

Conclusion

In conclusion, we have demonstrated a facile, two step synthesis of an 18-atom ringed tetraimidazolium ligand that employed 1,2-bis-(trifoxy)ethane as the key dielectrophile. The ligand can be prepared on a multi-gram scale quickly and cleanly without the use of dilute solvent conditions. This 18-atom ringed tetraimidazolium (**2**) ligates to form monomeric transition metal complexes such as **4**. The phenyl variant has recently demonstrated success as an aziridination catalyst,[22] thus verifying the fact that the strong sigma donor strength plays a large role in catalysis and the stabilization of metal-ligand bonds.

Figure 1.6. An example electrospray ionization mass spectrum measured for an acetonitrile solution of $[(^{Me,Et}TC^{H})IrH](OTf)_2$ and $[(^{Me,Et}TC^{H})RhH](OTf)_2$. (A) The inset shows a highlight for the $[(^{Me,Et}TC^{H})IrH]^{+2}$ ion, which is seen at 271.1 *m*/*z*. (B) The insets show highlights for the $[(^{Me,Et}TC^{H})RhH]^{+2}$ and $\{[(^{Me,Et}TC^{H})RhH](OTf)\}^{+}$ ions, which are seen at 226.0 and 601.1 *m*/*z*, respectively.

A

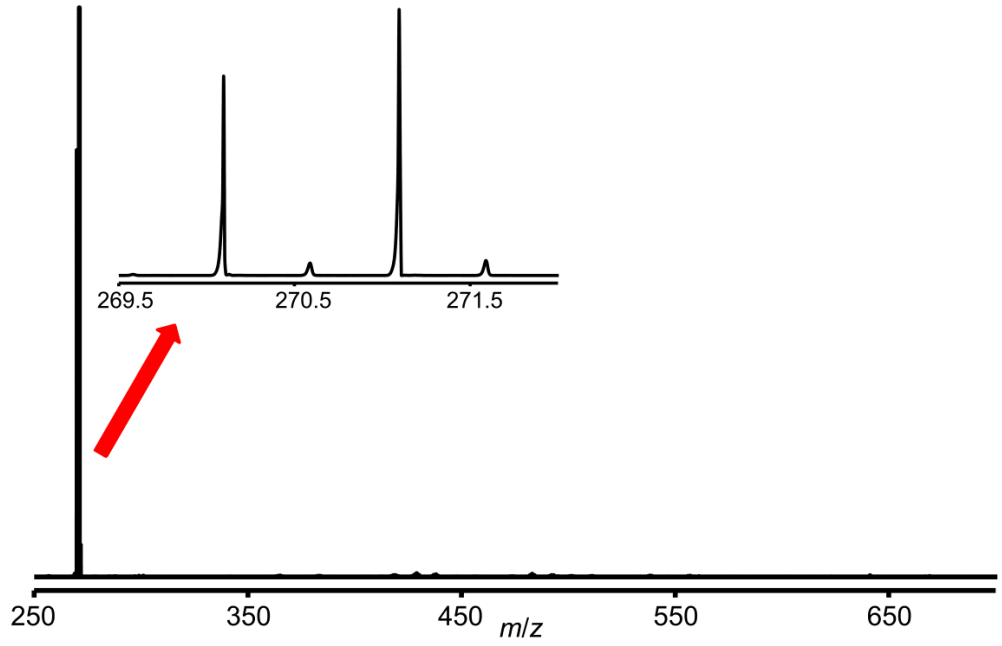
269.5
270.5
271.5
250
350
450
m/z
550
650

B

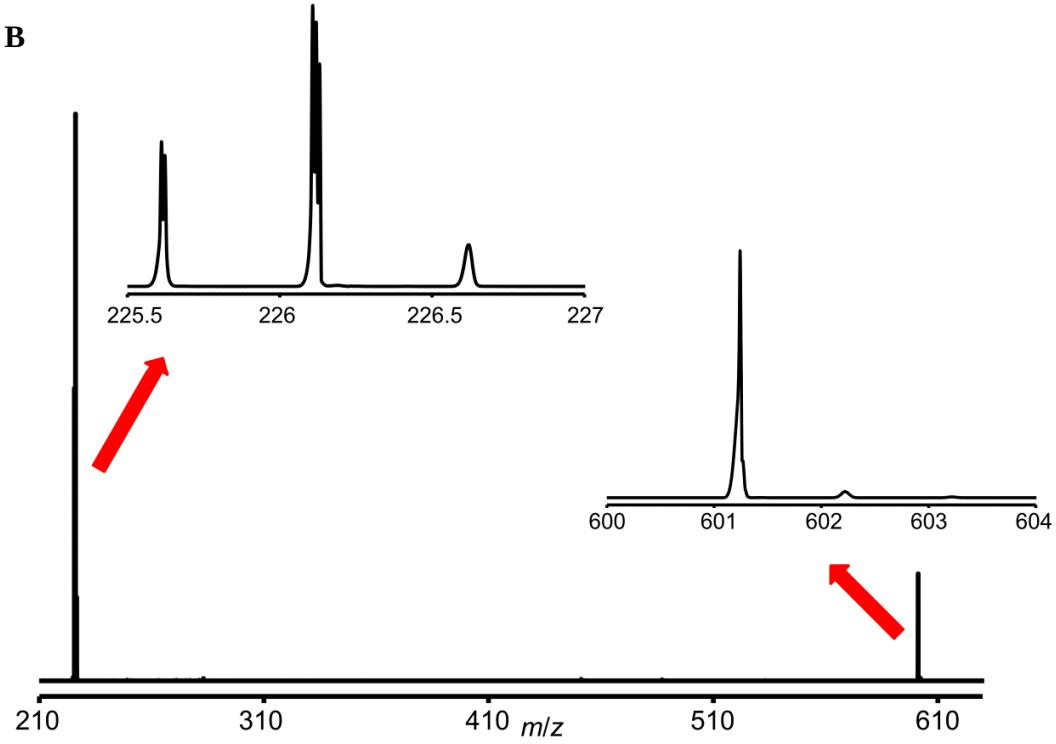
225.5
226
226.5
227
600
601
602
603
604
210
310
410
m/z
510
610

Experimental

Syntheses of organic compounds were performed under normal atmospheric conditions. Syntheses of metal complexes were performed under a dry nitrogen atmosphere with the use of either a dry box or standard Schlenk techniques. Solvents were dried on an Innovative Technologies (Newburgport, MA) Pure Solv MD-7 Solvent Purification System and degassed by three freeze-pump-thaw cycles on a Schlenk line to remove O_2 prior to use. DMSO-d_6, acetonitrile-d_3, and chloroform-d were degassed by three freeze-pump-thaw cycles prior to drying over activated molecular sieves. These NMR solvents were then stored under N_2 in a glovebox. The compounds 1,1'-methylene(bis-imidazole) (**1**)[17, 18] and 1,2-diyl-bis(trifluoromethanesulfonate)ethane (also called 1,2-bis-(trifoxy)ethane)[19] were prepared as described previously. All other reagents were purchased from commercial vendors and used without purification. ^{1}H, ^{13}C{^{1}H}, and ^{19}F NMR spectra were recorded at ambient temperature on a Varian Mercury 300 MHz or a Varian INOVA 600 MHz narrow-bore broadband system. ^{1}H and ^{13}C NMR chemical shifts were referenced to the residual solvent. ^{19}F NMR chemical shifts are reported relative to an external standard of neat $CFCl_3$. All mass spectrometry analyses were conducted at the Mass Spectrometry Center located in the Department of Chemistry at the University of Tennessee. The DART analyses were performed using a JEOL AccuTOF-D time-of-flight (TOF) mass spectrometer with a DART (direct analysis in real time) ionization source from JEOL USA, Inc. (Peabody, MA). The ESI/MS analyses were performed using a QSTAR Elite quadrupole time-of-flight (QTOF) mass spectrometer with an electrospray ionization source from AB Sciex (Concord, Ontario, Canada). All mass spectrometry sample solutions were prepared in acetonitrile. Infrared spectra were collected on a Thermo Scientific Nicolet iS10 with

a Smart iTR accessory for attenuated total reflectance. Carbon, hydrogen, and nitrogen analyses were obtained from Atlantic Microlab, Norcross, GA.

Synthesis of ($^{Me,Et}TC^{H}$)$(OTf)_4$, 2. 1,1'-methylene(bis-imidazole) (**1**) (7.39 g, 0.0499 mol) was dissolved in acetonitrile (220 mL) in a 500 mL round bottom flask and 1,2-diyl-bis(trifluoromethanesulfonate)ethane (16.3 g, 0.0499 mol) was then slowly added into the stirring solution. The solution was heated to reflux and stirred for 2 days. The solution was then filtered hot through a 60 mL fine sintered-glass frit and a white solid was collected. The white solid was then dried under reduced pressure to give the product (3.73 g, 15.8% yield). Crystals were obtained by vapor diffusion of diethyl ether into a concentrated DMSO solution. ^{1}H NMR (DMSO-d_6, 300.1 MHz): δ 8.99 (s, 4H), 8.07 (s, 4H), 7.87 (s, 4H), 6.52 (s, 4H), 4.80 (s, 8H). ^{13}C NMR (DMSO-d_6, 75.46 MHz): δ 137.7, 123.6, 123.1, 120.7 (q, J_{FC} = 322 Hz), 58.5, 48.9. ^{19}F NMR (DMSO-d_6, 282.3 MHz): δ -77.1. IR (neat): 3110, 1578, 1553, 1369, 1273, 1247, 1226, 1150, 1075, 1028, 886, 858, 774, 724 cm^{-1}. ESI/MS (*m/z*): $[M\text{-}OTf]^{+}$ 799.1, $[M\text{-}2OTf]^{2+}$ 325.0, $[M\text{-}3OTf]^{3+}$ 167.1, $[M\text{-}4OTf]^{4+}$ 88.1. Anal. Calcd for $C_{22}H_{24}F_{12}N_8O_{12}S_4$: C, 27.85; H, 2.55; N, 11.81. Found: C, 27.92; H, 2.47; N, 11.74.

Synthesis of ($^{Me,Et}TC^{H}$)$(I)_4$. In a 120 mL jar with a Teflon lid, acetonitrile (70 mL) and ($^{Me,Et}TC^{H}$)$(OTf)_4$ (**2**) (3.12 g, 0.00329 mol) were added and stirred. DMSO (14 mL) was added dropwise until all solids dissolved. Tetrabutylammonium iodide (12.2 g, 0.0329 mol) was then dissolved in acetonitrile (25 mL) in a 100 mL beaker. The tetrabutylammonium iodide solution was poured into the 120 mL jar immediately forming a white precipitate. The acetonitrile mixture stirred overnight and the white solid was collected on a 60 mL fine sintered-glass frit. The white solid was subsequently washed with THF (2 x 30 mL) and acetonitrile (1 x 30 mL) on the 60 mL fine sintered-glass frit. The white solid was then dried under reduced pressure to yield

the product (2.28 g, 80.5% yield). ^{1}H NMR (DMSO-d_6, 300.1 MHz): δ 9.11 (s, 4H), 8.11 (s, 4H), 7.91 (s, 4H), 6.58 (s, 4H), 4.84 (s, 8H). ^{13}C NMR (DMSO-d_6, 75.46 MHz): δ 137.6, 123.5, 123.0, 58.4, 48.7. IR (neat): 3094, 3023, 1563, 1550, 1441, 1327, 1170, 1153, 1022, 824, 764, 750, 728 cm^{-1}. Anal. Calcd for $C_{18}H_{24}I_4N_8$: C, 25.14; H, 2.81; N, 13.03. Found: C, 25.09; H, 3.07; N, 12.39.

Synthesis of (^{Me,Et}TC^{H})(Cl)$_4$. In a 20 mL vial, (^{Me,Et}TC^{H})(I)$_4$ (0.105 g, 0.110 mmol) was added to 10 mL of CH_3CN then dissolved with 1 mL DMSO. Slowly, a 1 mL solution of tetrabutylammonium chloride (0.123 g, 0.441 mmol) in CH_3CN was added to the dissolved macrocycle, immediately forming a white precipitate. The solution stirred for an hour and was subsequently filtered over a 15 mL fine sintered frit. The filtrate was dried under reduced pressure, leaving the pure white solid (0.0500 g, 92.4% yield). ^{1}H NMR (DMSO-d_6, 300.1 MHz): δ 9.94 (s, 4H), 8.11 (s, 4H), 7.82 (s, 4H), 6.71 (s, 4H), 4.90 (s, 8H). IR (neat): 3355, 3080, 1566, 1554, 1445, 1367, 1332, 1175, 1157, 1108, 1028, 832, 775, 730, 663 cm^{-1}.

Synthesis of (^{Me,Et}TC^{H})(PF$_6$)$_4$. In a 20 mL vial, (^{Me,Et}TC^{H})(I)$_4$ (0.105 g, 0.122 mmol) was dissolved in 10 mL of CH_3CN. Thallium hexafluorophosphate dissolved in 2 mL of CH_3CN was added, immediately crashing out a white solid. The mixture stirred for an hour and was subsequently filtered over a 15 mL fine sintered frit. The filtrate was dried under reduced pressure, leaving the pure white solid (0.106 g, 93.3% yield). ^{1}H NMR (DMSO-d_6, 300.1 MHz): δ 8.97 (s, 4H), 8.06 (s, 4H), 7.86 (s, 4H), 6.52 (s, 4H), 4.79 (s, 8H). ^{19}F NMR (DMSO-d_6, 282.3 MHz): δ: -72.6 (d, J = 706Hz).

Synthesis of [(^{Me,Et}TC^{H})Pt](OTf)$_2$, 4. (^{Me,Et}TC^{H})(OTf)$_4$ (**2**) (0.174 g, 0.184 mmol) was dissolved in DMSO (1 mL) in a 20 mL vial. Platinum(II) iodide (0.0824 g, 0.184 mmol) was dissolved in 1 mL of DMSO and was added to the (^{Me,Et}TC^{H})(OTf)$_4$ solution. Triethylamine

(0.0762 g, 0.753 mmol) was then added to the reaction mixture. This solution was heated to 85 °C and stirred for 48 h. After the reaction mixture was removed from the heat and allowed to cool to room temperature, thallium(I) trifluoromethanesulfonate (0.130 g, 0.367 mmol) was dissolved in DMSO (1 mL) and was added to the reaction mixture. This mixture was stirred for 15 min and then filtered over Celite to remove thallium(I) iodide. DMSO was then removed under reduced pressure to leave the crude solid. The crude solid was washed with THF (3 x 10 mL) and dried under reduced pressure leaving a white solid. To further purify the white solid, it was dissolved in acetonitrile (2 mL), and the resulting solution was then filtered over Celite, and crystallized via vapor diffusion of diethyl ether into the acetonitrile solution. White crystals were collected and dried under reduced pressure to give the pure product (0.0715 g, 46.3% yield). ^{1}H NMR (DMSO-d_6, 300.1 MHz): δ 7.68 (d, J = 1.8 Hz, 4H), 7.57 (d, J = 2.1 Hz, 4H), 6.40 (d, J = 12.9 Hz, 2H), 5.95 (d, J = 13.5 Hz, 2H), 4.86 (m, 4H), 4.61 (m, 4H). ^{13}C NMR (DMSO-d_6, 150.9 MHz): 157.8 (s and Pt satellites, $J_{Pt\text{-}C}$ = 942 Hz for ^{195}Pt (^{195}Pt = 33.8% abundance)), 123.3, 121.6, 120.6 (q, $J_{F\text{-}C}$ = 322 Hz), 62.5, 48.7. ^{19}F NMR (DMSO-d_6, 282.3 MHz): δ -77.0. IR (neat): 3131, 1574, 1428, 1244, 1224, 1152, 1026, 857, 812, 757, 707 cm^{-1}. ESI/MS (*m/z*): [M-OTf]$^{+}$ 692.1, [M-2OTf]$^{2+}$ 271.6. Anal. Calcd for $C_{20}H_{20}F_6N_8O_6PtS_2$: C, 28.54; H, 2.40; N, 13.31. Found: C, 28.67; H, 2.21; N, 13.16.

Synthesis of [(^{Me,Et}TC^{H})IrH](OTf)$_2$. In a 20 mL vial, (^{Me,Et}TC^{H})(OTf)$_4$ (**2**) (0.0300 g, 0.0316 mmol) was dissolved in approximately 1 mL of DMSO. Triethylamine (0.0105 g, 0.104 mmol) was added to the solution followed by chloro(1,5-cyclooctadiene)iridium(I) dimer (0.00850 g, 0.0127 mmol) dissolved in 1 mL of DMSO. The solution stirred for two hours at 60 °C then 2 hours at 80 °C and finally 1 hour at 110 °C. After said time, the reaction was turned down to 90 °C for 48 hrs. The solution was then cooled to room temperature and thallium triflate

(0.0179 g, 0.0506 mmol) was added. Thallium chloride crashed out and the solution was filtered over Celite. The solution was pumped to a solid and washed with pentane. ESI/MS (*m*/*z*): [M-OTf]$^{+}$ 691.1, [M-2OTf]$^{2+}$ 271.2.

Synthesis of [($^{Me,\ Et}$TC^{H})RhH](OTf)$_2$. In a 20 mL vial, (^{Me,Et}TC^{H})(OTf)$_4$ (0.0300 g, 0.0316 mmol) was dissolved in approximately 1 mL of DMSO. Triethylamine (0.0105 g, 0.104 mmol) was added to the solution followed by chloro(1,5-cyclooctadiene) rhodium(I) dimer (0.00624 g, 0.0127 mmol) dissolved in 1 mL of DMSO. The solution stirred for two hours at 60 °C then 2 hours at 80 °C and finally 1 hour at 110 °C. After said time, the reaction was turned down to 90 °C for 48 hrs. The solution was then cooled to room temperature and thallium triflate (0.0179 g, 0.0506 mmol) was added. Thallium chloride crashed out and the solution was filtered over Celite. The solution was pumped to a solid and washed with pentane. ESI/MS (*m*/*z*): [M-OTf]$^{+}$ 601.2, [M-2OTf]$^{2+}$ 226.1.

X-ray Structure Determinations. X-ray diffraction measurements were performed on single crystals coated with Paratone oil and mounted on Kaptan loops. Each crystal was frozen under a stream of N_2 while data were collected on a Bruker APEX diffractometer. A matrix scan using at least 12 centered reflections was used to determine initial lattice parameters. Reflections were merged and corrected for Lorenz and polarization effects, scan speed, and background using SAINT 4.05. Absorption corrections, including odd and even ordered spherical harmonics were performed using SADABS, if necessary. Space group assignments were based upon systematic absences, *E* statistics, and successful refinement of the structure. The structure was solved by direct methods with the aid of successive difference Fourier maps, and was refined against all data using the SHELXTL 5.0 software package.

References

(1) (a) Nugent, W. A.; Mayer, J. M. *Metal-ligand multiple bonds: the chemistry of transition metal complexes containing oxo, nitrido, imido, alkylidene, or alkylidyne ligands*; Wiley: New York, 1988. (b) Lin, Z.; Hall, M. B. *Coord. Chem. Rev.* **1993**, *123*, 149.

(2) (a) Rohde, J.-U.; In, J.-H.; Lim, M. H.; Brennessel, W. W.; Bukowski, M. R.; Stubna, A.; Muenck, E.; Nam, W.; Que, L. *Science* **2003**, *299*, 1037. (b) Li, F.; England, J.; Que, L. *J. Am. Chem. Soc.* **2010**, *132*, 2134. (c) Meyer, K.; Bill, E.; Mienert, B.; Weyhermueller, T.; Wieghardt, K. *J. Am. Chem. Soc.* **1999**, *121*, 4859. (d) Berry, J. F.; Bill, E.; Bothe, E.; DeBeer George, S.; Mienert, B.; Neese, F.; Wieghardt, K. *Science* **2006**, *312*, 1937.

(3) (a) Scepaniak, J. J.; Fulton, M. D.; Bontchev, R. P.; Duesler, E. N.; Kirk, M. L.; Smith, J. M. *J. Am. Chem. Soc.* **2008**, *130*, 10515. (b) Vogel, C.; Heinemann, F. W.; Sutter, J.; Anthon, C.; Meyer, K. *Angew. Chem., Int. Ed.* **2008**, *47*, 2681. (c) Betley, T. A.; Peters, J. C. *J. Am. Chem. Soc.* **2004**, *126*, 6252. (d) Brown, S. D.; Betley, T. A.; Peters, J. C. *J. Am. Chem. Soc.* **2003**, *125*, 322.

(4) (a) Jenkins, D. M.; Betley, T. A.; Peters, J. C. *J. Am. Chem. Soc.* **2002**, *124*, 11238. (b) Hu, X.; Meyer, K. *J. Am. Chem. Soc.* **2004**, *126*, 16322. (c) Shay, D. T.; Yap, G. P. A.; Zakharov, L. N.; Rheingold, A. L.; Theopold, K. H. *Angew. Chem., Int. Ed.* **2005**, *44*, 1508.

(5) (a) Kyba, E. P.; Davis, R. E.; Hudson, C. W.; John, A. M.; Brown, S. B.; McPhaul, M. J.; Liu, L.-K.; Glover, A. C. *J. Am. Chem. Soc.* **1981**, *103*, 3868. (b) Kyba, E. P.; Hudson, C. W.; McPhaul, M. J.; John, A. M. *J. Am. Chem. Soc.* **1977**, *99*, 8053. (c) Mizuta, T.; Okano, A.; Sasaki, T.; Nakazawa, H.; Miyoshi, K. *Inorg. Chem.* **1997**, *36*, 200.

(6) (a) Herrmann, W. A. *Angew. Chem., Int. Ed.* **2002**, *41*, 1290. (b) Diez-Gonzalez, S.; Marion, N.; Nolan S. P. *Chem. Rev.* **2009**, *109*, 3612.

(7) Strassner, T. *Top. Organomet. Chem.* **2007**, *22*, 125.

(8) Poyatos, M.; Mata, J. A.; Peris, E. *Chem. Rev.* **2009**, *109*, 3677.

(9) (a) Unger, Y.; Zeller, A.; Taige, M. A.; Strassner, T. *Dalton Trans.* **2009**, 4786. (b) Unger, Y.; Zeller, A.; Ahrens, S.; Strassner, T. *Chem. Commun.* **2008**, 3263.

(10) Quezada, C. A.; Garrison, J. C.; Tessier, C. A.; Youngs, W. J. *J. Organomet. Chem.* **2003**, *671*, 183.

(11) Lee, C.- S.; Pal, S.; Yang, W.- S.; Hwang, W.- S.; Lin, I. J. B. *J. Mol. Catal. A Chem.* **2008**, *280*, 115.

(12) Hahn, F. E.; Langenhahn, V.; Luegger, T.; Pape, T.; Le Van, D. *Angew. Chem., Int. Ed.* **2005**, *44*, 3759.

(13) (a) Sato, K.; Onitake, T.; Arai, S.; Yamagishi, T. *Heterocycles* **2003**, *60*, 779. (b) Shi, Z.; Thummel, R. P. *J. Org. Chem.* **1995**, *60*, 5935. (c) Wong, W. W. H.; Vickers, M. S.; Cowley, A. R.; Paul, R. L.; Beer, P. D. *Org. Biomol. Chem.* **2005**, *3*, 4201.

(14) McKie, R.; Murphy, J. A.; Park, S. R.; Spicer, M. D.; Zhou, S.- Z. *Angew. Chem., Int. Ed.* **2007**, *46*, 6525.

(15) Findlay, N. J.; Park, S. R.; Schoenebeck, F.; Cahard, E.; Zhou, S.- Z.; Berlouis, L. E. A.; Spicer, M. D.; Tuttle, T.; Murphy, J. A. *J. Amer. Chem. Soc.* **2010,** *132*, 15462.

(16) Park, S. R.; Findlay, N. J.; Garnier, J.; Zhou, S.; Spicer, M. D.; Murphy, J. A. *Tetrahedron* **2009**, *65*, 10756.

(17) Diez-Barra, E.; De la Hoz, A.; Sanchez-Migallon, A.; Tejeda, J. *Heterocycles* **1992**, *34*, 1365.

(18) Claramunt, R. M.; Elguero, J.; Meco, T. *J. Heterocycl. Chem.* **1983**, *20*, 1245.

(19) Lindner, E.; Von Au, G.; Eberle, H. J. *Chem. Ber.* **1981**, *114*, 810.

(20) Tapu, D.; Dixon, D. A.; Roe, C. *Chem. Rev.* **2009**, *109*, 3385.

(21) (a) Fehlhammer, W. P.; Bliss, T.; Kernbach, U.; Bruedgam, I. *J. Organomet. Chem.* **1995**, *490*, 149. (b) Herrmann, W. A.; Schwarz, J.; Gardiner, M. G.; Spiegler, M. *J. Organomet. Chem.* **1999**, *575*, 80.

(22) Cramer, S. A.; Jenkins, D. M. *J. Am. Chem. Soc.* **2011**, *133*, 1934.

Chapter 2

Designing a Macrocycle that is Isostructural and Isoelectronic to a Porphyrin

A version of this chapter was orginially published by Heather M. Bass, S. Alan Cramer, A. Scott McCullough, Karl J. Berstein, Chris R. Murdock, and David M. Jenkins:

Bass, H. M.; Cramer, S. A.; McCullough, A. S.; Bernstein, K. J.; Murdock, C. R.; Jenkins, D. M., "Employing Dianionic Macrocyclic Tetracarbenes To Synthesize Neutral Divalent Metal Complexes." *Organometallics* **2013,** *32*, 2160-2167.

Abstract

Two 16-atom ringed, borate-based macrocyclic tetraimidazoliums ($^{BH_2,Me}TC^{Me}$)$(I)_2$ and ($^{B(Me)_2,Me}TC^{H}$)$(Br)_2$ were synthesized. These macrocycles are isostructural to porphyrins and upon deprotonation should be isoelectronic to porphyrins. Due to the addition of the two borate moieties, divalent metal complexes formed on either of these two ligands will have an overall neutral charge. Unfortunately, we were unable to isolate complexes on ($^{BH_2,Me}TC^{Me}$)$(I)_2$ due to the inherent instability of the B-H bond. Although the formation of metal complexes using ($^{B(Me)_2,Me}TC^{H}$)$(Br)_2$ has not been thoroughly explored, we believe they should be able to be isolated since the B-H bond has been replaced by a more stable B-Me bond.

Introduction

Macrocycles, such as porphyrins, play roles in both natural and synthetic chemical reactions. In nature, porphyrins can be found in heme-containing proteins, such as hemoglobin and myoglobin. In hemoglobin, a heme group consisting of a porphyrin ring bound to an iron center allows for O_2 activation and transportation.[1] In fine chemical synthesis, porphyrins have been used for aziridination,[2] epoxidation,[3] and cyclopropanation[4] reactions. Porphyrins are prime candidates for these types of natural processes and synthetic reactions due to the fact that they

are di-anionic and block four-coordination sites in an equatorial plane around a transition metal center (Figure 2.1). In addition to blocking four coordination sites, structurally a porphyrin is flat, thus allowing free access to the metal center for reactions. By adjusting the donor strength of the ligand and using the base porphyrin scaffold, a novel ligand system can be developed that would allow for enhanced activity and novel reactivity. Unfortunately, only one strong neutral isostructural ligand has been synthesized to date, Hahn's 16-atom ringed templating reaction.[5] As discussed previously, this reaction uses harsh reagents and is not viable for a wide variety of metals.[5] We proposed a 16-atom ringed tetraimidazolium precursor using geminal triflates that would be suitable for a wide variety of transition metals and that would be isostructural to a porphyrin (Scheme 2.1).

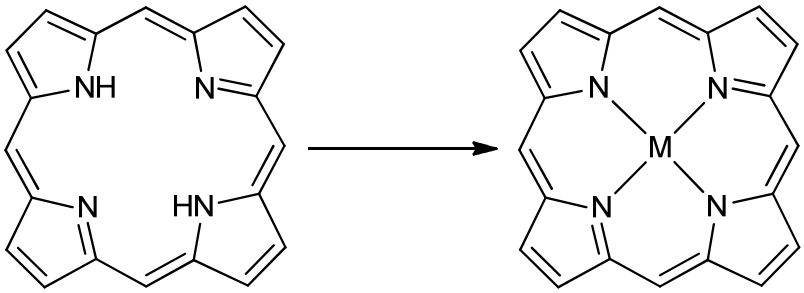

Figure 2.1. Structure of a porphyrin macrocycle.

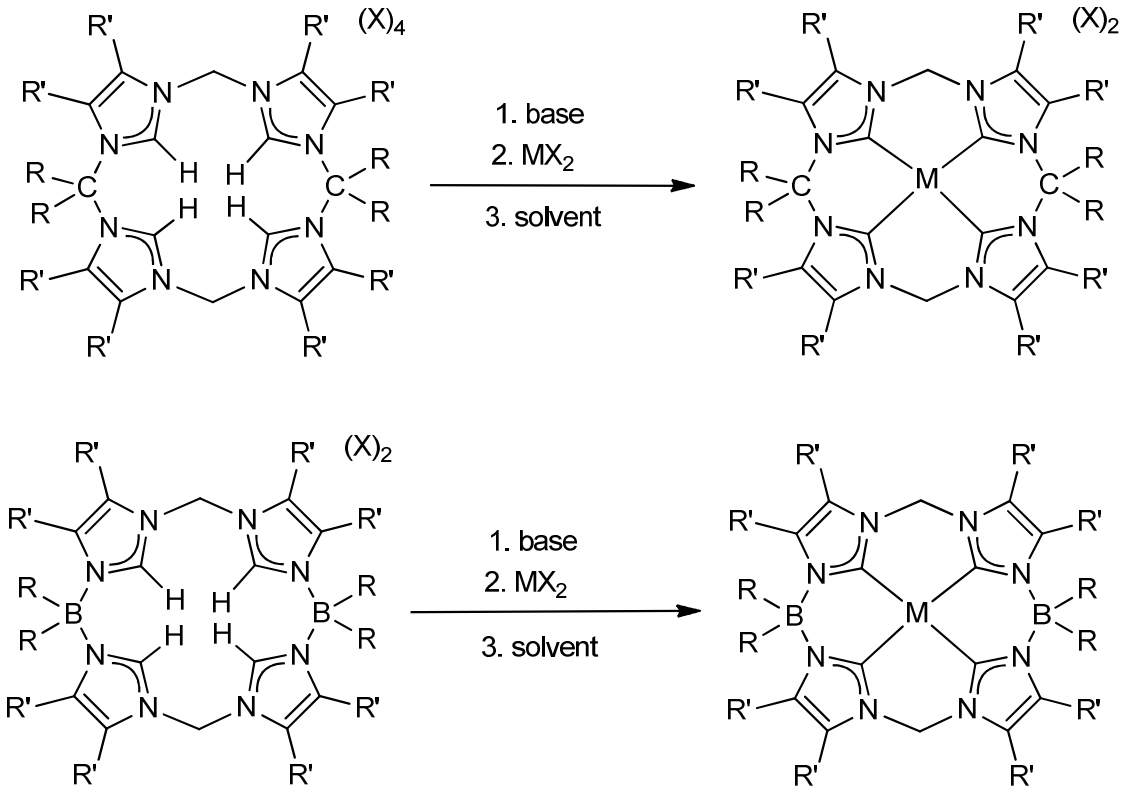

Scheme 2.1. Proposed 16-atom ringed tetraimidazolium ligands. The all carbon variant is the neutral ligand (top), while the borate-based variant is the dianionic variant (bottom).

Besides synthesizing an isostructural ligand system, we also wanted our ligand to be isoelectronic to a porphyrin. One way to accomplish this task would be to insert borates into the macrocycle. Borate-based macrocycles allow for a lower overall charge, thus increasing solubility in nonpolar solvents such as toluene. Siebert's previous syntheses suggest that it would be possible to prepare a 16-atom ringed macrocyclic tetraimidazolium with borates in the backbone that could be ligated to form tetracarbenes (Figure 2.2.A).[6] In order to be isoelectronic to a porphyrin, this would mean inserting two borates in the overall scaffold. Siebert and coworkers synthesized imidazolium borate macrocycles that contained either four or five

imidazoliums per ring with an equal number of borates.[6] Notably, they were unable to form carbenes with these complexes, perhaps because their ratio of one borate moiety to one imidazolium decreased the acidity of the C2 proton.[6] In contrast, Fehlhammer[7] and Smith[8] independently prepared bis-dicarbene borate complexes on group 10 metals (Figure 2.2 B/C). Their complexes only had one borate moiety per two carbenes. By following Fehlhammer and Smith's approach of one borate per two carbenes, it should be possible to form isostructural, as well as, isoelectronic macrocycles to porphyrins.

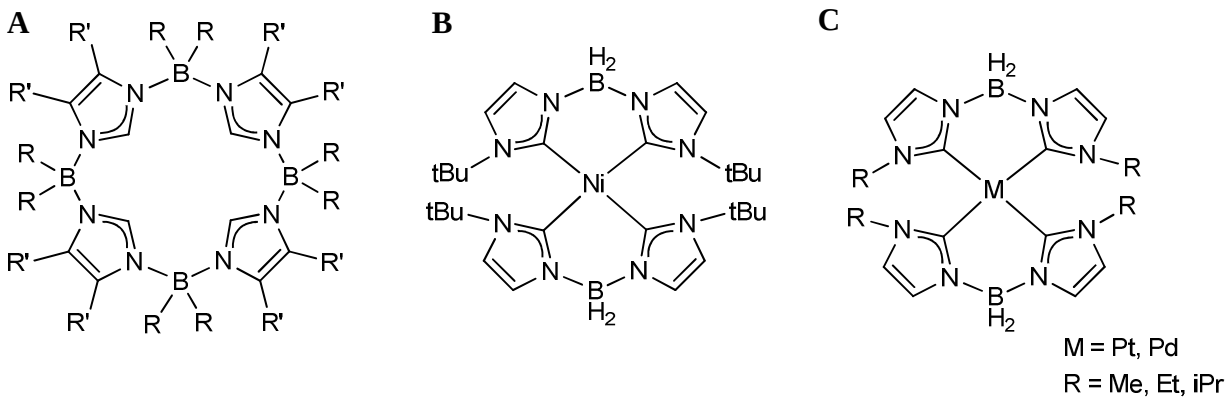

Figure 2.2. (A) Siebert's tetraimidazlium borate macrocycle, (B) Smith's bis-dicarbene nickel complex, and (C) Fehlhammer's bis-dicarbene platinum and palladium complexes.

Results and Discussion

Since previous results showed 1,2-bis-(trifloxy)ethane as a strong di-electrophile for the synthesis of our 18-atom ringed macrocycle,[9] a C_{2v} symmetric *gem*-triflate is critical for the synthesis of a neutral 16-atom ringed macrocycle. Notably, relatively few examples of symmetric *gem*-triflates have been synthesized and there are only three *gem*-triflates in literature,

which consist of Desmarteau's methyl-ditriflate,[10] Sterlin's 2,2-ditriflato-perfluoropropane,[11] and Martìnez's 7,7'-ditriflato-norbornane (Figure 2.3).[12] The most promising of these *gem*-triflates is the methyl-ditriflate; however, this synthesis involves extremely low temperatures under a dynamic vacuum, which is a synthetic apparatus that we do not possess.[10] Another approach is Sterlin's *gem*-triflates with the CF_3 groups off of the central carbon, which is readily susceptible to degradation. The easiest synthetic approach would be the synthesis of Martìnez's 7,7'-ditriflato-norbonane. Since 7-norbonone is quite difficult to synthesize, we proposed the use of commercially available cyclobutanone. Another advantage of using cyclobutanone is that the ß-hydrogens are sterically encumbered, as in Martìnez's compound, which eliminates the possibility of ß-hydride elimination. Solvents, ratios, and reaction times were examined; however, ^{19}F NMR suggested that in each attempt our product was degrading into triflic acid. After numerous failed attempts, our focus turned to the borate-based macrocycles.

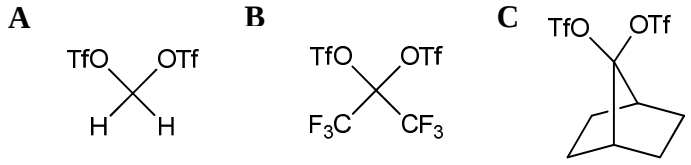

Figure 2.3. (A) Desmarteau's methyl ditriflate, (B) Sterlin's 2,2-ditriflato-perfluoro propane, and (C) Martinez's 7,7'-ditriflato-norbonane.

For the first borate-based 16-atom ringed macrocycle, we synthesized the diimidazole, 1,1'-methylene-bis(4,5-dimethylimidazole), in a manner similar to the synthesis of our previously synthesized phenyl variant.[9] For our key dielectrophile, we prepared iodoborane *in*

situ following the method of Smith.[8] The addition of **1** to iodoborane in acetonitrile resulted in the formation of ($^{BH_2,Me}TC^{Me}$)$(I)_2$ (**2**) in 33% yield (Scheme 2.2). Since Siebert was unable to synthesize a macrocycle with methyls off of the 4,5-position on the imidazoliums at the same time as methyls off of the borate due to sterics, for our second macrocycle we switched the position of the methyls to the borate and installed protons in the 4,5-positon. The second 16-atom ringed macrocycle that we synthesized involved the synthesis of the previous diimiazole from ($^{Me,Et}TC^{H}$)$(OTf)_4$.[9] In this instance, the key dielectrophile was the commercially available bromodimethylborane. The addition of bromodimethylborane to diimidazole **3** formed ($^{B(Me)_2,Me}TC^{H}$)$(Br)_2$ in a 75% yield. Unlike our previously prepared ligand precursors, such as ($^{Me,Et}TC^{Ph}$)$(OTf)_4$, **2** and **4** are only 16-atom macrocycles which are the same ring size as a porphyrin. Another direct contrast from our previously prepared ligand precursor is that **2** and **4** are dicationic in their imidazolium form, as opposed to tetracationic; hence they exhibit enhanced solubility in less polar solvents. When ligated to metals, they will become isoelectronic to porphyrins.

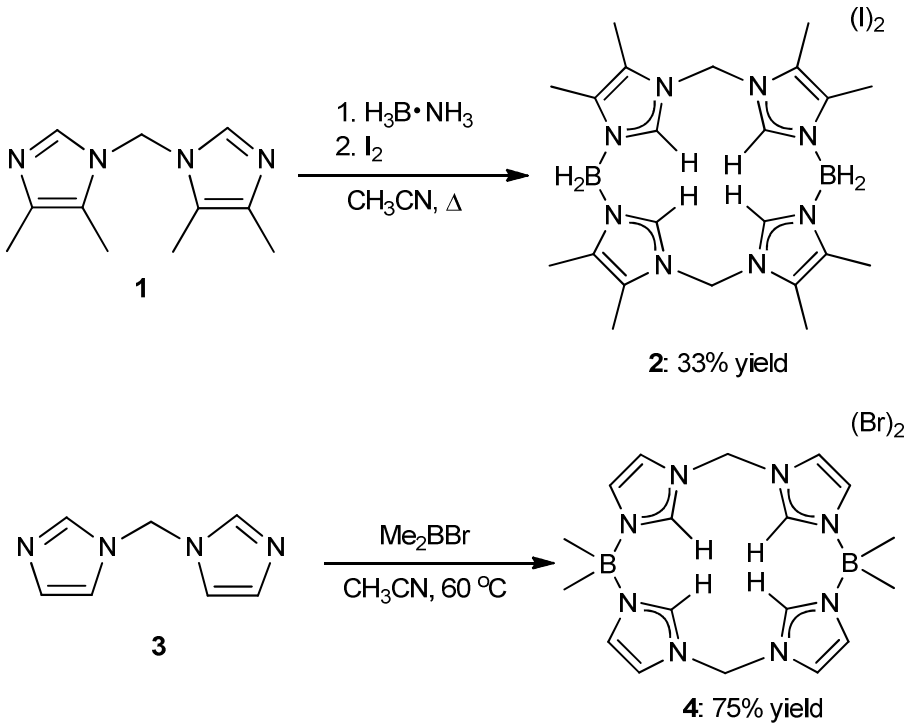

Scheme 2.2. Synthesis of ($^{BH_2,Me}TC^{Me}$)$(I)_2$ (**2**) and ($^{B(Me)_2,Me}TC^{H}$)$(Br)_2$ (**4**).

In order to confirm the formation of **2** and **4**, the peak splitting and isotopic ratios of **2** and **4** were examined by ESI/MS. The ESI/MS of **2** showed the correct peaks for $[(^{BH_2,Me}TC^{Me})]^{2+}$ and $[(^{BH_2,Me}TC^{Me})(I)]^{+}$ at 217.16 and 561.23 *m*/*z* (Figure 2.4), respectively, while the ESI/MS of **4** showed the correct peaks for $[(^{B(Me)_2,Me}TC^{H})]^{2+}$ and $[(^{B(Me)_2,Me}TC^{H})(Br)]^{+}$ at 189.13 and 457.18 *m*/*z*. Both spectra showed ½ mass unit splitting for the +2 peaks, as well as, 1 mass unit splitting for the +1 peaks along with the correct isotopic distribution. In some instances, however, **4** exhibited a +2 peak at 323.16 *m*/*z* of a hexameric species, which was confirmed by two sets of peaks in its ^{1}H NMR. Although we are unsure of which variables effect the hexameric formation, we were able to isolate the pure tetrameric species.

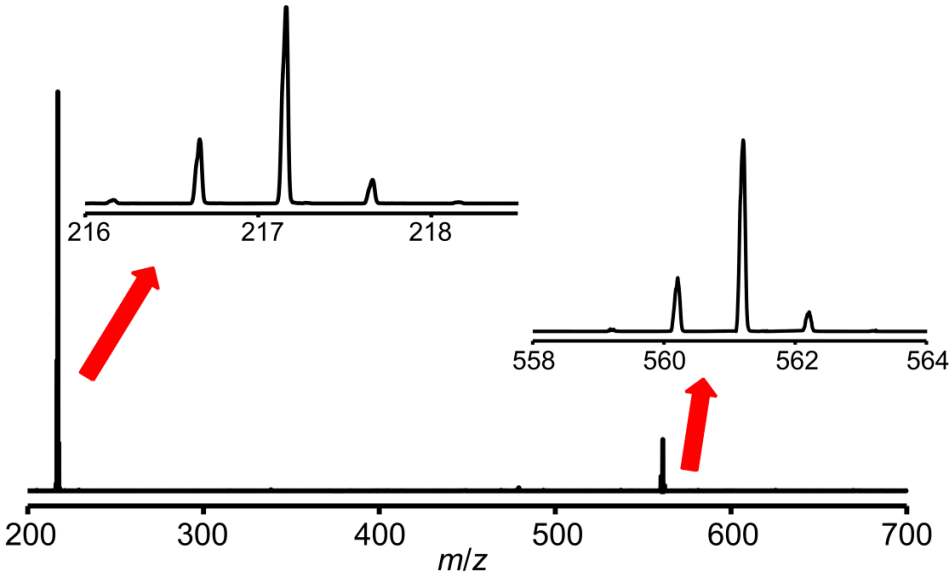

Figure 2.4. An example electrospray ionization mass spectrum measured for a DMSO/acetonitrile solution of **2**. The insets show highlights for $[(^{BH_2,Me}TC^{Me})]^{2+}$ and $[(^{BH_2,Me}TC^{Me})(I)]^{+}$ at 217.16 and 561.23 *m*/*z*, respectively.

Both macrocycles were characterized by multi-nuclear NMR which demonstrated the two-fold symmetry of **2** and **4** that is characteristic of isostructural ligand precursors previously prepared by our group.[9, 13, 14] The position of the ^{1}H resonance for the C2 imidazolium proton is particularly important in these macrocycles since it intimates its relative acidity[14] and, therefore, ease of deprotonation to form the free carbene. The peak positions for the C2 protons in DMSO-d_6 were found at 8.41 and 9.31 ppm for **2** and **4**, respectively. The average of these two values lies approximately in the same position of the C2 peak at 9.11 ppm for $(^{Me,Et}TC^{H})(I)_4$;[9] however, we see that **2** is slightly upfield and **4** is slightly downfield from our previous macrocycle $(^{Me,Et}TC^{H})(I)_4$. Since all three ligand precursors' NMR spectra were taken in DMSO-d_6 and contained similarly coordinating anions, it is likely the difference between the C2 proton values

arises primarily from the acidity of each, suggesting the C2 protons for **2** is slightly less acidic and for **4** is slightly more acidic than that of ($^{Me,Et}TC^{H}$)$(I)_4$. Siebert concluded that his macrocycles' inability to form carbene complexes was based, in part, on this low acidity of his C2 proton, whose resonance was found at 6.64 ppm in CD_2Cl_2 for his isostructural 16-atom ringed macrocycle ($^{BH_2,BH_2}TC^{Me}$) (Table 2.1).[8] In order to compare our ligand precursors to Siebert's, we collected the ^{1}H NMR spectrum of compound **2** in CD_2Cl_2. Notably, the C2 proton of **2** shifted slightly farther downfield to 9.14 ppm in CD_2Cl_2 versus 8.41 ppm in DMSO-d_6. A comprised list of the C2 values can be seen in Table 2.1. This difference in the peak position of the C2 proton of our ligand precursors (**2** and **4**) versus Siebert's macrocycle suggests our diborate macrocycles, **2** and **4**, are closer to their carbon bridged analogs, implying that it would be easier to deprotonate them to form the carbene *in situ*.

Table 2.1 ^{1}H NMR comparison of the relative C2 proton peaks of tetraimidazoliums **2** and **4** vs. our previous tetraimidazolium ($^{Me,Et}TC^{H}$)$(I)_4$ and Siebert's isostructural borate-based tetraimidazolium ($^{BH_2,BH_2}TC^{Me}$), which intimates relative acidity of the C2 proton.

Complex	**C2 peak position**
($^{BH_2,BH_2}TC^{Me}$)	6.64 (CD_2Cl_2)
($^{Me,Et}TC^{H}$)$(I)_4$	9.11 (DMSO-d_6)
($^{BH_2,Me}TC^{Me}$)$(I)_2$	9.14 (CD_2Cl_2) / 8.41 (DMSO-d_6)
($^{B(Me)_2,Me}TC^{H}$)$(Br)_2$	9.31 (DMSO-d_6)

As with our previous macrocycle, a crystal structure was necessary to verify the tetrameric species was formed as opposed to the dimeric species. Crystal structures of **2** and **4** were obtained via vapor diffusion of diethyl ether into dimethyl sulfoxide. In compounds **2** and **4** the imidazolium rings are nearly perpendicular to the plane of the macrocyclic ring which relieves repulsive strain between the C2 imidazolium hydrogens (Figure 2.5). Each imidazolium ring points in the opposite direction in regards to the ring next to it. This alternate twisting arrangement was described previously by Siebert on similar sized imidazolium-borate macrocycles.[8] The bond lengths and angles for **2** and **4** were comparable to one another except for the N-B-N bond angle, which was 107.1° for **2** and 103.3° for **4**. This difference arises due to the fact that the substituents off of the boron for **2** are protons, as opposed to bulkier methyls off of the boron on **4**.

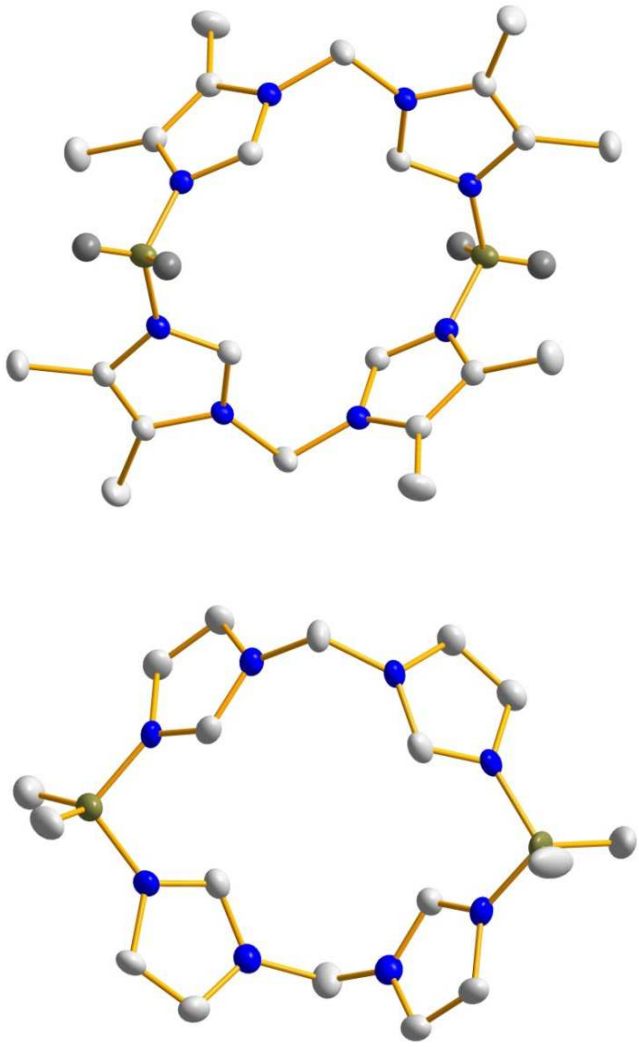

Figure 2.5. Crystal structures of ($^{BH_2,Me}TC^{Me}$)$(I)_2$ (**2**) (top) and ($^{B(Me)_2,Me}TC^{H}$)$(Br)_2$ (**4**) (bottom). Blue, gray, and olive ellipsoids (50% probability) represent N, C, and B, respectively. Counteranions and hydrogens have been omitted for clarity.

We pursued the synthesis of metal complexes using both a weak and strong base deprotonation strategy that we successfully employed to prepare [($^{Me,Et}TC^{H}$)Pt](OTf)$_2$ and [($^{Me,Et}TC^{Ph}$)Fe(NCCH$_3$)$_2$](PF$_6$)$_2$, respectively.[9,13] The use of a weak base, such as triethylamine, followed by the addition of a metal(II) halide resulted in the decomposition of both **2** and **4**, leading us to try the strong base approach. The macrocyclic tetraimidazolium borates were deprotonated with a strong base, such as *n*-butyllithium, followed by the addition of a metal(II) halide as seen in Scheme 2.3. For ($^{BH_2,Me}TC^{Me}$)(I)$_2$ (**2**), we were unsuccessful in obtaining any evidence of a stable metal complex despite trying a wide variety of bases, solvents, and temperatures; however, ESI/MS suggested that we were at least able to form highly unstable metal complexes on ($^{BH_2,Me}TC^{Me}$)(I)$_2$ with Pt, Pd, Ni, Fe, and Co. An example ESI/MS of [($^{BH_2,Me}TC^{Me}$)Pt–H]$^+$ is seen in Figure 2.6. What is unusual about this species is the fact that ($^{BH_2,Me}TC^{Me}$)Pt is a neutral compound and is seen as a +1 species in the ESI/MS. We suspect this anomaly of losing a proton arises from the fact that the B-H bond is highly unstable and is broken during ionization. Metal complexes supported by ($^{B(Me)_2,Me}TC^{H}$)(Br)$_2$ have not been investigated as thoroughly, hence the success of **4** as a ligand cannot be determined at this time.

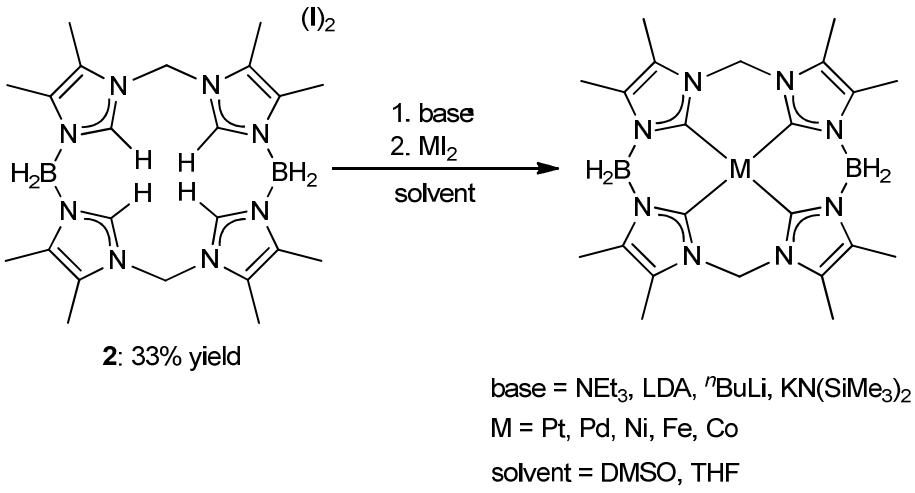

Scheme 2.3. Attempted reactions of **2** with various bases, metal (II) iodides, and solvents.

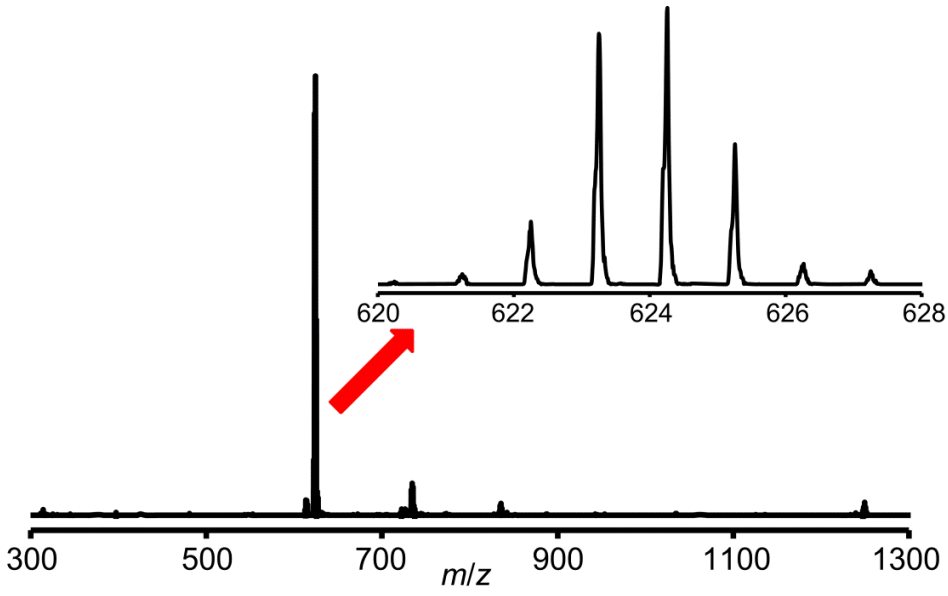

Figure 2.6. An example ESI/MS measured for a tetrahydrofuran solution of ($^{BH_2,Me}TC^{Me}$)Pt**.** The inset show highlight for the [($^{BH_2,Me}TC^{Me}$)Pt–H]$^+$ ion.

Conclusion

We synthesized two novel 16-atom ringed borate-based tetraimidazolium macrocycles. The borates decreased the overall charge of the macrocycles and allowed for increased solubility in nonpolar solvents when compared to our previous neutral variants. Although we were unable to synthesize stable metal complexes, ESI/MS suggests that we were able to deprotonate ($^{BH_2,Me}TC^{Me}$)$(I)_2$ (**2**) to form highly reactive metal complexes on Pt, Pd, Ni, Fe, and Co. The formation of metal complexes on ($^{B(Me)_2,Me}TC^{H}$)$(Br)_2$ (**4**) was not as thoroughly explored due to the concurrent formation of a suspected hexameric species in some instances although we were eventually able to exclusively isolate the tetrameric species. We suspect that metal complexes supported by ($^{B(Me)_2Me}TC^{H}$)$(Br)_2$ (**4**) might be less reactive than ($^{BH_2,Me}TC^{Me}$)$(I)_2$ (**2**) due to the presence of B-Me bonds as opposed to the substantially weaker and more reactive B-H bonds, which can potential be deprotonated with a base. If future results show **4** is capable of supporting metal complexes then we would have successfully synthesized an isostructural and isoelectronic structure to a porphyrin.

Experimental

Synthesis of 1,1'-methylene-bis(4,5-dimethyl-imidazole), 1. 4,5-dimethyl-imidazolium chloride (15.0 g, 0.114 mol) and potassium hydroxide (31.9 g, 0.568 mol) were added to a 1 L round bottom flask containing 500 mL of acetonitrile. This mixture was allowed to stir for 1 hour. Methylene chloride (48.2 g, 0.568 mol) was then added and stirred for an additional 2 days. The mixture was dried under reduced pressure to give a brownish, red solid. The solid was dissolved in 300 mL H_2O and the product was extracted with methylene chloride (3 x 125 mL). The organic layer was separated, dried with $MgSO_4$, and the solvent was removed under reduced pressure. Crystals were grown by dissolving the powder into methylene chloride and vapor diffusing in diethyl ether (3.97 g, 34.6% yield). Mp: 162-163 °C. ^{1}H NMR ($CDCl_3$, 300.08 MHz): δ 7.39 (s, 2H), 5.73 (s, 2H), 2.10 (d, *J* = 0.60 Hz, 6H), 2.08 (d, *J* = 0.60 Hz, 6H). ^{13}C NMR ($CDCl_3$, 75.46 MHz): δ 135.2, 134.8, 121.6, 53.6, 12.5, 8.4. IR (neat): 3095, 2918, 1597, 1492, 1451, 1421, 1386, 1355, 1275, 1224, 1184, 1012, 943, 841, 787, 771, 703, 674 cm^{-1}. DART/MS (*m*/*z*): $[M+H]^+$ 205.2. Anal. Calcd for $C_{11}H_{16}N_4$: C, 64.68; H, 7.89; N, 27.43. Found: C, 64.60; H, 7.84; N, 27.24.

Synthesis of ($^{BH_2,Me}TC^{Me}$)$(I)_2$, 2. Under an atmosphere of N_2, trimethylamine borane complex (0.271 g, 3.71 mmol) was dissolved in 25 mL of acetonitrile in a 50 mL round bottom flask. Over a 10 min period, iodine (0.471 g, 1.86 mmol) was gradually added to the solution. Once all of the iodine was in solution, the mixture stirred for 30 min. Following the 30 min, 1,1'-methylene-bis(4,5-dimethyl-imidazole) (0.750 g, 3.71 mmol) was added followed by 1 hr of stirring. After the hour elapsed, the round bottom was heated to reflux (90-94 °C) under N_2 for 5 days. The solution was dried under reduced pressure to give a faint yellow solid. The solid was washed with methylene chloride (3 x 20 mL) and filtered over a 30 mL fine sintered-glass frit.

The remaining solid was dried under reduced pressure giving the product as a white solid powder (0.414 g, 32.6% yield). Crystals were grown by dissolving the white powder into DMSO and vapor diffusing in diethyl ether. Dp: 260-262 °C. ^{1}H NMR (DMSO-d_6, 300.08 MHz): δ 8.41 (s, 4H), 6.41 (s, 4H), 3.25 (s, B-H, 4H), 2.30 (s, 12H), 2.16 (s, 12H). (CD_2Cl_2, 499.74 MHz): δ 9.13 (s, 4H), 6.46 (s, 4H), 3.38 (s, B-H, 4H), 2.33 (s, 12H), 2.25 (s, 12H). ^{13}C NMR (DMSO-d_6, 125.66 MHz): δ 137.3, 129.0, 125.8, 40.4, 9.3, 8.0. (CD_2Cl_2, 125.66 MHz): δ 136.6, 131.7, 126.2, 30.1, 10.4, 9.5. ^{11}B NMR (DMSO-d_6, 128.42 MHz): δ -10.8. IR (neat): 2960, 2444, 1620, 1542, 1433, 1356, 1240, 1184, 1156, 1046, 900, 809, 699 cm^{-1}. HR-ESI/MS (*m*/*z*): $[M\text{-}I]^+$ 561.2299, $[M\text{-}2I]^{2+}$ 217.1620 (found); $[M\text{-}I]^+$ 561.2296, $[M\text{-}2I]^{2+}$ 217.1623 (calcd).

Synthesis of ($^{B(Me)_2,Me}TC^{H}$)(Br)$_2$, 4. Under an atmosphere of N_2, 1,1'-methylene(bis-imidazole) (0.562 g, 3.79 mmol) was dissolved in approximately 50 mL of acetonitrile. The solution was place in the freezer for 30 minutes. Upon removal, bromodimethylborane (0.458 g, 3.79 mmol) was added to the solution immediately forming a white precipitate. The reaction stirred for one hour, allowing it to reach room temperature. It was then pumped out of the glovebox and placed on a reflux condenser under a steady flow of N_2. The slurry refluxed for three days. It was then filtered over a 60 mL fine sintered frit and washed with acetonitrile (2 X 20 mL) and diethyl ether (2 X 20 mL). The resulting white solid was dried under reduced pressure resulting in a pure product (0.765 g, 75.1% yield). ^{1}H NMR (DMSO-d_6, 300.08 MHz): δ 9.31 (s, 4H), 7.96 (s, 4H), 7.55 (s, 4H), 6.54 (s, 4H), 0.29 (s, 12 H). HR-ESI/MS(*m*/*z*): $[M\text{-}Br]^+$ 457.1863, $[M\text{-}2Br]^{2+}$ 189.1266 (found); $[M\text{-}Br]^+$ 457.1806, $[M\text{-}2Br]^{2+}$ 189.1312 (calcd).

References

(1) Tolman, W. B., Ed. *Activation of Small Molecules: Organometallic and Bioinorganic Perspectives*; Wiley-VCH: Weinheim, Germany, 2006.

(2) Fantauzzi, S.; Caselli, A.; Gallo, E. *Dalton Trans.* **2009**, 5434.

(3) Rose, E.; Andrioletti, B.; Zrig, S.; Quelquejeu-Ethève, M. *Chem. Soc. Rev.* **2005**, 34, 573.

(4) Che, C.; Huang, J. *Coord. Chem. Rev.* **2002**, 231, 151.

(5) Hahn, F. E.; Langenhahn, V.; Luegger, T.; Pape, T.; Le Van, D. *Angew. Chem., Int. Ed.* **2005**, *44*, 3759.

(6) (a) Weiss, A.; Pritzkow, H.; Siebert, W. *Angew. Chem., Int. Ed.* **2000**, *39*, 547. (b) Weiss, A.; Barba, V.; Pritzkow, H.; Siebert, W. *J. Organomet. Chem.* **2003**, *680*, 294.

(7) Fränkel, R.; Kniczek, J.; Ponikwar, W.; Nöth, H.; Polborn, K.; Fehlhammer, W. P. *Inorg. Chim. Acta* **2001**, *312*, 23.

(8) Nieto, I.; Bontchev, R. P.; Smith, J. M. *Eur. J. Inorg. Chem.* **2008**, 2476.

(9) Bass, H. M.; Cramer, S. A.; Price, J. L.; Jenkins, D. M. *Organometallics* **2010**, *29*, 3235.

(10) Katsuhara, Y.; Desmarteau, D. D. *J. of Fluorine Chem.* **1980**, 16, 257.

(11) Avetisyan, E. A.; Cherstkov, V. F.; Tumanskii, B. L.; Sterlin, S. R. *Russ. Chem. Bull.* **1998**, 47, 2429-2433.

(12) Martínez, A. G.; Ríos, I. E.; Vilar, E. T. *Synthesis* **1979**, 382-383.

(13) Cramer, S. A.; Jenkins, D. M. *J. Am. Chem. Soc.* **2011**, *133*, 19342.

(14) Lu, Z.; Cramer, S. A.; Jenkins, D. M. *Chem. Sci.* **2012**, *3*, 3081.

(15) Cremer, T.; Kolbeck, C.; Lovelock, K. R. J.; Paape, N.; Woelfel, R.; Schulz, P. S.; Wasserschied, P.; et al. *Chem. Eur. J.* **2010**, *16*, 9018.

Chapter 3

An 18-Atom Ringed, Dianionic Macrocycle

A version of this chapter was orginially published by Heather M. Bass, S. Alan Cramer, A. Scott McCullough, Karl J. Berstein, Chris R. Murdock, and David M. Jenkins:

Bass, H. M.; Cramer, S. A.; McCullough, A. S.; Bernstein, K. J.; Murdock, C. R.; Jenkins, D. M., "Employing Dianionic Macrocyclic Tetracarbenes To Synthesize Neutral Divalent Metal Complexes." *Organometallics* **2013,** *32*, 2160-2167.

Abstract

The 18-atom ringed, borate-based macrocyclic tetraimidazolium, ($^{B(Me)_2,Et}TC^{H}$)$(Br)_{2,}$ was formed in a two-step process with an 84% yield. By employing divalent metal salts, we were able to synthesize the neutral metal complexes ($^{B(Me)_2,Et}TC^{H}$)Pd and ($^{B(Me)_2,Et}TC^{H}$)Ni that were soluble in non-polar solvents, such as benzene and toluene. DFT calculations were performed on ($^{B(Me)_2,Et}TC^{H}$)Ni and the hypothetical [($^{Me,Et}TC^{H}$)Ni]$^{2+}$ to determine the electronic difference the addition of two borate moieties makes on ($^{B(Me)_2,Et}TC^{H}$)Ni. In addition, we formed trivalent metal complexes on manganese and iron, as well as, began initial investigations into forming stable complexes with metal-ligand multiple bonds on [($^{B(Me)_2,Et}TC^{H}$)Fe(THF)]PF_6.

Introduction

In myriad instances, the addition of a borate moiety to the backbone of tridentate ligands has led to fascinating reactivity that is distinct from that exhibited by complexes with isostructural ligands featuring carbon in the same position.[1] Addition of a borate decreases the overall charge of a metal complex, often allowing for increased solubility in nonpolar solvents. In addition to increasing solubility, a borate positioned near the metal center can subtly change the electronic structure of the complex.[2] This seemingly small tweak in electron donation

properties of the ligand can induce novel oxidation states and spin states at the metal center which leads to innovative reactivity.[3]

These phenomena have been documented extensively for tripodal ligands for both triphosphines and tricarbenes when comparing the neutral versus anionic versions.[4] In the case of the triphosphine ligands, the Peters group has shown that the tris(phosphino)borate ligand can support complexes that stabilize novel iron-nitrogen bonds that can then be functionalized.[5] For the tricarbenes, both the neutral and anionic versions have been found to support metal-ligand multiple bonds;[6] however, the anionic version has stabilized unprecedented oxidation states for iron nitrides that exhibited reactivity in instances where complexes with the neutral version of the tricarbene ligand did not.[7] Despite the importance of these tripodal ligands with a borate in the backbone, to date, there are no known tetracarbenes with borates in the macrocyclic ring.

Macrocyclic tetracarbene ligands are a class of strong σ-donor ligands that were first reported by Hahn via a templating synthesis on platinum in 2005.[8] Since his publication, macrocyclic tetraimidazoliums have now been employed to prepare a wide variety of transition metal tetracarbene complexes.[9] Many of these complexes have demonstrated important properties such as electron transfer reagents,[9b, 9d] aziridination catalysis,[9e, 10] and stabilization of non-heme iron oxos.[9g] Despite the growing importance of this class of macrocyclic N-heterocyclic carbene (NHC) ligands, no examples with borates in the macrocycle have been prepared. Nevertheless, previous syntheses suggest that it would be possible to prepare a macrocyclic tetraimidazolium with borates in the backbone that could be ligated to form tetracarbenes. Siebert and coworkers synthesized imidazolium borate macrocycles that contained either four or five imidazoliums per ring with an equal number of borates.[11] While they noted that they were unable to form carbenes with these complexes, perhaps because the borates

decrease the acidity of the C2 proton, they demonstrated that this type of cyclic structure is possible.[11] In contrast, Fehlhammer[12] and Smith[13] independently prepared bis-dicarbene borate complexes on group 10 metals. Their complexes only had one borate moiety per two carbenes. Previous research from our group proved that we could synthesize a 16-atom ringed tetraimidazolium with one borate per two imidazoliums; however, we were still unable to form metal complexes. We intend to meld these concepts, as well as, our previous 18-atom ringed macrocyclic tetracarbene complexes in order to make new 18-atom ringed macrocyclic tetracarbene borate complexes.

The expansion of the family of macrocyclic tetracarbenes to include examples with borates in the macrocycle would be advantageous for two reasons. First, metal complexes will have a reduced charge that will increase their solubility in nonpolar solvents. Improved solubility in non-coordinating solvents like toluene is particularly beneficial for catalytic reactions, such as the aforementioned aziridination.[9e] Second, the addition of borates should improve the electron donating ability of the carbenes to the metal, if the imidazolium can be successfully deprotonated. This electron donation comparison can be investigated through spectroscopic methods[14] as well as TD-DFT calculations.[15] The combined properties of increased electron donation and reduced charge on the complex may assist in stabilizing metal ions in high valent oxidation states in the same manner that Smith and Peters demonstrated with tripodal borate ligands.[5c, 5g, 5i, 7c-e, 16] Herein, we describe the first synthesis of an 18-atom ringed borate containing macrocyclic tetracarbene ligand and provide multiple examples of complexation on palladium, nickel, manganese, and iron. Unlike Siebert's macrocyclic rings, we were able to synthesize exclusively the tetraimidazolium as the sole product.[11] The ligand precursor and metal complexes were characterized by single crystal X-ray crystallography and spectroscopic

techniques. Finally, DFT and TD-DFT calculations were performed on structurally similar neutral and cationic nickel complexes to assist in comparing the electron donor strength of these novel tetracarbene ligands.

Synthesis and characterization of the macrocyclic ligand

Since we have demonstrated that the 18-atom ring size for a tetracarbene macrocycle is favorable for ligation to a wide variety of transition metals,[9f] and since we were unable to ligate our 16-atom ringed borate macrocycles, we were also interested in preparing a borate macrocycle of the same size as ($^{Me,Et}TC^{Ph}$)$(OTf)_4$. Since haloboranes are excellent dielectrophiles, we capitalized on this by using commercially available bromodimethylborane as the dielectrophile and previously reported 1,2-diimidazoleethane (**1**) as the diimidazole component.[17] Addition of bromodimethylborane to 1,2-diimidazoleethane in two portions followed by heating to 60 °C for 24 h yielded the macrocycle, ($^{B(Me)_2,Et}TC^{H}$)$(Br)_2$ (**2**), as a pure white powder in 84% yield (Scheme 3.1). Ligand precursor **2** can be prepared on over a 10 gram scale in high yield in only two steps, which makes this precursor to a tetracarbene ligand highly advantageous.

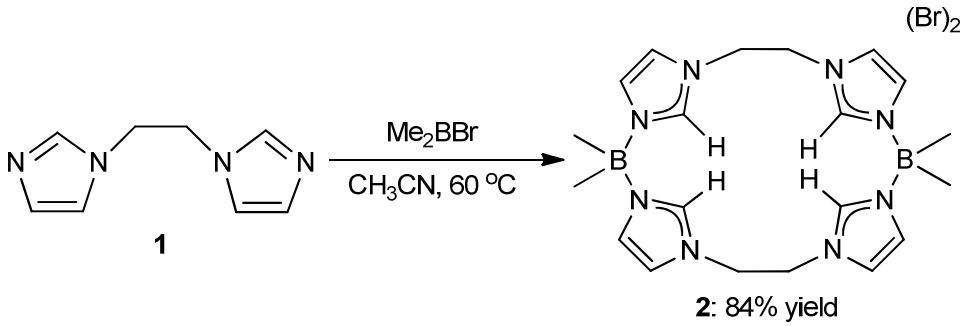

Scheme 3.1. Synthesis of ($^{B(Me)_2,Et}TC^{H}$)$(Br)_2$ (**2**).

The 18-atom ringed borate macrocycle was characterized by multi-nuclear NMR which demonstrated the two-fold symmetry of **2** that is characteristic of isostructural ligand precursors previously prepared by our group.[9c] As with our 16-atom ringed borate macrocycles, the position of the ^{1}H resonance for the C2 imidazolium proton is particularly important since this intimates its relative acidity[18] and, therefore, ease of deprotonation to form the free carbene. The peak position for the C2 proton in DMSO-d_6 was found at 8.71 ppm for **2**. This value is slightly upfield of the C2 peak position of 9.11 ppm for ($^{Me,Et}TC^{H}$)$(I)_4$ [9c] and lies between the peak position of ($^{BH_2,Me}TC^{Me}$)$(I)_2$ and ($^{B(Me)_2,Me}TC^{H}$)$(Br)_2$ at 8.41 ppm and 9.31 ppm, respectively. Since all of the ligands' NMRs were taken in DMSO-d_6 and contained similarly coordinating anions, it is likely the difference between the C2 proton values arises primarily from the acidity of each, suggesting the C2 proton of **2** is slightly less acidic that our previous neutral variant of ($^{Me,Et}TC^{H}$)$(I)_4$. Siebert concluded that his macrocycles' inability to form carbene complexes was based, in part, on this low acidity of his C2 proton, whose resonance was found at 6.64 ppm in CD_2Cl_2 for his ($^{BH_2,BH_2}TC^{Me}$) 16-atom ringed macrocycle.[11a] Since **2** was not sufficiently soluble in CD_2Cl_2 to obtain a ^{1}H NMR, we examined the trend of the C2 proton that we had seen with ($^{BH_2,Me}TC^{Me}$)$(I)_2$ in CD_2Cl_2. Notably, the C2 proton of ($^{BH_2,Me}TC^{Me}$)$(I)_2$ shifted slightly farther downfield to 9.14 ppm in CD_2Cl_2 versus 8.41 ppm in DMSO-d_6. Since the C2 peak of **2** is already farther downfield than the C2 peak of ($^{BH_2,Me}TC^{Me}$)$(I)_2$, it can be concluded that in CD_2Cl_2 **2** will be even farther than 9.14 ppm, hence **2** is more acidic than Siebert's macrocycle. This difference in the peak position of the C2 proton of our ligand precursor **2** versus Siebert's macrocycle suggests our diborate macrocycle, **2**, is closer to its carbon bridged analogs, implying that it would be easier to deprotonate **2** to form the carbene *in situ*.

In addition to spectroscopic studies, ($^{B(Me)_2,Et}TC^{H}$)$(Br)_2$ was characterized by single crystal X-ray diffraction. Suitable crystals for X-ray diffraction were obtained by vapor diffusion of diethyl ether into a methanol/water mixture for **2**. Unlike our 16-atom ringed counterparts, where each imidazolium ring points in the opposite direction in regards to the ring next to it, macrocycle **2** has all four imidazolium rings pointing out of the plane in the same direction (Figure 3.1). This orientation insinuates that the ring has less strain than its 16-atom ringed counterparts and thus is easier to orient the imidazoliums toward a single central metal center.

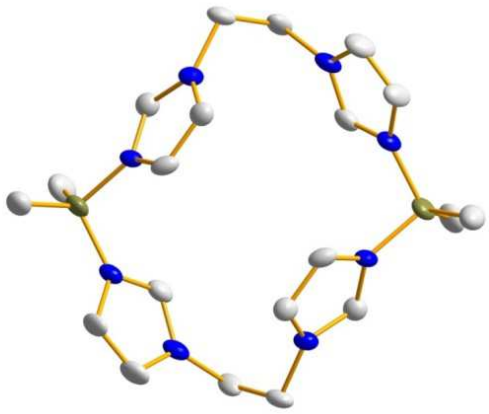

Figure 3.1. X-ray crystal structure of ($^{B(Me)_2,Et}TC^{H}$)$(Br)_2$, **2**. Blue, gray, and olive ellipsoids (50% probability) represent N, C, and B, respectively. Counteranions, solvent molecules, and hydrogens have been omitted for clarity.

Synthesis and characterization of the nickel and palladium complexes

We pursued the synthesis of metal complexes using a similar strong base deprotonation strategy that was successfully employed to prepare [($^{Me,Et}TC^{Ph}$)Fe(NCCH$_3$)$_2$](PF$_6$)$_2$.[9e] The macrocyclic tetraimidazolium borates were deprotonated with a strong base, such as *n*-butyllithium, followed by the addition of a metal(II) halide. Since group 10 metals tend to be more stable than other transition metals and readily form square planar complexes, our first attempts were synthesizing palladium and nickel complexes. We employed the 18-atom macrocycle, ($^{B(Me)_2,Et}TC^{H}$)(Br)$_2$ (**2**), *n*-butyllithium as the base, and nickel(II) or palladium(II) iodide to form ($^{B(Me)_2,Et}TC^{H}$)Pd (**3**) and ($^{B(Me)_2,Et}TC^{H}$)Ni (**4**) both in approximately 10% yield (Scheme 3.2). The low yield of these reactions is not surprising and was seen in our previous neutral systems before the synthesis of a silver transmetalling reagent.[9c, 9e] Compounds **3** and **4** are stable in air and are soluble in nonpolar solvents such as toluene.

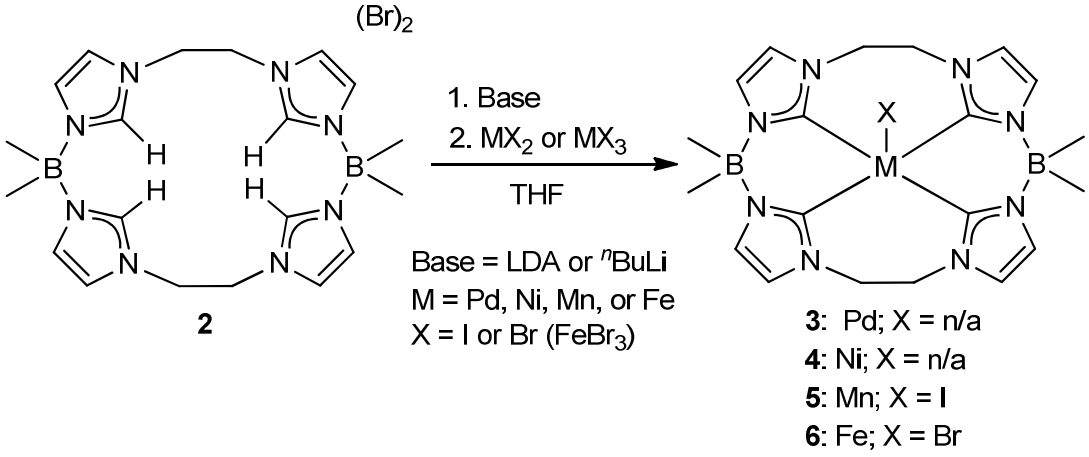

Scheme 3.2. Synthesis of metal complexes on **2** using a strong base deprotonation strategy.

Several rationales could explain the success of forming stable tetracarbene complexes with **2** and not our 16-atom ringed borate macrocycles. First, the boron moieties cannot be deprotonated in the presence of base when they have methyl substituents as in complex **2**; however, Siebert prepared a 16-atom macrocyclic ring with methyls attached to the boron and was still unable to synthesize tetracarbene complexes. [11b] In addition, we have not thoroughly investigated ($^{B(Me)_2,Me}TC^{H}$)$(Br)_2$ to make a conclusive assessment of its success at forming metal complexes. Third, the substituents on the 4,5-positions of the imidazolium are different for ($^{BH_2,Me}TC^{Me}$)$(I)_2$ (methyls) and **2** (protons). In regards to this difference between the 4,5-substituents, we have been able to prepare metal complexes with our neutral macrocyclic carbene ligands that have protons or phenyls in the 4,5-positions,[9c] so we believe that this effect is negligible. Fourth, the size of the pocket on the inside of the macrocycle may matter for ligation. The 18-atom ring size macrocycle has been demonstrated to fit a wide variety of transition metals,[9f] but to our knowledge, no one has prepared a macrocyclic tetracarbene from the imidazolium precursor with a 16-atom ringed example. Nevertheless, Hahn was successful in preparing a tetracarbene complex on platinum via a templating synthesis that does not appear to be significantly distorted from the expected idealized square plane.[8] Finally, the electronic differences between a methyl and ethyl linker between the imidazoliums cannot be ruled out as favoring stabilizing complexes for the larger ring ligand precursor **2**. While we can cannot rule out the size of the pocket of the macrocycle as a factor, we believe that the increased electron donation from having longer carbon chains between the imidazolium rings combined with the inability to deprotonate the borate moieties are the primary reasons that **2** more easily forms complexes than our 16-atom ringed variants in the presence of strong bases.

Both the palladium (**3**) and nickel (**4**) complexes are square planar complexes and were characterized by HR-DART/MS, multi-nuclear NMR, and single crystal X-ray crystallography. Unlike their cationic counterparts, [(^{Me,Et}TC^{Ph})Pd](OTf)$_2$ and [(^{Me,Et}TC^{Ph})Ni](OTf)$_2$,[9f] compounds **3** and **4** are not charged and an adducted hydrogen gave the expected cationic product of $[M+H]^+$ in a HR-DART/MS with values of 509.1736 *m*/*z* for **3** and 461.2053 *m*/*z* for **4** in acetonitrile solutions. In both spectra, a second set of peaks at 491.1489 *m*/*z* for **3** and 445.1743 *m*/*z* for **4** were seen, which equated to the loss of a methyl group from one of the borate moieties. The loss of this methyl group causes the boron moiety to become neutral, leaving the overall charge of the complex as +1 as seen in the DART/MS. This fragmentation occurs upon ionization.

Diastereotopic splitting in both the ^{1}H and ^{13}C NMR demonstrates that the macrocyclic rings for both the nickel and palladium complexes are rigid in solution at room temperature. The methyl carbons that are bound to the boron atom are diastereotopic and show distinct resonances in the ^{13}C NMR. The protons on the ethylene moiety are diastereotopic as well and have discrete resonances in the ^{1}H NMR. This rigidity in solution had been seen on all of the other square planar complexes that we have prepared with 18-atom tetracarbene macrocyclic ligands.[9c, 9f] The two boron atoms of **3** and **4** are equivalent by ^{11}B NMR spectroscopy and the resonances were found at -2.0 ppm for **3** and -0.6 ppm for **4**.

One experimental method which can measure the σ-donor strength of NHCs is the relative ^{13}C NMR resonance of the carbene carbon.[14b, 14c] Generally, the more downfield the shift for similar complexes, the stronger the σ-donor strength of the NHC.[14b, 14c] A comparison of these resonances for the isostructural nickel complexes, [(^{Me,Et}TC^{Ph})Ni](OTf)$_2$ and ($^{B(Me)_2,Et}$TC^{H})Ni (**4)**, shows that their peak positions in CD_3CN are at 170.7 and 174.7 ppm, respectively (Table 3.1).[9f] A similar trend was noted for the palladium complexes, although the

difference between the cationic and neutral complexes is smaller, 168.1 ppm for [($^{Me,Et}TC^{Ph}$)Pd](OTf)$_2$ and 171.3 ppm for ($^{B(Me)_2,Et}TC^{H}$)Pd (**3**) both in CD_3CN (Table 3.1).[9f] Similar results are demonstrated when comparing homoleptic divalent Pt complexes with two dicarbene ligands. Strassner's[19] cationic complex has a carbene resonance in the ^{13}C NMR at 162.7 ppm while Fehlhammer's[20] neutral borate complex has a carbene resonance at 168.8 ppm. Even though counteranions can have a slight effect on this position, the effect is small relative to difference in the resonances in these complexes.[12, 20] These results suggest that **2** may be a slightly stronger σ-donor compared to the cationic varieties, such ($^{Me,Et}TC^{Ph}$)(OTf)$_4$ and ($^{Me,Et}TC^{H}$)(OTf)$_4$, that we have previously synthesized.

Table 3.1. Comparison of relative carbene peak postions as a measure of σ-donor strength.

Metal complex	**Carbene peak position (ppm)**
[($^{Me,Et}TC^{Ph}$)Ni](OTf)$_2$	170.7 (CD_3CN)
($^{B(Me)_2,Et}TC^{H}$)Ni	174.7 (CD_3CN)
[($^{Me,Et}TC^{Ph}$)Pd](OTf)$_2$	168.1 (CD_3CN)
($^{B(Me)_2,Et}TC^{H}$)Pd	171.3 (CD_3CN)

Both metal complexes **3** and **4** were crystallized by vapor diffusion of pentane into a concentrated benzene solution. A side view of the crystal structures show the ligand puckering due to the borate and the ethylene linkers, which are above and below the carbene-metal plane (Figure 3.2). The ethylene linkers are staggered to relieve any steric strain between the two

groups. By measuring the distance of the metal within the carbene plane, we see that both ($^{B(Me)_2,Et}TC^{H}$)Pd and ($^{B(Me)_2,Et}TC^{H}$)Ni are almost exactly in the plane with an out-of-plane distance of 0.00 Å and 0.03 Å, respectively. Complexes **3** and **4** are isostructural to complexes that we have previously prepared with neutral macrocyclic tetracarbene ligands. ($^{B(Me)_2,Et}TC^{H}$)Pd has slightly longer Pd-C bonds (0.02 Å) compared to isostructural [($^{Me,Et}TC^{Ph}$)Pd](OTf)$_2$,[9f] but nearly identical bond lengths when compared to a macrocyclic tetracarbene complex that has a larger 24-atom macrocyclic ring, [($^{Pr,Pr}TC^{H}$)Pd](I)$_2$.[9a] In a similar manner, the *trans* C-Pd-C' bond angles for **3** are 174.4(1)° and 174.8(1)° which is slightly more distorted from a perfect square plane than the other two macrocyclic tetracarbene palladium complexes.[9a, 9f] In agreement with the results of **3**, ($^{B(Me)_2,Et}TC^{H}$)Ni has longer bond lengths than the isostructural cationic complexes, such as [($^{Me,Et}TC^{Ph}$)Ni](OTf)$_2$ and [($^{Pr,Pr}TC^{H}$)Ni](I)$_2$.[9d, 9f] Notably, the C-Ni bond lengths of **4** are considerably shorter than the C-Ni bond lengths of Smith's bis-di(carbene)borate nickel complex, whose elongated bonds are due to the complex's opposing *tert*-butyl groups that create significant steric repulsion between each bidentate ligand.[13] A compiled list of these bond lengths and angles can be seen in Table 3.2.

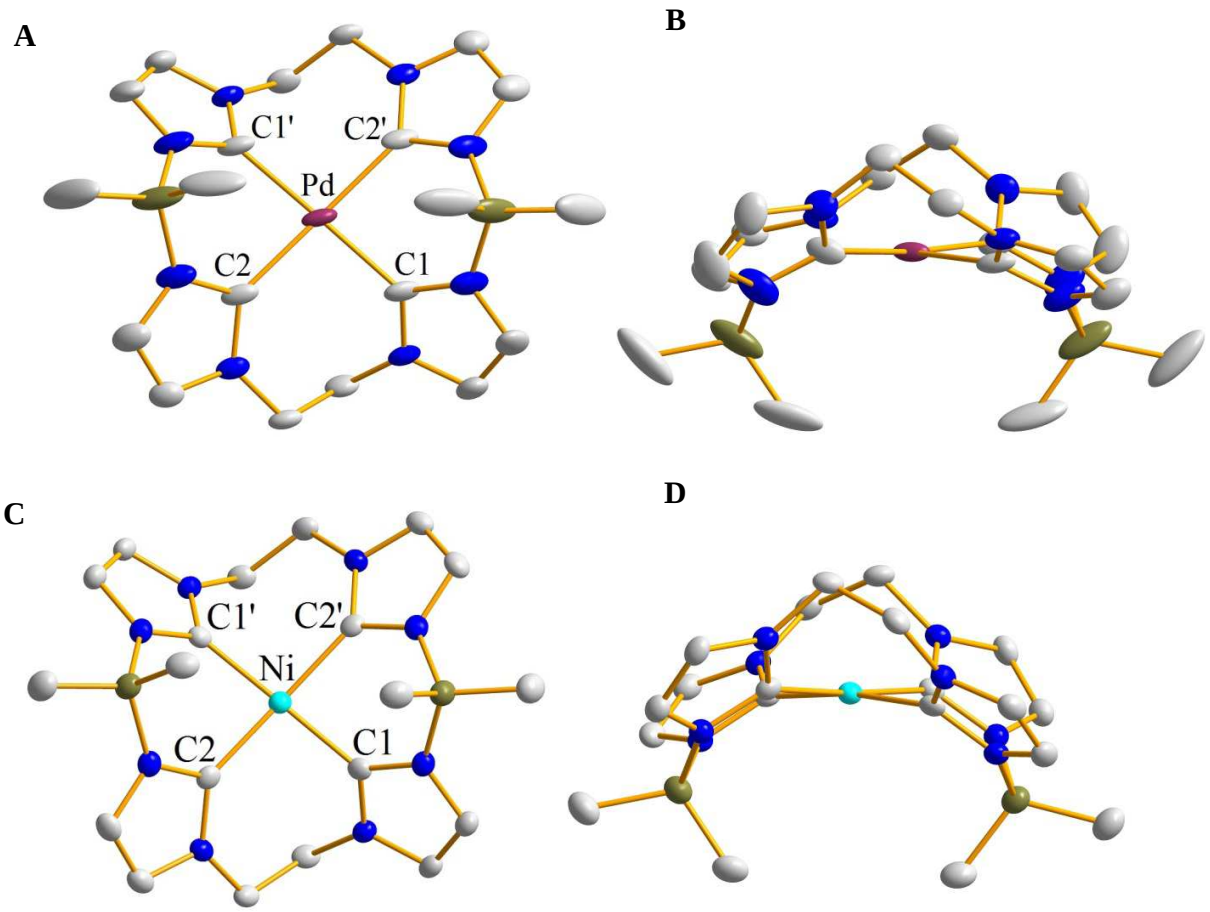

Figure 3.2. Crystal structures of (A) **3** top-down view, (B) **3** side-on view, (C) **4** top-down view, and (D) **4** side-on view. Plum, teal, blue, gray, and olive ellipsoids (50% probability) represent Pd, Ni, N, C, and B respectively. Hydrogens have been omitted for clarity.

Table 3.2. Selected bond lengths (Å) and angles (°) for ($^{B(Me)_2,Et}TC^{H}$)Pd, (**3**) (top) and ($^{B(Me)_2,Et}TC^{H}$)Ni, (**4**) (bottom).

M-C/ C-M-C	**Bond Length (Å)/ Bond Angle (°)**
Pd-C1	2.015(2) Å
Pd-C2	2.057(2) Å
C1-Pd-C1’	174.40(13)°
C2-Pd-C2’	174.82(12)°
C1-Pd-C2	94.31(9)°
C2-Pd-C1’	85.95(9)°

M-C/ C-M-C	**Bond Length (Å)/ Bond Angle (°)**
Ni-C1	1.928(3) Å
Ni-C2	1.892(3) Å
C1-Ni-C1’	171.97(19)°
C2-Ni-C2’	175.8(2)°
C1-Ni-C2	86.56(14)°
C2-Ni-C1’	93.73(14)°

DFT calculations for nickel complexes

In order to gain a better understanding of the effects of installing two borate moieties in the macrocycle, we performed DFT calculations on our nickel complexes and evaluated the corresponding d-orbital splitting. We chose the nickel complexes specifically to compare them to the already published DFT results of the structurally similar compounds, ($^{Pr,Pr}TC^{H}$)Ni and [($^{Pr,Pr}TC^{H}$)Ni]$^{2+}$, prepared by Murphy.[9d] The former compound facilitates fascinating reduction reactions due to its unusual ligand-based radical.[9d] Our DFT calculations were performed with NWChem using functional B3LYP and basis set 6-31g**. Single point electronic structure calculations were performed on ($^{B(Me)_2,Et}TC^{H}$)Ni and [($^{Me,Et}TC^{Ph}$)Ni]$^{2+}$ using the experimentally determined X-ray coordinates and a singlet ground state. Each structure was allowed to relax to a global minimum without the use of geometric constraints. Time-dependent DFT (TD-DFT) energy calculations were performed on the optimized ground state DFT geometries also using functional B3LYP and basis set 6-31g**.

An energy minimization for ($^{B(Me)_2,Et}TC^{H}$)Ni (**4**) shows no appreciable change in the Ni-C bond distances versus the experimental structure and only a small change in the C-Ni-C bond angles as seen in Table 3.3. The calculated orbital splitting diagram for **4** shows that the LUMO is centered primarily on the p_z orbitals on the carbene carbons and their adjacent nitrogens (Figure 3.3A). The LUMO p_z orbital of **4** is consistent with the calculated LUMO for [($^{Pr,Pr}TC^{H}$)Ni]$^{2+}$.[9d] However, the HOMO orbital for **4** is a d_z^2 orbital (Figure 3.3B) and not a ligand based orbital as was observed on [($^{Pr,Pr}TC^{H}$)Ni]$^{2+}$.[9d] The other orbitals with energies that are near the HOMO and LUMO orbitals are consistent with typical square planar d^8 complexes.

Table 3.3. Experimentally obtained data compared to DFT calculations using NWChem using functional B3LYP and basis set 6.31g**.

	Experimental		**Calculated**	**Calculated**
Complex	**($^{B(Me)_2,Et}TC^{H}$)Ni**	**Complex**	**($^{B(Me)_2,Et}TC^{H}$)Ni**	**[($^{Me,Et}TC^{H}$)Ni]$^{2+}$**
Ni-C1 (Å)	1.927(3)	Ni-C1 (Å)	1.9304	1.9296
Ni-C2 (Å)	1.891(3)	Ni-C2 (Å)	1.8926	1.8853
C1-Ni-C2 (°)	93.8(1)	Ni-C3 (Å)	1.9304	1.9298
C1-Ni-C2’ (°)	86.5(1)	Ni-C4 (Å)	1.8926	1.8854
C1-Ni-C1’ (°)	172.0(2)	C1-Ni-C2 (°)	93.311	87.684
C2-Ni-C2’(°)	175.8(2)	C2-Ni-C3 (°)	87.237	92.519
		C3-Ni-C4 (°)	93.311	87.677
		C1-Ni-C4 (°)	87.237	92.536
		C1-Ni-C3 (°)	167.409	168.369
		C2-Ni-C4 (°)	175.006	177.948

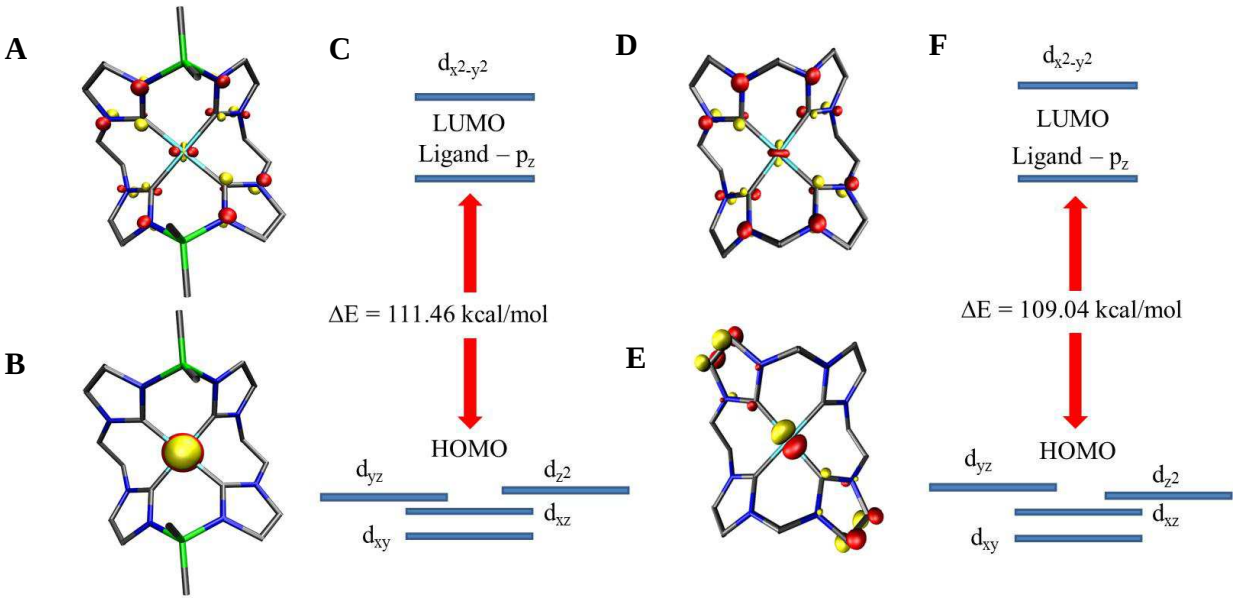

Figure 3.3. (A) LUMO of ($^{B(Me)_2,Et}TC^H$)Ni. (B) HOMO of ($^{B(Me)_2,Et}TC^H$)Ni. (C) Orbital splitting diagram of ($^{B(Me)_2,Et}TC^H$)Ni obtained from TD-DFT calculations. (D) LUMO of [($^{Me,Et}TC^H$)Ni]$^{2+}$. (E) HOMO of [($^{Me,Et}TC^H$)Ni]$^{2+}$. (F) Orbital splitting diagram of [$^{Me,Et}TC^H$)Ni]$^{2+}$ obtained from TD-DFT calculations. All calculations used NWChem/B3LYP/6-31g**.

To help determine if the change in the HOMO orbital is due to the boron atoms being part of the macrocycle, we performed the same calculation on previously described [($^{Me,Et}TC^{Ph}$)Ni]$^{2+}$.[9f] In a similar manner to **4**, there is almost no change in the metal ligand bond lengths, but a slightly more appreciable flexing which causes one of the *trans* C-Ni-C bond angles to contract. Notably, the LUMO is the same ligand based p_z orbital that we observed for **4** and a similar d-orbital splitting pattern was found for [($^{Me,Et}TC^{Ph}$)Ni]$^{2+}$. However, a direct comparison was problematic since several ligand based orbitals were interspersed between the LUMO and the highest occupied d-orbital. All of these orbitals have electron density primarily on the phenyl rings of the macrocyclic ligand.

To simplify the interpretation of the DFT results, an additional calculation was performed on the hypothetical complex [($^{Me,Et}TC^{H}$)Ni]$^{2+}$. The phenyl rings on the 4 and 5 positions of each carbene ring for [($^{Me,Et}TC^{Ph}$)Ni]$^{2+}$ were removed and replaced by hydrogen atoms and then the calculation was performed as described previously. In the same manner as **4**, the LUMO remains a p_z-ligand based orbital (Figure 3.3D), but for [($^{Me,Et}TC^{H}$)Ni]$^{2+}$ the HOMO is now a d_{yz} orbital (Figure 3.3E). This change in HOMO orbital is likely due to the near degeneracy of the d_z^2, d_{yz}, and d_{xz} orbitals. The simplified structure of [($^{Me,Et}TC^{H}$)Ni]$^{2+}$ allows for a closer comparison of the HOMO-LUMO gap between the cationic and neutral complexes. The HOMO-LUMO gap for [($^{Me,Et}TC^{H}$)Ni]$^{2+}$ is 109.04 kcal/mol (Figure 3.3F) which is slightly smaller than the calculated value of 111.46 kcal/mol for ($^{B(Me)_2,Et}TC^{H}$)Ni (Figure 3.3C).

We can draw two conclusions from the DFT calculations. First, the tetracarbene borate macrocycles appear to have comparable σ-donor strength as their neutral counterparts. This conjecture is supported by the experimental evidence of the ^{13}C NMR which shows that the carbene resonance is only slightly shifted by the addition of borates to the macrocycle. Both the

experimental and theoretical observations suggest that the borate containing macrocycles may be slightly more electron donating with regards to their nickel complexes. Second, the calculations suggest that it is the size of the macrocyclic ring and the accompanying change in torsion angle of the NHC rings in relation to the metal-ligand plane (formed by four carbons and the nickel) that affect the energies of the ligand-based HOMO orbital and not the presence of boron atoms in the macrocyclic ring.

Synthesis and Characterization of Manganese and Iron Complexes

We were interested in exploring other first-row transition metals due to the fact that they have been found to form highly reactive metal-ligand multiple, particularly iron species.[21] Our first focus was on synthesizing a macrocyclic manganese tetracarbene complex due to the fact that only one tetracarbene on manganese has been synthesized to date and it was a bis-bidentate carbene as opposed to a macrocyclic tetracarbene.[22] ($^{B(Me)_2,Et}TC^{H}$)MnI (**5**) was synthesized by *in situ* deprotonation of ($^{B(Me)_2,Et}TC^{H}$)$(Br)_2$ with lithium diisopropylamide followed by the addition of MnI_2 (Scheme 3.2). The manganese underwent a redox reaction forming a Mn(III) metal complex with a bound iodide, creating a five coordinate complex. Since manganese oxidized to the +3 state, we decided to use an iron(III) starting material to make ($^{B(Me)_2,Et}TC^{H}$)FeBr. For the synthesis of this complex, *n*-butyllithium was used as the strong base to deprotonate ($^{B(Me)_2,Et}TC^{H}$)$(Br)_2$ followed by the addition of $FeBr_3$ (**6**) (Scheme 3.2). Again a five coordinate species with a bound bromide was formed.

Crystal structures for **5** and **6** were obtained in an identical method to **3** and **4** via vapor diffusion of pentane into a concentrated benzene solution. As in the aforementioned cases, a side view shows a puckering of the linkers (Figure 3.4). This puckering and the corresponding

location of the methyls off of the borate, block the underside of the metal, which is beneficial in blocking a backside attack and in leaving one position open for catalytic reactivity. Unlike the previous square planar complexes (**3** and **4**), the geometry of **5** and **6** lies between square pyramidal and trigonal bipyramidal with C-M-X angles at 104.17(9)° and 95.38(8)° (center of symmetry) for **5** and 110.25(18)°, 110.28(19)°, 93.93(18)°, and 92.51(19)° for **6** (Table 3.5). The ethylene bridges are now eclipsed, as opposed to staggered, and the halide is pointed away from the upper carbons of the ethyl-bridge. The addition of a halide in the apical position leads to the metal centers being further out of the plane at 0.35 Å and 0.41 Å for ($^{B(Me)_2,Et}TC^{H}$)MnI and ($^{B(Me)_2,Et}TC^{H}$)FeBr, respectively, which can be seen in Figure 3.4.

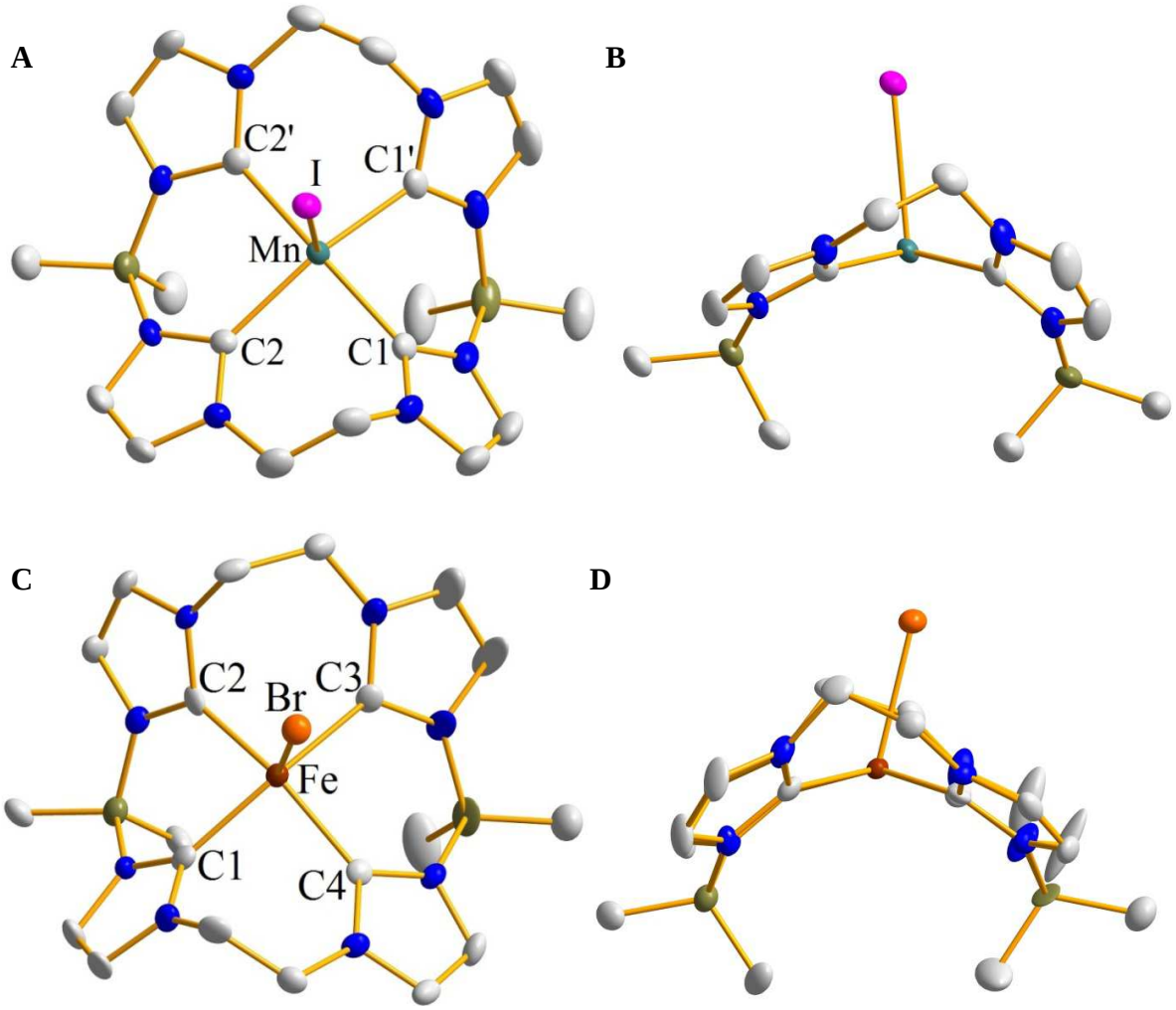

Figure 3.4. Crystal structures of (A) **5** top-down view, (B) **5** side-on view, (C) **6** top-down view, and (D) **6** side-on view. Aqua, brick red, fuchsia, orange, blue, gray, and olive ellipsoids (50% probability) represent Mn, Fe, I, Br, N, C, and B respectively. Hydrogens have been omitted for clarity.

Table 3.4. Selected bond lengths (Å) and angles (°) for ($^{B(Me)_2,Et}TC^{H}$)MnI, (**5**) (left) and ($^{B(Me)_2,Et}TC^{H}$)FeBr, (**6**) (right).

M-X/ X-M-X	**Bond Length (Å)/ Bond Angle (°)**	**M-X/ X-M-X**	**Bond Length (Å)/ Bond Angle (°)**
Mn-I	2.9051(8) Å	Fe-Br	2.5261(12) Å
Mn-C1	2.070(3) Å	Fe-C1	2.044(6) Å
Mn-C2	2.108(3) Å	Fe-C2	2.041(6) Å
C1-Mn-C2’	160.19(12)°	C1-Fe-C2	90.9(3)°
C1-Mn-C2	89.06(12)°	C1-Fe-C3	155.8(2)°
C1-Mn-C1’	83.15(18)°	C2-Fe-C3	88.3(2)°
C2-Mn-C2’	92.33(17)°	C2-Fe-C4	157.2(3)°
I-Mn-C1	104.17(9)°	Br-Fe-C1	110.25(18)°
I-Mn-C2	95.38(8)°	Br-Fe-C2	110.30(19)°
		Br-Fe-C3	93.93(18)°
		Br-Fe-C4	92.49(18)°

As previously stated, late transition metals with metal-ligand multiple bonds are quite reactive species and have been postulated as intermediates in biological systems.[21] These systems include, but are not limited to high-valent iron-oxo and iron-nitrido species for dioxygen activation[23] and dinitrogen activation,[23c, 24] respectively. Our primary focus was synthesizing some of these reactive intermediates using ($^{B(Me)_2,Et}TC^{H}$)FeBr, as well as, exploring the catalytic properties of ($^{B(Me)_2,Et}TC^{H}$)FeBr. Our first attempt was to synthesize an Fe(V) nitride starting from our Fe(III) precursor. Typically, iron-nitrides are stable in lower oxidation states; however, there are a few examples of highly reactive Fe(V)-nitridos[21, 25] and one example of an Fe(VI)-nitrido compound.[21, 25b, 26] Since the formation of a metal azido species is one of the most common routes for preparing a nitride species,[25b] the first step was to convert our ($^{B(Me)_2,Et}TC^{H}$)FeBr (**6**) to ($^{B(Me)_2,Et}TC^{H}$)FeN_3 (**7**). Sodium azide was added to ($^{B(Me)_2,Et}TC^{H}$)FeBr and heated to 60 ˚C overnight resulting in ($^{B(Me)_2,Et}TC^{H}$)FeN_3 (Scheme 3.3). Confirmation of this species was determined by X-ray crystallography, as well as, FTIR. Overlaying the IRs of ($^{B(Me)_2,Et}TC^{H}$)FeBr (**6**) and ($^{B(Me)_2,Et}TC^{H}$)FeN_3 (**7**), we noted growth of the large azide stretch at approximately 2040 cm^{-1}. The crystal structure of ($^{B(Me)_2,Et}TC^{H}$)FeN_3 is seen in Figure 3.4. Following the methodologies of Smith,[25] we then irradiated ($^{B(Me)_2,Et}TC^{H}$)FeN_3 with a mercury lamp leading to the formation of an iron(III)-iron(IV) (**8**) bridging nitride, as opposed to a monomeric Fe(V) nitride (Scheme 3.3). Formation of a dimeric complex is attributed to the inherent instability of a high valent iron nitride, as well as, the fact that ($^{B(Me)_2,Et}TC^{H}$)Fe does not have bulky groups surrounding the apical position to prevent dimerization. Similar Fe(III)-Fe(IV) bridging nitrides have been documented in several μ-nitriobis[tetraphenylporphyrinatioiron)] complexes,[27] with Fe-N bond lengths of approximately

1.66 Å [27b, 27f] compared to our Fe-N bond length of 1.80 Å. A crystal structure of **8** was obtained via layering of THF with pentane and is shown in Figure 3.5.

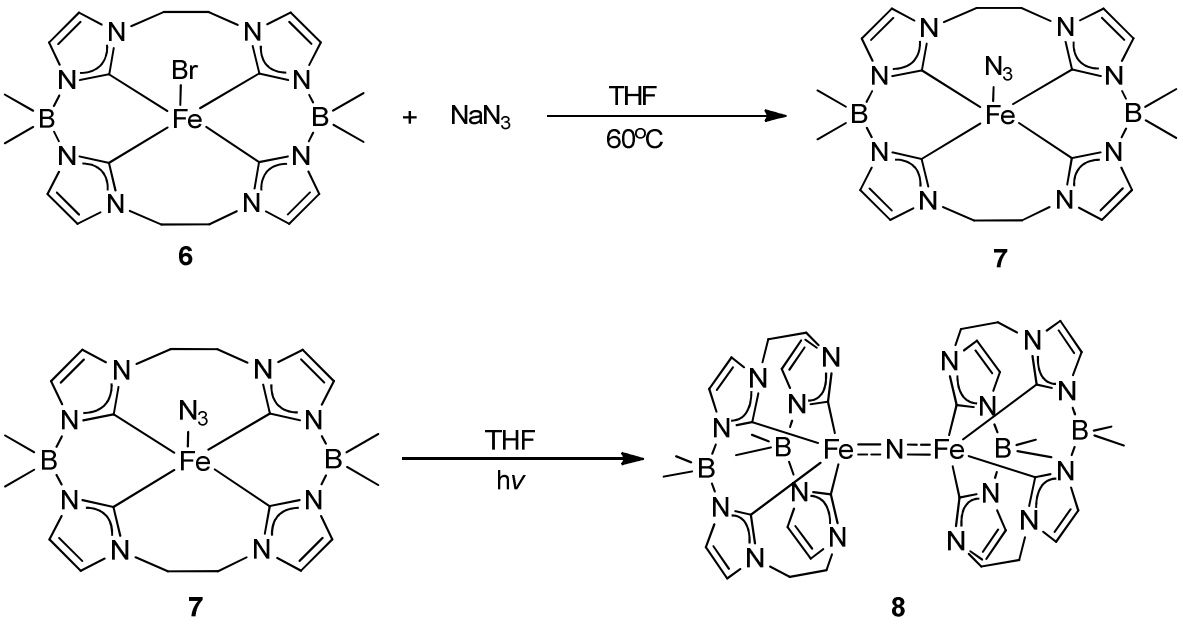

Scheme 3.3. Two-step synthesis for the formation of [($^{B(Me)_2,Et}TC^{H}$)Fe]$_2$N (**8**).

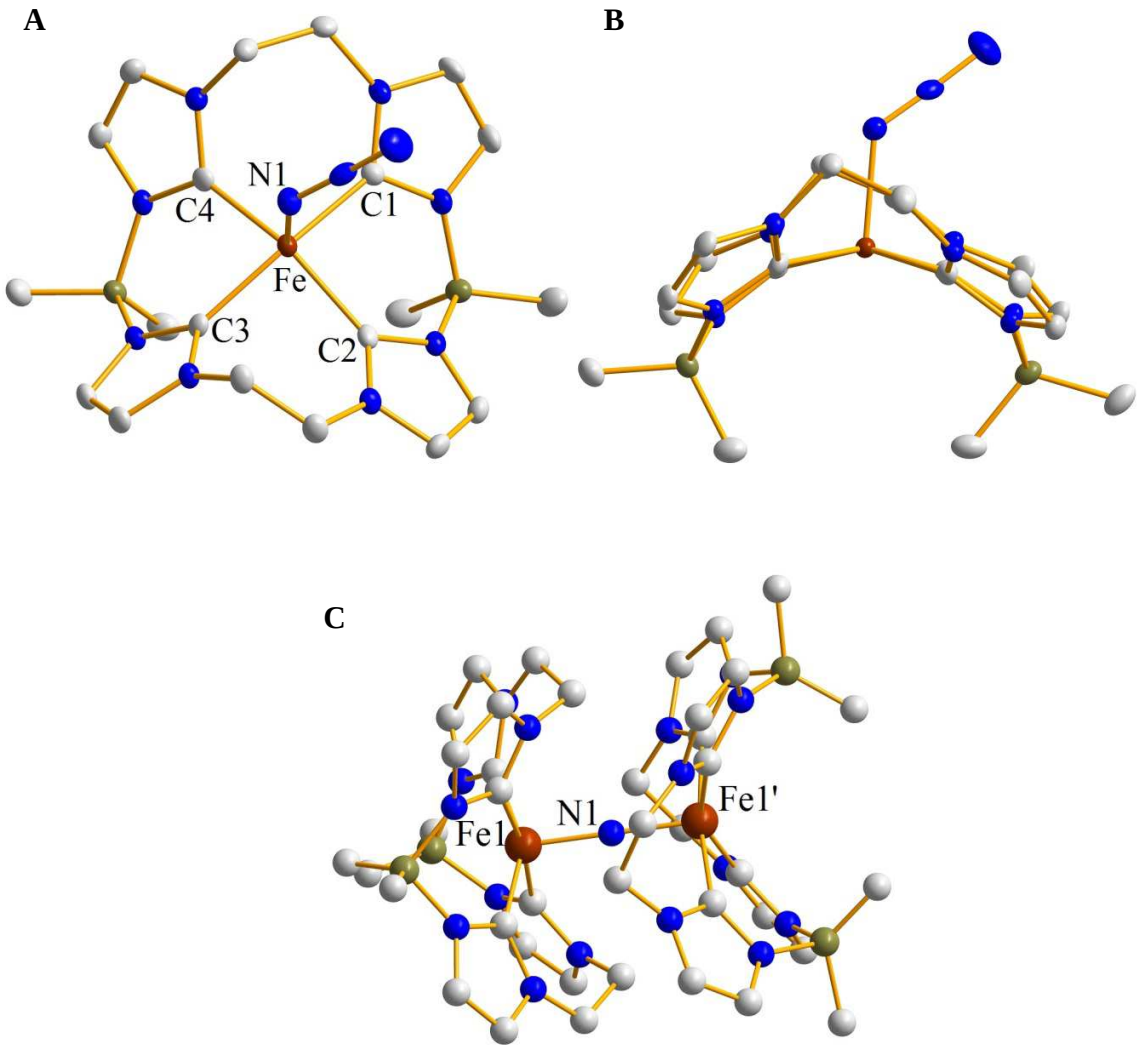

Figure 3.5. Crystal structure of ($^{B(Me)_2,Et}TC^{H}$)FeN_3 (**7**) from (A) a top-down and (B) a side-on view and (C) [($^{B(Me)_2,Et}TC^{H}$)Fe]$_2$N (**8**). Brick red, blue, gray, and olive ellipsoids (50% probability) represent Fe, N, C, and B respectively. Hydrogen atoms and counteranions have been omitted for clarity.

Table 3.5. Selected bond lengths (Å) and angles (°) for ($^{B(Me)_2,Et}TC^{H}$)FeN_3, (**7**) (top) and [($^{B(Me)_2,Et}TC^{H}$)Fe]$_2$N, (**8**) (bottom).

M-X/ X-M-X	**Bond Length (Å)/ Bond Angle (°)**
Fe-C1	2.040(2) Å
Fe-C2	2.046(2) Å
Fe-N1	2.0150(18) Å
C1-Fe-C2	90.93(8)°
C1-Fe-C3	160.18(8)°
C2-Fe-C3	89.18(9)°
C2-Fe-C4	157.13(9)°

M-X/ X-M-X	**Bond Length (Å)/ Bond Angle (°)**
Fe1-N	1.8029(2) Å
N-Fe2	1.8029(2) Å
Fe1-N-Fe2	180.0°
C1-Fe1-C3	151.63(2)°
C2-Fe1-C4	171.28(3)°

Since our group's previous system [($^{Me,Et}TC^{Ph}$)Fe($NCCH_3$)$_2$](PF_6)$_2$ was an effective catalyst for aziridination reactions,[9e] we decided to pursue the effectiveness of ($^{B(Me)_2,Et}TC^{H}$)FeBr as a catalyst. Since having a bound anion may inhibit the reactivity of a catalyst, it was necessary to remove the halide. Removing the halide involved adding thallium hexafluorophosphate to a solution of ($^{B(Me)_2,Et}TC^{H}$)FeBr to precipitate thallium bromide. A single crystal for X-ray crystallography was obtained via vapor diffusion of pentane into THF. The crystal structure of [($^{B(Me)_2,Et}TC^{H}$)Fe(THF)](PF_6) (**9**) is seen in Figure 3.6. As seen by the side view of the crystal structure, the apical ligand is almost perpendicular to the metal-carbene plane and the ethylene bridges are in the staggered conformation.

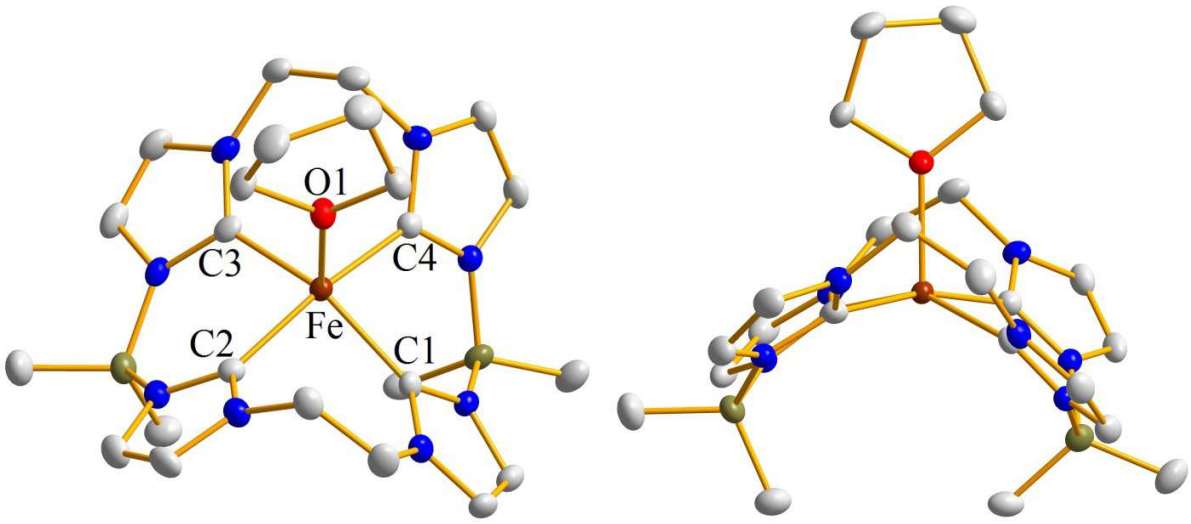

Figure 3.6. Crystal structure of [($^{B(Me)_2,Et}TC^{H}$)Fe(THF)](PF_6) (**9**) from a top-down (right) and a side-on view (left). Brick red, red, blue, gray, and olive ellipsoids (50% probability) represent Fe, O, N, C, and B respectively. Hydrogen atoms and counteranions have been omitted for clarity.

Table 3.6. Selected bond lengths (Å) and angles (°) for [($^{B(Me)_2,Et}TC^{H}$)Fe(THF)](PF_6), (**9**).

M-X/ X-M-X	**Bond Length/ Bond Angle**
Fe-C1	2.047(4) Å
Fe-C2	1.998(4) Å
Fe-O1	2.084(3) Å
C1-Fe-C2	88.80(15)°
C1-Fe-C3	149.82(15)°
C2-Fe-C3	88.48(15)°
C2-Fe-C4	166.00(15)°
O1-Fe-C1	108.66(13)°
O1-Fe-C2	95.06(13)°
O1-Fe-C3	101.52(13)°
O1-Fe-C4	98.95(13)°

In order to measure the success of [($^{B(Me)_2,Et}TC^{H}$)Fe(THF)](PF_6) as a catalyst, we set up several aziridination reactions. Various solvents, alkenes, and organic azides were tested along with various alkene to azide ratios. Although we were unsuccessful in the formation of the aziridine, we did notice the formation of an imide species in ESI/MS using 1-azidoadamante and 4-azidobenzonitrile as the nitrene source. In order to increase the imide product peak, we used a 20-fold excess of our organic azide (Scheme 3.4), which increased the ratio of the imide peak (607.31 *m*/*z* for 1-azidoadamante and 574.20 *m*/*z* for 4-azidobenzonitrile) in relation to the starting material (458.20 *m*/*z*), as seen in Figure 3.7. Iron imides are important intermediates for a variety of group transfer reactions.[28] Although there have been several Fe(II)/Fe(III) imides prepared in literature,[29] there are relatively few Fe(IV) and Fe(V) imides[30] due to the relative instability of such species. This evidence suggests we have potentially synthesized an Fe(V) imide species.

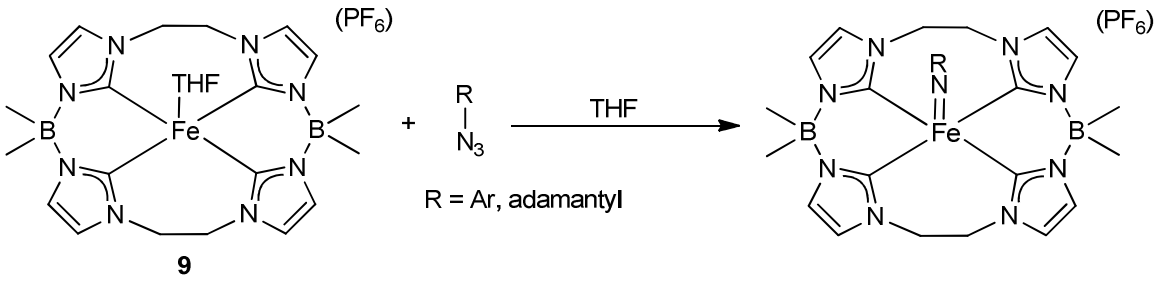

9

Scheme 3.4. Reaction for the formation of an Fe(V) imide.

A

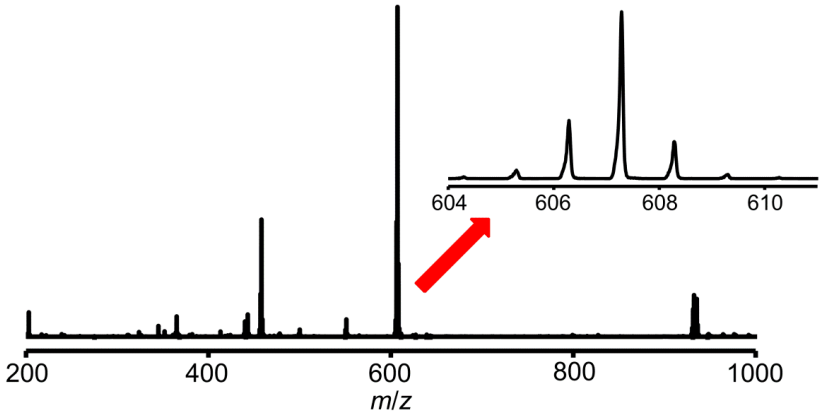

B

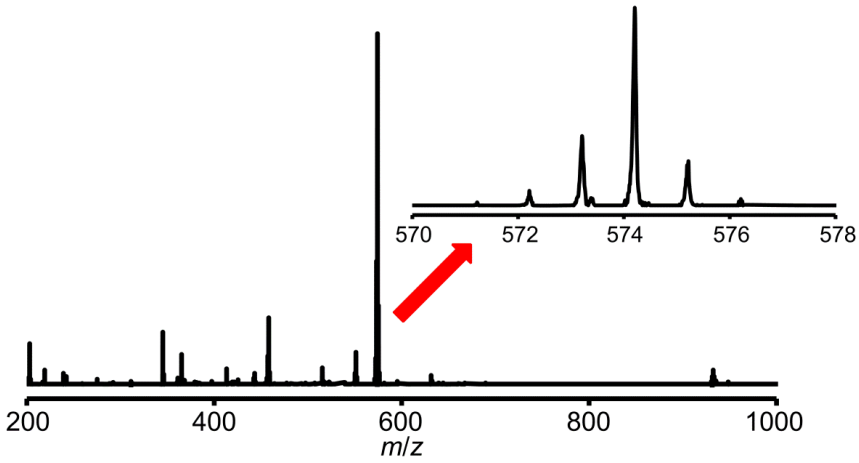

Figure 3.7. An example HR-ESI/MS measured for a tetrahydrofuran solution of (A) [($^{B(Me)_2,Et}TC^{H}$)Fe=Nadamantyl](PF$_6$) and (B) [($^{B(Me)_2,Et}TC^{H}$)Fe=NC$_6$H$_4$CN](PF$_6$)**.** The insets show highlights for the +1 peak of both [($^{B(Me)_2,Et}TC^{H}$)Fe=Nadamantyl]$^+$ and [($^{B(Me)_2,Et}TC^{H}$)Fe=NC$_6$H$_4$CN]$^+$ at 607.28 and 574.20 *m*/*z*.

In order to conclusively confirm the formation of the Fe(V) imide species, we will need to obtain an X-ray crystal structure, as well as, other spectroscopic methods. Preliminary attempts show that these species decompose after two days at room temperature, hence working at lower temperatures will be necessary. If we are able to isolate the imide intermediate, it will be necessary to add an alkene to it to see if it forms an aziridine.

Conclusion

In conclusion, we have synthesized the first examples of metal tetracarbene complexes prepared from a macrocyclic imidazolium borate ligand. The macrocyclic imidazolium borate ligand was characterized by spectroscopic and structural methods. The addition of a strong base, such as *n*-butyllithium, followed by addition of a metal(II) iodide allowed the formation of neutral divalent tetracarbene complexes when using the 18-atom ringed variant of the macrocyclic tetracarbene. The nickel and palladium complexes are square planar and structurally and spectroscopically similar to bis-dicarbene complexes that have been previously prepared. TD-DFT calculations and NMR results suggest that the 18-atom ringed borate containing macrocycle is at least as strong of a σ-donor as our previously prepared isostructural ligand.

In addition to our divalent, square planar nickel and palladium complexes, we have also synthesized trivalent, five coordinate manganese and iron complexes. More importantly, ($^{B(Me)_2,Et}TC^{H}$)MnI is the first example of a manganese supported macrocyclic tetracarbene. Using ($^{B(Me)_2,Et}TC^{H}$)FeBr, we have also been able to synthesize a bridging Fe(III)/Fe(IV) nitride, as well as, acquire ESI/MS evidence of various Fe(V) imide species. Further research is necessary to isolate and react each Fe(V) imide species.

Despite their structural similarity, this new class of tetracarbene complexes offers two potential advantages over similar compounds synthesized from neutral macrocyclic ligands. First, the metal complexes are quite soluble in nonpolar solvents, such as toluene, which should be advantageous for a host of catalytic reactions. Second, the addition of borate into the macrocyclic ring may allow for unique reactivity in a similar manner to the tripodal carbenes and phosphines, particularly when these ligands are ligated to metals which form non-saturated complexes. We believe that these macrocyclic tetracarbene borates allow for the possibility of preparing a wide variety of metal complexes with this class of strong σ-donor ligand.

Experimental

Synthesis of ($^{B(Me)_2,Et}TC^{H}$)$(Br)_2$, 2. In a 500 mL round bottom flask, 1,1'-ethylenediimidazole (5.00 g, 30.7 mmol) was dissolved in 100 mL of acetonitrile. Bromodimethylborane (7.43 g, 60.1 mmol) was pipetted into the acetonitrile solution and allowed to stir for 30 min. After the 30 min elapsed, a second portion of 1,1'-ethylenediimidazole (5.00 g, 30.7 mmol) was added to the flask. The resulting solution was brought out of the glove box and put on a reflux condenser under a steady stream of N_2. The reaction was heated to 60 °C and stirred for 24 hr. After 24 hr, the solution was filtered over a 150 mL fine sintered glass frit. The collected white precipitate was then washed with diethyl ether (3 x 100 mL) and dried under reduced pressure leaving the white product (14.6 g, 83.6%). Crystals were grown by dissolving the white powder into a 50/50 MeOH/H_2O mixture and vapor diffusing in diethyl ether. Mp: 115-117°C. ^{1}H NMR (DMSO-d_6, 499.74 MHz): δ 8.71 (s, 4H), 7.24 (s, 4H), 7.22 (s, 4H), 4.63 (s, 8H), 0.13 (s, 12H). ^{13}C NMR (DMSO-d_6, 125.66 MHz): δ 137.3, 123.5, 121.5, 48.13, 8.82. ^{11}B NMR (DMSO-d_6, 128.42 MHz): δ -3.5. IR(neat): 3106, 3059, 2935, 1542, 1440, 1410, 1366, 1304, 1252, 1120, 1085, 1044, 972, 944, 874, 795, 761, 671, 658 cm^{-1}. HR-ESI/MS (*m*/*z*): $[M\text{-}Br]^+$ 485.2128, $[M\text{-}2Br]^{2+}$ 203.1462 (found); $[M\text{-}Br]^+$ 485.2123, $[M\text{-}2Br]^{2+}$ 203.1466 (calcd). Anal. Calcd for $C_{20}H_{32}B_2N_8Br_2$: C, 42.44; H, 5.70; N, 19.80. Found: C, 41.47; H, 5.74; N, 19.06.

Synthesis of ($^{B(Me)_2,Et}TC^{H}$)Pd, 3. In a 100-mL round bottom flask, 30 mL of tetrahydrofuran was added to $[^{B(Me)_2,Et}TC^{H}](Br)_2$ (0.525 g, 0.927 mmol). The mixture was stirred for 10 min, forming a slurry. ^{n}BuLi (2.50 M, 1.48 mL, 3.71 mmol) was added to the solution and allowed to react for 15 min. The solution changed from a white slurry to a yellow solution. After

the 15 min elapsed, palladium (II) iodide (0.334 g, 0.927 mmol), dissolved in 20 mL of heated tetrahydrofuran, was added to the yellow solution. The reaction immediately turned light brown and was stirred overnight. The reaction mixture was then filtered over a 60 mL fine sintered glass frit and the resulting THF solution was placed under reduced pressure to yield a white powder. The product was extracted with 3 x 30 mL of benzene and then concentrated to 10 mL. Crystalline product could be obtained via a vapor diffusion of pentane into the concentrated benzene solution (0.0398 g, 8.45% yield). Mp: 108-110°C dec. ^{1}H NMR ($CDCl_3$, 499.74 MHz): δ 7.10 (s, 4H), 6.74 (s, 4H), 4.85 (dd, J_1 = 14.8 Hz, J_2 = 7.7 Hz, 4H), 4.22 (dd, J_1 = 14.5 Hz, J_2 = 7.7 Hz, 4H), 0.33 (s, 6H), 0.23 (s, 6H). (CD_3CN, 499.74 MHz): δ 7.07 (s, 4H), 6.94 (s, 4H), 4.86 (dd, J_1 = 14.8 Hz, J_2 = 7.7 Hz), 4.30 (dd, J_1 = 14.8 Hz, J_2 = 7.7 Hz), ^{13}C NMR ($CDCl_3$, 125.66 MHz): δ 170.1, 122.7, 118.8, 48.7, 16.7 (br), 8.6 (br). (CD_3CN, 125.66 MHz): δ 171.3, 122.8, 120.4, 49.3, 17.5 (br), 8.6 (br). ^{11}B NMR ($CDCl_3$, 128.42 MHz): δ -2.0. IR(neat): 2924, 1452, 1443, 1423, 1402, 1336, 1293, 1241, 1217, 1156, 1111, 1073, 1038, 1014, 956, 943, 836, 795, 737, 720, 701, 673 cm^{-1}. HR-DART/MS (*m*/*z*): $[M+H]^+$ 509.17594 (found); $C_{20}H_{29}B_2N_8Pd$ 509.17361 (calcd).

Synthesis of ($^{B(Me)_2,Et}TC^{H}$)Ni, 4. In a 100-mL round bottom flask, 30 mL of tetrahydrofuran was added to ($^{B(Me)_2,Et}TC^{H}$)$(Br)_2$ (0.351g, 0.619 mmol). The mixture was stirred for 10 minutes, forming a slurry. ^{n}BuLi (2.50 M, 0.991 mL, 2.48 mmol) was added to the solution and allowed to react for 15 min. The mixture changes from a white slurry to a yellow solution. After 15 min elapsed, nickel(II) iodide (0.194 g, 0.619 mmol), dissolved in 20 mL of heated tetrahydrofuran, was added to the yellow solution. The reaction immediately turned light brown and was stirred overnight. The reaction was then filtered over a 60 mL fine sintered glass frit and the resulting THF solution was dried under reduced pressure to a light yellow powder.

The product was extracted with benzene (3 x 30 mL), concentrated to 10 mL, and crystallized via vapor diffusion of pentane to give the pure, yellow crystalline product (0.0406 g, 9.89% yield). Mp: 112-115°C dec. ^{1}H NMR ($CDCl_3$, 499.74 MHz): δ 7.05 (s, 4H), 6.70 (s, 4H), 4.95 (dd, J_1 = 14.5 Hz, J_2 = 6.8 Hz, 4H), 4.21 (dd, J_1 = 14.0, J_2 = 7.3 Hz, 4H), 0.42 (s, 6H), 0.25 (s, 6H). (CD_3CN, 499.74 MHz): δ 7.02 (s, 4H), 6.88 (s, 4H), 4.95 (dd, J_1 = 14.5 Hz, J_2 = 7.5 Hz, 4H), 4.27 (dd, J_1 = 14.5 Hz, J_2 = 7.3 Hz), 0.30 (s, 6H), 0.17 (s, 6H). ^{13}C NMR ($CDCl_3$, 125.66 MHz): δ 173.6, 123.1, 118.8, 48.0, 16.5 (br), 9.3(br). (CD_3CN, 125.66 MHz) 174.7, 123.2, 48.5, 16.9 (br), 9.9 (br). ^{11}B NMR ($CDCl_3$, 128.42 MHz): δ -0.6. IR (neat): 2923, 1452, 1422, 1403, 1332, 1295, 1239, 1212, 1152, 1085, 1070, 1041, 955, 942, 841, 797, 736, 725, 704, 672 cm^{-1}. HR-DART/MS (*m*/*z*): $[M+H]^+$ 461.20530 (found); $C_{20}H_{29}B_2N_8Ni$ 461.20623 (calcd).

Synthesis of ($^{B(Me)_2,Et}TC^H$)MnI, 5. In a 20-mL vial, 4 mL of tetrahydrofuran were added to ($^{B(Me)_2,Et}TC^H$)$(Br)_2$ (0.210 g, 0.390 mmol). Lithium diisopropylamide (0.167 g, 1.56 mmol) dissolved in 4 mL of tetrahydrofuran was added to the solution and stirred for 20 minutes. Upon addition of the base, the solution turned orange. Manganese(II) iodide (0.121 g, 0.390 mmol) dissolved in 3 mL of tetrahydrofuran was added to the solution and stirred overnight. The solution was pumped to a solid. The product was extracted with benzene (3 X 30 mL), concentrated to 10 mL, and crystallized via vapor diffusion of pentane to give the pure crystalline product. Further characterization is ongoing by a member of Dr. David M. Jenkins' group.

Synthesis of ($^{B(Me)_2,Et}TC^H$)FeBr, 6. In a 100-mL round bottom flask, 20 mL of tetrahydrofuran were added to ($^{B(Me)_2,Et}TC^H$)$(Br)_2$ (0.351g, 0.619 mmol). The reaction stirred for 10 minutes, forming a slurry. ^{n}BuLi (2.5 M, 0.991 mL, 2.48 mmol) was added to the solution and allowed to react for 15 minutes. The solution changed from a white slurry to a yellow solution.

After 15 min. elapsed, iron(III) bromide (0.194 g, 0.619 mmol), dissolved in 20 mL of heated tetrahydrofuran, was added to the yellow solution. Immediately, the reaction turned light brown and the reaction stirred overnight. The reaction was then filtered over a 60 mL fine sintered frit and the resulting THF solution was pumped to a yellow, green powder. The product was extracted with 3 X 30 mL of benzene, pumped to a concentrated amount, and crystallized via vapor diffusion of pentane to give the pure, red/green crystalline product (0.0223 g, 10.1% yield). ^{1}H NMR (CD_3CN, 499.74 MHz): δ 29.42, -5.76, -14.41, -18.68. IR(neat): 2927, 1463, 1417, 1403, 1303, 1284, 1208, 1155, 1118, 1085, 1063, 1034, 979, 944, 796, 738, 732, 706, 678 cm^{-1}. DART MS (*m*/*z*): $[M+H]^+$ 538.08. Anal. Calcd for $C_{20}H_{28}B_2N_8FeBr$: C, 44.66; H, 5.25; N, 20.83. Found: C, 45.41; H, 5.41; N, 20.30.

Synthesis of ($^{B(Me)_2,Et}TC^{H}$)FeN_3, 7. In a 20-mL vial, **(**$^{B(Me)2,Et}TC^{H}$)FeBr (0.0310 g, 0.0576 mmol) was dissolved in 3 mL tetrahydrofuran. Sodium azide (0.00370 g, 0.0576 mmol), dissolved in 2 mL of tetrahydrofuran, was added to the stirring solution. The reaction stirred overnight at 60 ^{o}C forming a greenish solution with brown particulate. After cooling, the solution was filtered over Celite and crystallized via vapor diffusion of pentane to give the pure, orange/reddish crystalline product (0.0248 g, 86.1% yield). IR(neat): 2916, 2848, 2044, 1461, 1418, 1403, 1327, 1285, 1209, 1154, 1117, 1068, 1049, 947, 795, 753, 736, 708, 673 cm^{-1}.

Synthesis of [($^{B(Me)_2,Et}TC^{H}$)Fe]$_2$N, 8. In a 20-mL vial, ($^{B(Me)_2,Et}TC^{H}$)$Fe^{III}N_3$ (0.0383 g, 0.0766 mmol) was dissolved in 3 mL of tetrahydrofuran. The vial was set under a mercury lamp for 1 hr and stirred, turning the solution from a reddish orange to a dark red. The resulting solution was layered with pentane and crystallized at -35 ^{o}C. (Further investigation and characterization is ongoing)

Synthesis of [($^{B(Me)_2,Et}TC^H$)Fe^{III}](PF$_6$), 9. In a 20-mL vial, ($^{B(Me)_2,Et}TC^H$)FeBr (0.0866 g, 0.161 mmol) was dissolved in 3 mL of tetrahydrofuran. Thallium hexafluorophosphate (0.0562 g, 0.161 mmol), dissolved in 2 mL of tetrahydrofuran, was added immediately forming a white precipitate (TlBr) and changing the color of the solution from a greenish brown to a vibrant reddish orange. The reaction stirred for an hour to ensure that all of the ($^{B(Me)_2,Et}TC^H$)FeBr had reacted. It was then filtered over Celite, to remove the white solid. The resulting solution was setup for crystallization via vapor diffusion with pentane. The product was obtained as reddish orange crystals (0.0893 g, 92.0% yield). (Note – collected yellow crystals with the same IR as red.) IR(neat): 3138, 2933, 1543, 1455, 1420, 1404, 1298, 1214, 1159, 1119, 1071, 1048, 960, 946, 825, 740, 703, 670 cm^{-1}. ESI/MS (*m*/*z*): [M-PF$_6$]$^+$ 458.20.

Synthesis of [($^{B(Me)_2,Et}TC^H$)Fe^V=Nadamamtyl](PF$_6$). In a 20-mL vial, [($^{B(Me)_2,Et}TC^H$)Fe^{III}](PF$_6$) (0.0189 g, 0.0280 mmol) was dissolved in 3 mL of tetrahydrofuran. An excess of 1-azidoadamantane (0.0993 g, 0.560 mmol) was added to the solution and stirred at room temperature for 1 day. The solution changed from a reddish orange to a dark red color. The reaction was filtered over Celite and crystalized via layering of pentane at -35 ^{o}C. ESI/MS (*m*/*z*): [M-PF$_6$]$^+$ 607.32. (Further investigation and characterization is ongoing)

Synthesis of [($^{B(Me)_2,Et}TC^H$)Fe=NC$_6$H$_4$CN](PF$_6$). In a 20-mL vial, [($^{B(Me)_2,Et}TC^H$)Fe^{III}](PF$_6$) (0.0109 g, 0.0161 mmol) was dissolved in 3 mL of tetrahydrofuran. An excess of 4-azidobenzonitrile (0.0456 g, 0.323 mmol) was added to the solution and stirred at room temperature for 1 day. The solution changed from a reddish orange to a dark green color. The reaction was pumped to a solid and washed with diethyl ether. After each wash the solid was dried under reduced pressure. The resulting dark green powder was dissolved in tetrahydrofuran

and crystallized via vapor diffusion with diethyl ether. IR(neat): 3142, 2933, 2215, 1596, 1553, 1496, 1458, 1418, 1294, 1211, 1168, 1151, 1121, 1039, 946, 825, 738, 705, 677 cm^{-1}. ESI/MS (*m*/*z*): $[M\text{-}PF_6]^+$ 574.20. (Further investigation and characterization is ongoing)

References

(1) (a) Saouma, C. T.; Peters, J. C. *Coord. Chem. Rev.* **2011**, *255*, 920. (b) Gunay, A.; Theopold, K. H. *Chem. Rev.* **2010**, *110*, 1060. (c) Mehn, M. P.; Peters, J. C. *J. Inorg. Biochem.* **2006**, *100*, 634. (d) Riordan, C. G. *Coord. Chem. Rev.* **2010**, *254*, 1815. (e) Reger, D. L. *Comments Inorg. Chem.* **1999**, *21*, 1. (f) Bigmore, H. R.; Lawrence, S. C.; Mountford, P.; Tredget, C. S. *Dalton Trans.* **2005**, 635. (g) Hu, X.; Castro-Rodriguez, I.; Meyer, K. *J. Am. Chem. Soc.* **2004**, *126*, 13464. (h) Evans, M. E.; Li, T.; Vetter, A. J.; Rieth, R. D.; Jones, W. D. *J. Org. Chem.* **2009**, *74*, 6907. (i) Thyagarajan, S.; Shay, D. T.; Incarvito, C. D.; Rheingold, A. L.; Theopold, K. H. *J. Am. Chem. Soc.* **2003**, *125*, 4440. (j) Shay, D. T.; Yap, G. P. A.; Zakharov, L. N.; Rheingold, A. L.; Theopold, K. H. *Angew. Chem., Int. Ed.* **2005**, *44*, 1508. (k) Egan, J. W., Jr.; Haggerty, B. S.; Rheingold, A. L.; Sendlinger, S. C.; Theopold, K. H. *J. Am. Chem. Soc.* **1990**, *112*, 2445. (l) Mukherjee, A.; Cranswick, M. A.; Chakrabarti, M.; Paine, T. K.; Fujisawa, K.; Munck, E.; Que, L., Jr. *Inorg. Chem.* **2010**, *49*, 3618. (m) Schebler, P. J.; Mandimutsira, B. S.; Riordan, C. G.; Liable-Sands, L. M.; Incarvito, C. D.; Rheingold, A. L. *J. Am. Chem. Soc.* **2001**, *123*, 331.

(2) (a) Smith, J. M. *Comments Inorg. Chem.* **2008**, *29*, 189. (b) Jenkins, D. M.; Peters, J. C. *J. Am. Chem. Soc.* **2005**, *127*, 7148. (c) Fujisawa, K.; Ono, T.; Ishikawa, Y.; Amir, N.; Miyashita, Y.; Okamoto, K.-I.; Lehnert, N. *Inorg. Chem.* **2006**, *45*, 1698.

(3) (a) Scepaniak, J. J.; Harris, T. D.; Vogel, C. S.; Sutter, J.; Meyer, K.; Smith, J. M. *J. Am. Chem. Soc.* **2011**, *133*, 3824. (b) Mehn, M. P.; Brown, S. D.; Paine, T. K.; Brennessel, W. W.; Cramer, C. J.; Peters, J. C.; Que, L., Jr. *Dalton Trans.* **2006**, 1347. (c) Thomas, C. M.; Peters, J. C. *Angew. Chem., Int. Ed.* **2006**, *45*, 776. (d) Jenkins, D. M.; Peters, J. C. *J. Am. Chem. Soc.* **2003**, *125*, 11162. (e) Jenkins, D. M.; Betley, T. A.; Peters, J. C. *J. Am. Chem. Soc.* **2002**, *124*,

11238. (f) Jenkins, D. M.; Di, B. A. J.; Allen, M. J.; Betley, T. A.; Peters, J. C. *J. Am. Chem. Soc.* **2002**, *124*, 15336. (g) Lu, C. C.; Saouma, C. T.; Day, M. W.; Peters, J. C. *J. Am. Chem. Soc.* **2007**, *129*, 4. (h) Suess, D. L. M.; Tsay, C.; Peters, J. C. *J. Am. Chem. Soc.* **2012**, *134*, 14158. (i) Forshaw, A. P.; Smith, J. M.; Ozarowski, A.; Krzystek, J.; Smirnov, D.; Zvyagin, S. A.; Harris, T. D.; Karunadasa, H. I.; Zadrozny, J. M.; Schnegg, A.; Holldack, K.; Jackson, T. A.; Alamiri, A.; Barnes, D. M.; Telser, J. *Inorg. Chem.* **2013**, *52*, 144.

(4) (a) Hu, X.; Meyer, K. *J. Organomet. Chem.* **2005**, *690*, 5474. (b) Vogel, C. S.; Heinemann, F. W.; Khusniyarov, M. M.; Meyer, K. *Inorg. Chim. Acta* **2010**, *364*, 226. (c) Nakai, H.; Tang, Y.; Gantzel, P.; Meyer, K. *Chem. Commun.* **2003**, 24. (d) Hu, X.; Castro-Rodriguez, I.; Meyer, K. *J. Am. Chem. Soc.* **2003**, *125*, 12237. (e) Hu, X.; Castro-Rodriguez, I.; Meyer, K. *Chem. Commun.* **2004**, 2164. (f) Betley, T. A.; Peters, J. C. *Inorg. Chem.* **2003**, *42*, 5074. (g) MacBeth, C. E.; Thomas, J. C.; Betley, T. A.; Peters, J. C. *Inorg. Chem.* **2004**, *43*, 4645. (h) Lu, C. C.; Peters, J. C. *Inorg. Chem.* **2006**, *45*, 8597. (i) Nieto, I.; Cervantes-Lee, F.; Smith, J. M. *Chem. Commun.* **2005**, 3811. (j) Nieto, I.; Bontchev, R. P.; Ozarowski, A.; Smirnov, D.; Krzystek, J.; Telser, J.; Smith, J. M. *Inorg. Chim. Acta* **2009**, *362*, 4449. (k) Cowley, R. E.; Bontchev, R. P.; Duesler, E. N.; Smith, J. M. *Inorg. Chem.* **2006**, *45*, 9771. (l) Munoz, S. B.; Foster, W. K.; Lin, H.-J.; Margarit, C. G.; Dickie, D. A.; Smith, J. M. *Inorg. Chem.* **2012**, *51*, 12660. (m) Forshaw, A. P.; Bontchev, R. P.; Smith, J. M. *Inorg. Chem.* **2007**, *46*, 3792. (n) Sacconi, L.; Ghilardi, C. A.; Mealli, C.; Zanobini, F. *Inorg. Chem.* **1975**, *14*, 1380. (o) Heinze, K.; Huttner, G.; Zsolnai, L.; Schober, P. *Inorg. Chem.* **1997**, *36*, 5457. (p) Schober, P.; Soltek, R.; Huttner, G.; Zsolnai, L.; Heinze, K. *Eur. J. Inorg. Chem.* **1998**, 1407. (q) Mayer, H. A.; Kaska, W. C. *Chem. Rev.* **1994**, *94*, 1239.

(5) (a) Brown, S. D.; Betley, T. A.; Peters, J. C. *J. Am. Chem. Soc.* **2003**, *125*, 322. (b) Brown, S. D.; Peters, J. C. *J. Am. Chem. Soc.* **2005**, *127*, 1913. (c) Rohde, J.-U.; Betley, T. A.; Jackson, T. A.; Saouma, C. T.; Peters, J. C.; Que, L., Jr. *Inorg. Chem.* **2007**, *46*, 5720. (d) Moret, M.-E.; Peters, J. C. *J. Am. Chem. Soc.* **2011**, *133*, 18118. (e) Saouma, C. T.; Lu, C. C.; Peters, J. C. *Inorg. Chem.* **2012**, *51*, 10043. (f) Saouma, C. T.; Muller, P.; Peters, J. C. *J. Am. Chem. Soc.* **2009**, *131*, 10358. (g) Thomas, C. M.; Mankad, N. P.; Peters, J. C. *J. Am. Chem. Soc.* **2006**, *128*, 4956. (h) Betley, T. A.; Peters, J. C. *J. Am. Chem. Soc.* **2003**, *125*, 10782. (i) Hendrich, M. P.; Gunderson, W.; Behan, R. K.; Green, M. T.; Mehn, M. P.; Betley, T. A.; Lu, C. C.; Peters, J. C. *Proc. Natl. Acad. Sci. U.S.A.* **2006**, *103*, 17107. (j) Anderson, J. S.; Moret, M.-E.; Peters, J. C. *J. Am. Chem. Soc.* **2013**, *135*, 534.

(6) (a) Hu, X.; Meyer, K. *J. Am. Chem. Soc.* **2004**, *126*, 16322. (b) Kropp, H.; King, A. E.; Khusniyarov, M. M.; Heinemann, F. W.; Lancaster, K. M.; DeBeer, S.; Bill, E.; Meyer, K. *J. Am. Chem. Soc.* **2012**, *134*, 15538. (c) Cowley, R. E.; Bontchev, R. P.; Sorrell, J.; Sarracino, O.; Feng, Y.; Wang, H.; Smith, J. M. *J. Am. Chem. Soc.* **2007**, *129*, 2424. (d) Nieto, I.; Ding, F.; Bontchev, R. P.; Wang, H.; Smith, J. M. *J. Am. Chem. Soc.* **2008**, *130*, 2716.

(7) (a) Smith, J. M.; Subedi, D. *Dalton Trans.* **2012**, *41*, 1423. (b) Scepaniak, J. J.; Bontchev, R. P.; Johnson, D. L.; Smith, J. M. *Angew. Chem., Int. Ed.* **2011**, *50*, 6630. (c) Scepaniak, J. J.; Vogel, C. S.; Khusniyarov, M. M.; Heinemann, F. W.; Meyer, K.; Smith, J. M. *Science* **2011**, *331*, 1049. (d) Scepaniak, J. J.; Young, J. A.; Bontchev, R. P.; Smith, J. M. *Angew. Chem., Int. Ed.* **2009**, *48*, 3158. (e) Scepaniak, J. J.; Fulton, M. D.; Bontchev, R. P.; Duesler, E. N.; Kirk, M. L.; Smith, J. M. *J. Am. Chem. Soc.* **2008**, *130*, 10515. (f) Vogel, C.; Heinemann, F. W.; Sutter, J.; Anthon, C.; Meyer, K. *Angew. Chem., Int. Ed.* **2008**, *47*, 2681.

(8) Hahn, F. E.; Langenhahn, V.; Luegger, T.; Pape, T.; Le Van, D. *Angew. Chem., Int. Ed.* **2005**, *44*, 3759.

(9) (a) McKie, R.; Murphy, J. A.; Park, S. R.; Spicer, M. D.; Zhou, S.-z. *Angew. Chem., Int. Ed.* **2007**, *46*, 6525. (b) Park, S. R.; Findlay, N. J.; Garnier, J.; Zhou, S.; Spicer, M. D.; Murphy, J. A. *Tetrahedron* **2009**, *65*, 10756. (c) Bass, H. M.; Cramer, S. A.; Price, J. L.; Jenkins, D. M. *Organometallics* **2010**, *29*, 3235. (d) Findlay, N. J.; Park, S. R.; Schoenebeck, F.; Cahard, E.; Zhou, S.-z.; Berlouis, L. E. A.; Spicer, M. D.; Tuttle, T.; Murphy, J. A. *J. Am. Chem. Soc.* **2010**, *132*, 15462. (e) Cramer, S. A.; Jenkins, D. M. *J. Am. Chem. Soc.* **2011**, *133*, 19342. (f) Lu, Z.; Cramer, S. A.; Jenkins, D. M. *Chem. Sci.* **2012**, *3*, 3081. (g) Meyer, S.; Klawitter, I.; Demeshko, S.; Bill, E.; Meyer, F. *Angew. Chem., Int. Ed.* **2013**, *52*, 901.

(10) Jenkins, D. M. *Synlett* **2012**, *23*, 1267.

(11) (a) Weiss, A.; Pritzkow, H.; Siebert, W. *Angew. Chem., Int. Ed.* **2000**, *39*, 547. (b) Weiss, A.; Barba, V.; Pritzkow, H.; Siebert, W. *J. Organomet. Chem.* **2003**, *680*, 294.

(12) Fränkel, R.; Kniczek, J.; Ponikwar, W.; Nöth, H.; Polborn, K.; Fehlhammer, W. P. *Inorg. Chim. Acta* **2001**, *312*, 23.

(13) Nieto, I.; Bontchev, R. P.; Smith, J. M. *Eur. J. Inorg. Chem.* **2008**, 2476.

(14) (a) Baker, M. V.; Barnard, P. J.; Brayshaw, S. K.; Hickey, J. L.; Skelton, B. W.; White, A. H. *Dalton Trans.* **2005**, 37. (b) Tapu, D.; Dixon, D. A.; Roe, C. *Chem. Rev.* **2009**, *109*, 3385. (c) Yuan, D.; Huynh, H. V. *Organometallics* **2012**, *31*, 405.

(15) (a) Wasbotten, I. H.; Ghosh, A. *Inorg. Chem.* **2007**, *46*, 7890. (b) Nagura, K.; Saito, S.; Froehlich, R.; Glorius, F.; Yamaguchi, S. *Angew. Chem., Int. Ed.* **2012**, *51*, 7762. (c) Mendez, F.; Garcia-Garibay, M. A. *J. Org. Chem.* **1999**, *64*, 7061. (d) Xu, X.; Kim, S. H.; Zhang, X.; Das, A. K.; Hirao, H.; Hong, S. H. *Organometallics* **2013**, *32*, 164.

(16) Betley, T. A.; Peters, J. C. *J. Am. Chem. Soc.* **2004**, *126*, 6252.

(17) Wu, L. P.; Yamagiwa, Y.; Kuroda-Sowa, T.; Kamikawa, T.; Munakata, M. *Inorg. Chim. Acta* **1997**, *256*, 155.

(18) Cremer, T.; Kolbeck, C.; Lovelock, K. R. J.; Paape, N.; Woelfel, R.; Schulz, P. S.; Wasserscheid, P.; Weber, H.; Thar, J.; Kirchner, B.; Maier, F.; Steinrueck, H.-P. *Chem. Eur. J.* **2010**, *16*, 9018.

(19) Unger, Y.; Zeller, A.; Ahrens, S.; Strassner, T. *Chem. Commun.* **2008**, 3263.

(20) Fehlhammer, W. P.; Bliss, T.; Kernbach, U.; Bruedgam, I. *J. Organomet. Chem.* **1995**, *490*, 149.

(21) Berry, J. F. *Comm. Inorg. Chem.* **2009**, *30*, 28.

(22) (a) Lee, D. Y.; Sun, H. Y.; Park, J. W.; Son, S. U. Organic Electrolyte Solution and Redox Flow Cell having it. US 20110195283, August 11, 2011. (b) Lee, M.- J.; Oh, D.- J.; Hwang, S.- S. Redox Flow Battery. US 20120171530, July 12, 2012.

(23) (a) de Montellano, P. R., Ed. *Cytochrome P450 Structure, Mechanism, and Biochemistry*; Plenum Press: New York, 1986. (b) Lippard, S. J.; Berg, J. M. *Principles of Bioinorganic Chemistry*; University Science Books: Mill Valley, 1994. (c) Tollman, W. B., Ed. *Activation of Small Molecules: Organometallic and Biorganic Perspectives*; Wiley-VCH: Weinheim, Germany, 2006.

(24) Hoffman, B. M.; Dean, D. R.; Seefeldt, L. C. *Acc. Chem. Res.*, **2009**, *42*, 609.

(25) (a) Scepaniak, J. J.; Vogel, C. S.; Khusniyarov, M. M.; Heinemann, F. W.; Meyer, K.; Smith, J. M. *Science* **2011,** *331*, 1049. (b) Smith, J. M.; Subedi, D. *Dalton Trans.* **2012**, *41*, 1423. (c) Wagner, W. D.; Nakamoto, K. *J. Amer. Chem. Soc.* **1988**, *110*, 4044. (d) Wagner, W. D.; Nakamoto, K. *J. Amer. Chem. Soc.* **1989**, *111*, 1590.

(26) Berry, J. F.; Bill, E.; Bothe, E.; DeBeer George, S.; Mienert, B.; Neese, F.; Wieghardt, K; *Science*, **2006**, *312*, 1937.

(27) (a) Summerville, D. A.; Cohen, I. A. *J. Amer. Chem. Soc.* **1976**, *98*, 1747. (b) Scheidt, W. R.; Summerville, D. A.; Cohen, I. A. *J. Amer. Chem. Soc.* **1976**, *98*, 6623. (c) Tatsumi, K.; Hoffman, R. *J. Amer. Chem. Soc.* **1981**, *103*, 3328. (d) Bottomley, L. A.; Garrett, B. B. *J. Amer. Chem. Soc.* **1982**, *104*, 1260. (e) English, D. R.; Hendrickson, D. N.; Suslick, K. S. *Inorg. Chem.* **1985**, *24*, 122. (f) Kienast, A.; Homborg, H. *Z. Anorg. Allg. Chem.* **1998**, *624*, 233.

(28) Eikey, R. A.; Abu-Omar, M. M. *Coord. Chem. Rev.* **2003**, *243*, 83.

(29) (a) Brown, S. D.; Peters, J. C. *J. Amer. Chem. Soc.* **2004**, *126*, 4538. (b) Brown, S. D.; Betley, T. A.; Peters, J. C. *J. Am. Chem. Soc.* **2003**, *125*, 322. (c) Betley, T. A.; Peters, J. C. *J. Amer. Chem. Soc.* **2003**, *125*, 10782. (d) Brown, S. D.; Peters, J. C. *J. Amer. Chem. Soc.* **2005**, *127*, 1913.

(30) Thomas, C. M.; Mankad, N. P.; Peters, J. C. *J. Amer. Chem. Soc.* **2006,** *128*, 4956.

Chapter 4

Aziridine Reactions and Aryl Phosphine Bonding

Abstract

Three types of reactions were performed using the catalyst [(^{Me,Et}TC^{Ph})Co(OTf)](OTf). Although [(^{Me,Et}TC^{Ph})Co(OTf)](OTf) did not catalyze the attempted epoxidation and cyclopropanation reactions using the tested conditions, [(^{Me,Et}TC^{Ph})Co(OTf)](OTf) did catalyze aziridination reactions. Besides investigating the catalytic properties of [(^{Me,Et}TC^{Ph})Co(OTf)](OTf), we investigated the bonding mode of aryl phosphines on metal surfaces. The bonding mode was investigated via SERS using various 2º and 3º aryl phosphines.

Introduction for Aziridination, Epoxidation and Cyclopropanation

Three membered rings, such as cyclopropanes, epoxides, and aziridines are important biologically[1] and in fine chemical synthesis.[1a-b] For example, azinomycin[2] and mitomycin[3] are examples of aziridines that have antitumor and antibiotic properties. All of these cyclic structures are also used as synthons due to their ring-strain. They are typically used in the formation of new bonds, though ring-opening reactions.[4] Typically, cyclopropanes are formed through the use of a diazo-compound that lose N_2 in order to form cyclopropanes.[5] Epoxides are typically formed through the use of reagents, such as peroxides or iodosobenzene in a $C_2 + O_1$ addition reaction.[5c, 6] Previously, aziridine reactions used hypervalent iodine[5c, 7] or tosyl azides[5c, 8] both of which were not atom economical and difficult to remove,[7, 8] making the synthesis of aziridines more difficult than that of cyclopropanes and epoxides. By using azides as oppose to these nitrene reagents, aziridines have a direct $C_2 + N_1$ route in which N_2 is released as the sole byproduct like diazo-compounds.[9] Our group recently took advantage of using azides as aziridine precursors and had success catalyzing the first examples of a tri- and tetrasubstituted alkene to form an

azide.[10] We are interested in further investigating these aziridine reactions using a different metal for our catalyst, as well as, screening its success in cyclopropanation and epoxidation reactions.

Catalysis Results

S. Alan Cramer's [($^{Me,Et}TC^{Ph}$)Fe($NCCH_3$)$_2$](PF_6)$_2$ catalyst from our group was the first example of a catalyst that successfully formed aziridines with tri- and tetrasubstituted alkenes.[10] We were interested in expanding the scope of the aziridination reaction to other metals using this ligand system in order to compare each metal's reactivity. This process involved the synthesis of the previously reported ($^{Me,Et}TC^{Ph}$)(OTf)$_4$[11] followed by the formation of the transmetallating reagent [{($^{Me,Et}TC^{Ph}$)Ag}$_2$Ag$_2$](OTf)$_4$ (**1**).[12] Once [{($^{Me,Et}TC^{Ph}$)Ag}$_2$Ag$_2$](OTf)$_4$ was purified, [{($^{Me,Et}TC^{Ph}$)Ag}$_2$Ag$_2$](OTf)$_4$ reacted with $CoCl_2$ in a CH_2Cl_2/THF solution to form the product [($^{Me,Et}TC^{Ph}$)Co(OTf)](OTf) (**2**) as previously described by Lu and coworkers.[12] The reactions for **1** and **2** are shown below in Scheme 4.1.

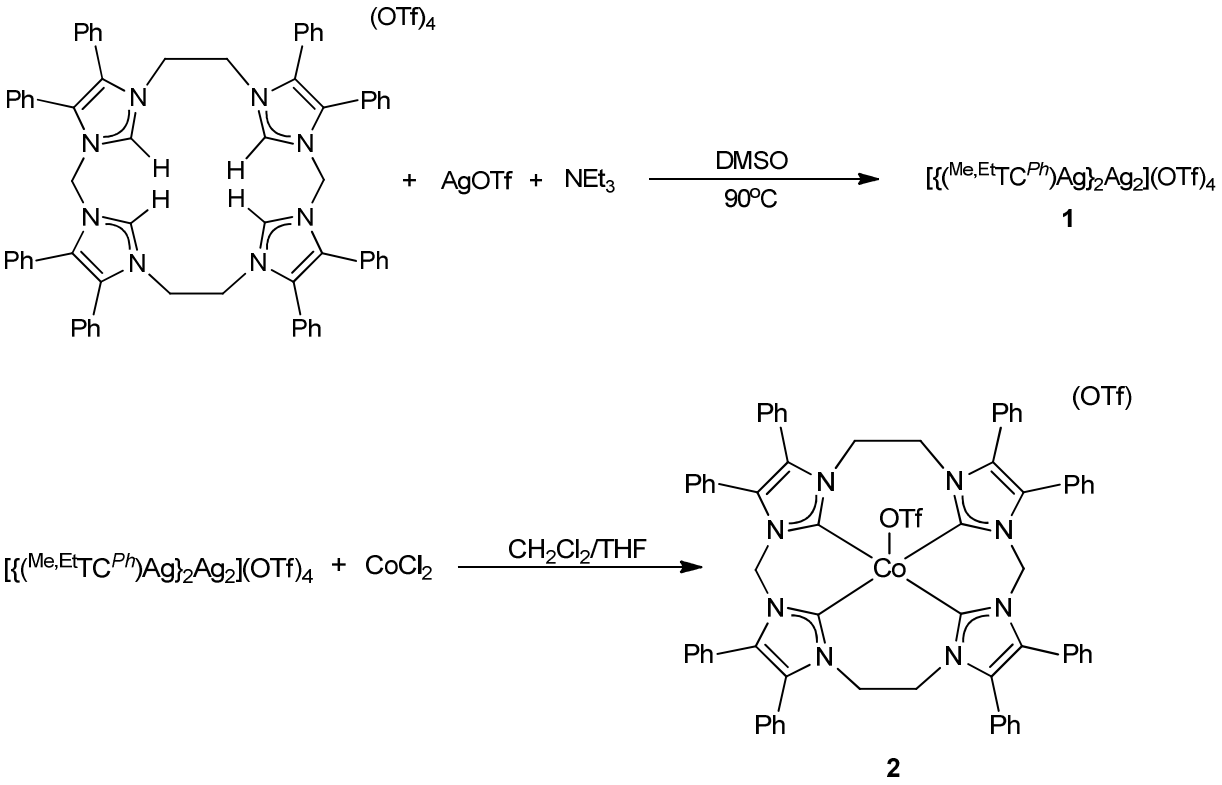

Scheme 4.1. Synthesis of [{(^{Me,Et}TC^{Ph})Ag}$_2$Ag$_2$](OTf)$_4$ (**1**) followed by the addition of $CoCl_2$ to form [(^{Me,Et}TC^{Ph})Co(OTf)](OTf) (**2**).

ESI/MS was taken in order to verify the formation of [{(^{Me,Et}TC^{Ph})Ag}$_2$Ag$_2$](OTf)$_4$ (**1**) and [(^{Me,Et}TC^{Ph})Co(OTf)](OTf) (**2**). Peaks associated with [{(^{Me,Et}TC^{Ph})Ag}$_2$Ag$_2$]$^{4+}$, {{(^{Me,Et}TC^{Ph})Ag}$_2$Ag$_2$](OTf)}$^{3+}$, and {{(^{Me,Et}TC^{Ph})Ag}$_2$Ag$_2$](OTf)$_2$}$^{2+}$ were found at 586.07, 831.41, and 1321.60 *m*/*z*, respectively with the correct isotopic distribution. For **2**, peaks associated with [(^{Me,Et}TC^{Ph})Co]$^{2+}$ and [(^{Me,Et}TC^{Ph})Co(OTf)]$^{1+}$ were found at 507.62 and 1166.23 *m*/*z*, respectively. The ESI/MS for [(^{Me,Et}TC^{Ph})Co(OTf)](OTf) is seen in Figure 4.1.

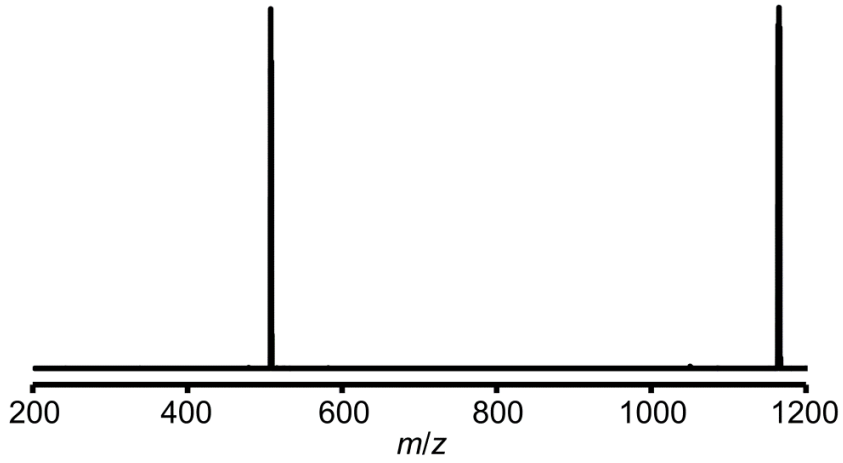

Figure 4.1. An example electrospray ionization mass spectrum measured for an acetonitrile solution of **2** exhibiting two peaks associated with $[(^{Me,Et}TC^{Ph})Co]^{2+}$ and $[(^{Me,Et}TC^{Ph})Co(OTf)]^{1+}$ at 507.6151 and 1166.2266 *m*/*z*, respectively.

In order to test the effectiveness of $[(^{Me,Et}TC^{Ph})Co(OTf)](OTf)$ as a catalyst, we set up various test reactions using similar conditions to those used in $[(^{Me,Et}TC^{Ph})Fe(NCCH_3)_2](PF_6)_2$.[10] All reactions were run in an excess of alkene with tolyl azide and either a 0.1 or a 1.0% catalyst loading (Scheme 4.2). GC/MS was run after the reaction stirred for 18 hours at 90 ^oC for preliminary confirmation of the formation of each azidirine. Since various products can exhibit the same mass, each product had to be purified by column chromotography using a 9:1 hexanes to ethyl acetate mixture. The most successful catalytic reaction involved using 1-decene and tolyl azide for the synthesis of 2-octyl-1-(p-tolyl)aziridine. Similar percent yields were obtained when using a 0.1% or a 1.0% catalyst loading (approximately 83%), which is in agreement with the 1.0% catalyst loading of $[(^{Me,Et}TC^{Ph})Fe(NCCH_3)_2](PF_6)_2$ of 82%.[10] A sample ^1H and ^{13}C NMR for 2-octyl-1-(p-tolyl)aziridine are shown below in Figure 4.2 and Figure 4.3, respectively.

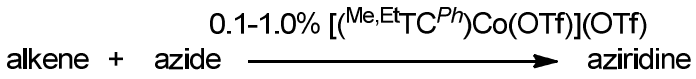

alkene	azide	catalyst percent	percent yield
	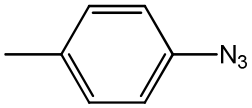	0.1	84.2%
	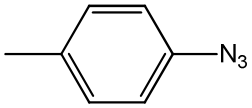	1	82.9%
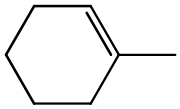	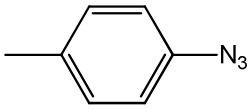	0.1	---
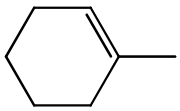	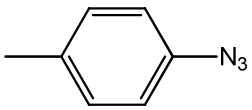	1	---

Scheme 4.2. General synthesis for the formation of aziridines starting from an alkene and an aryl azide.

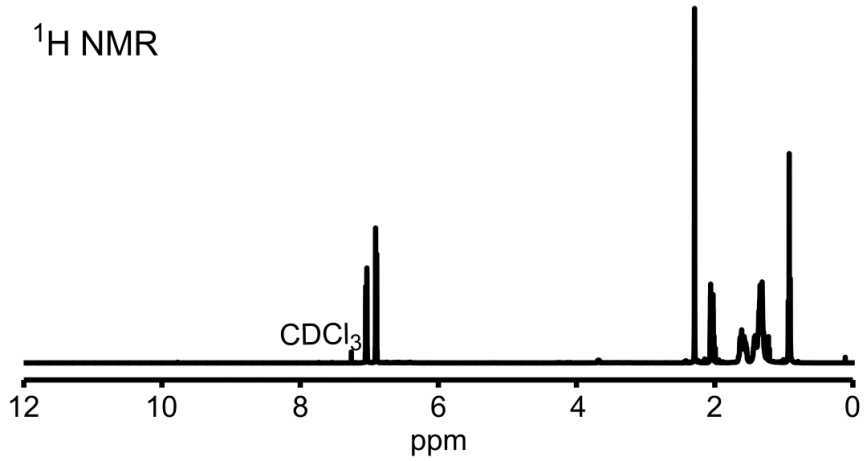

Figure 4.2. ^{1}H NMR of 2-octyl-1-(p-tolyl)aziridine in $CDCl_3$.

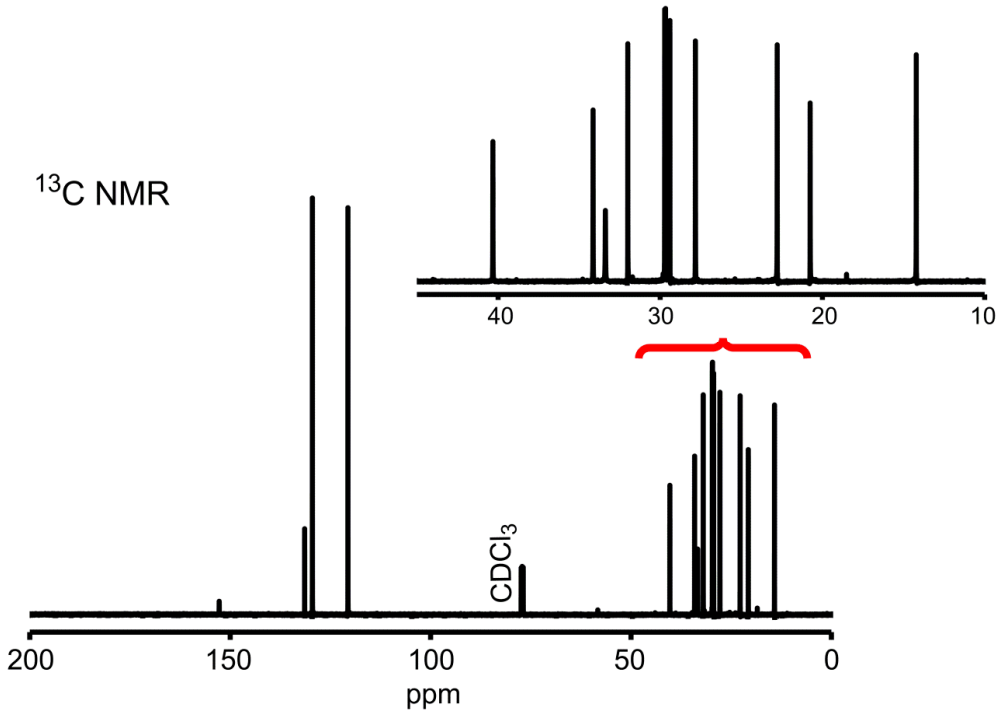

Figure 4.3. ^{13}C NMR of 2-octyl-1-(p-tolyl)aziridine in $CDCl_3$.

We were also interested in trying a cyclopropanation, as well as, an epoxidation reaction to explore the versatility of our catalyst. For the cyclopropanation reaction, we used the methods of Yadav[5a] and Belderrain[5b] involving the formation of cyclopropane via the use of a diazo-compound. Various ratios of cyclooctene and ethyl diazoacetate stirred in a solution of methylene chloride with either a 1% or 5% catalyst loading (Scheme 4.3). Notably, after 2 hours and 24 hours no product was visible on the GC/MS. For an epoxidation reaction, we tested iodosobenzene in an excess of cycloocetene with various catalyst loadings (Scheme 4.3). Again, GC/MS showed no evidence of a reaction. This evidence suggests that although [($^{Me,Et}TC^{Ph}$)Co(OTf)](OTf) is capable of aziridination reactions, it is not an effective catalyst for cyclopropanation or epoxidation reactions using the given conditions.

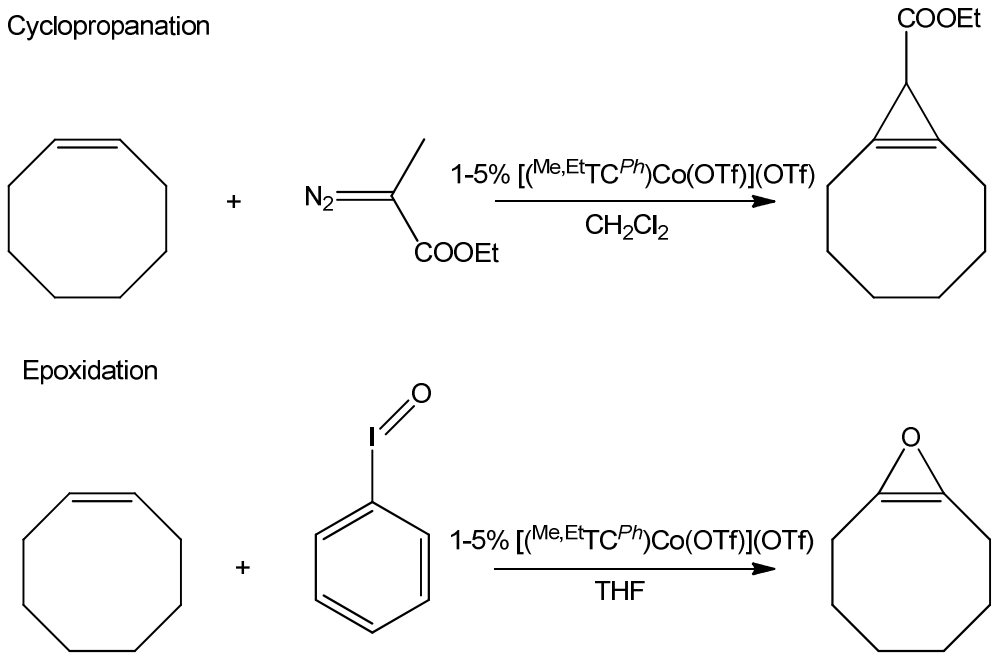

Scheme 4.3. General synthesis for cyclopropanation and epoxidation attempts.

Catalysis Conclusion

Developing the most efficient catalyst not only involves finding the most favorable reaction conditions, but also involves investigating various metals to serve as the metal center. Our group has begun doing this with the synthesis of the new catalyst, [($^{Me,Et}TC^{Ph}$)Co(OTf)](OTf). Preliminary results suggest that [($^{Me,Et}TC^{Ph}$)Co(OTf)](OTf) is as good of a catalyst as the previously reported [($^{Me,Et}TC^{Ph}$)Fe($NCCH_3$)$_2$](PF_6)$_2$ at least in the formation of 2-octyl-1-(p-tolyl)aziridine. Further investigation into tri- and tetrasubstituted alkenes is necessary for comparative purposes, as well as, further investigation into cyclopropanation and epoxidation reactions.

Introduction for Aryl Phosphines Investigations with Raman

R-groups typically bond to metals in either a covalent manner (X-type bond) or a Lewis acid/base type adduct (L-type bond). Aryl thiols are known to lose a proton in order to form strong covalent bonds to metals (Figure 4.4),[13] which is why they are typically used for making modifiable nanoparticle surfaces.[14] Although phosphorous is directly beside sulfur on the periodic table, the bonding motif of aryl phosphines to metal surfaces has yet to be explored. Our group decided to investigate the bonding motif of aryl phosphines by looking at secondary aryl phosphines, secondary aryl phosphine oxides, and tertiary phosphines.

Each type of aryl phosphine to be investigated can only bond to a surface in specific ways (Figure 4.4), thus allowing for a conclusion to be drawn through a process of elimination using surface enhanced Raman spectroscopy (SERS). By adding each group to a silver colloidal solution and then running SERS, we will be able to see which phosphines bond to the metal and which phosphines do not bond. Secondary aryl phosphines can bond by losing a proton and

forming an X-type bond in the same manner as aryl thiols or by donating the lone pair from phosphorous and forming an L-type bond, as depicted in Figure 4.4. By adding an oxide to a secondary phosphine, an X-type bond can still be formed by losing a proton; however, an L-type bond can only be formed if the lone pair from oxygen donates to the metal. Since all the X-type bonds are already used in bonding for a tertiary phosphine, only the lone pair from phosphorous is available for bonding in an L-type fashion. By investigating all three types of aryl phosphines, the bonding mode will be able to be determined, which will indicate its similarity or dissimilarity to aryl thiols.

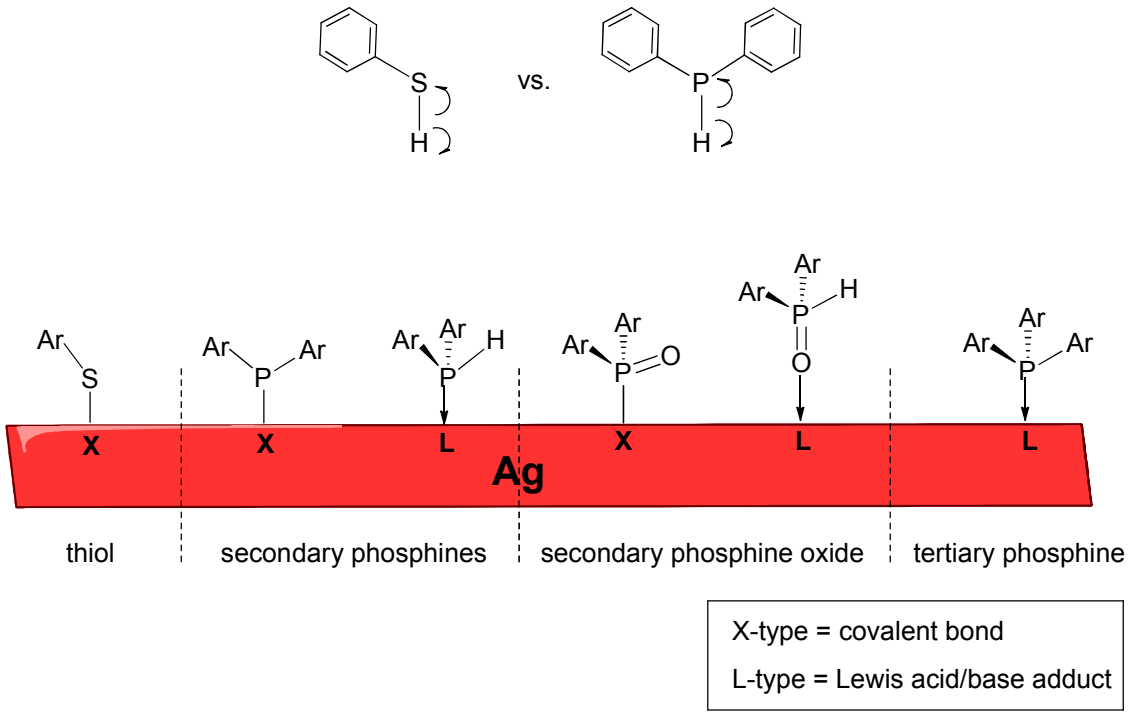

Figure 4.4. Bonding mode of aryl thiols on a silver surface vs. the potential bonding modes of secondary phosphines, secondary phosphine oxides, and tertiary phosphines.

Phosphine Results

The three secondary phosphines we used for our experiment were diphenylphosphine (dpp), bis[3,5-bis(trifluoromethyl)phenyl]phosphine (dppf), and bis[3,5-bis(trifluoromethyl)phenyl]phosphine oxide (dppfo) (Table 4.1). Diphenylphosphine and bis[3,5-bis(trifluoromethyl)phenyl]phosphine were commercially available; however, due to fluorescence issues we had to further purify them by sublimation. Bis[3,5-bis(trifluoromethyl)phenyl]phosphine oxide was synthesized by the methods of Pailloux;[15] however, we had to get rid of impurities through the combined use of a silica plug and petroleum ether washes. To ensure quality control, ^{1}H NMR in $CDCl_3$ was run on dppfo. The ^{1}H NMR of bis[3,5-bis(trifluoromethyl)phenyl]phosphine oxide, shown in Figure 4.5, exhibits a large splitting of the hydrogen attached directly to the phosphine with a *J*-coupling value of 504 MHz. The peak values and this *J*-coupling value were corroborated by Pailloux's reported values.[15]

Table 4.1. List of secondary phosphines, the secondary phosphine oxide, and tertiary phosphines used for experimentation.

Secondary Phosphines	Secondary Phosphine Oxide	Tertiary Phosphines
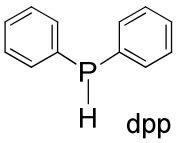 dpp 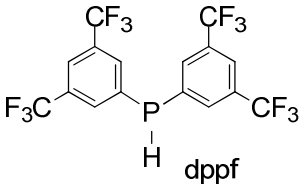 dppf	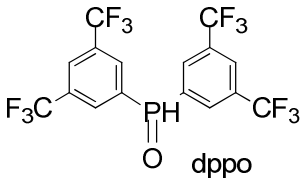 dppo	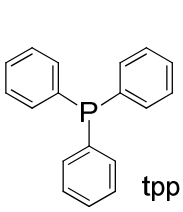 tpp 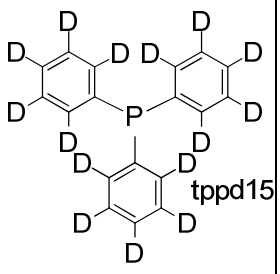 tppd15 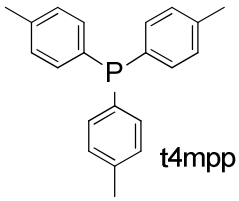 t4mpp 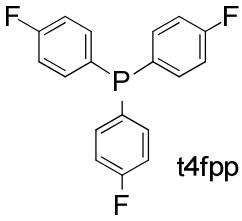 t4fpp

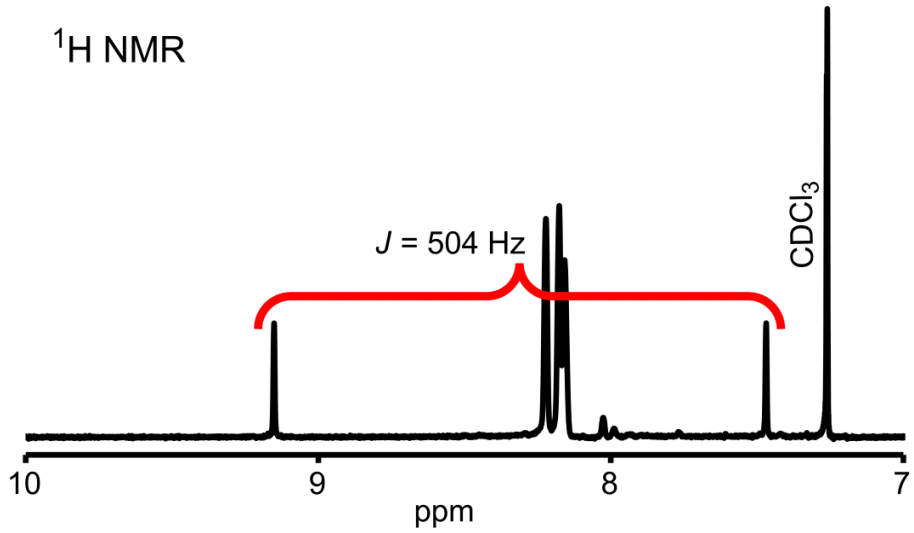

Figure 4.5. ^{1}H NMR of bis[3,5-bis(trifluoromethyl)phenyl]phosphine oxide in $CDCl_3$.

Once each of our secondary phosphines was clean, they were ready for testing. The first step in our experiment was running Raman on each secondary phosphine. The spectrum for each phosphine is seen in Figure 4.6. Many of the peaks from each of the three phosphines overlapped due to their structural similarities. One that is notably different in dppfo versus the other two is the peak at 1156.2 in the top spectrum, which confirms the presence of the P=O bond.

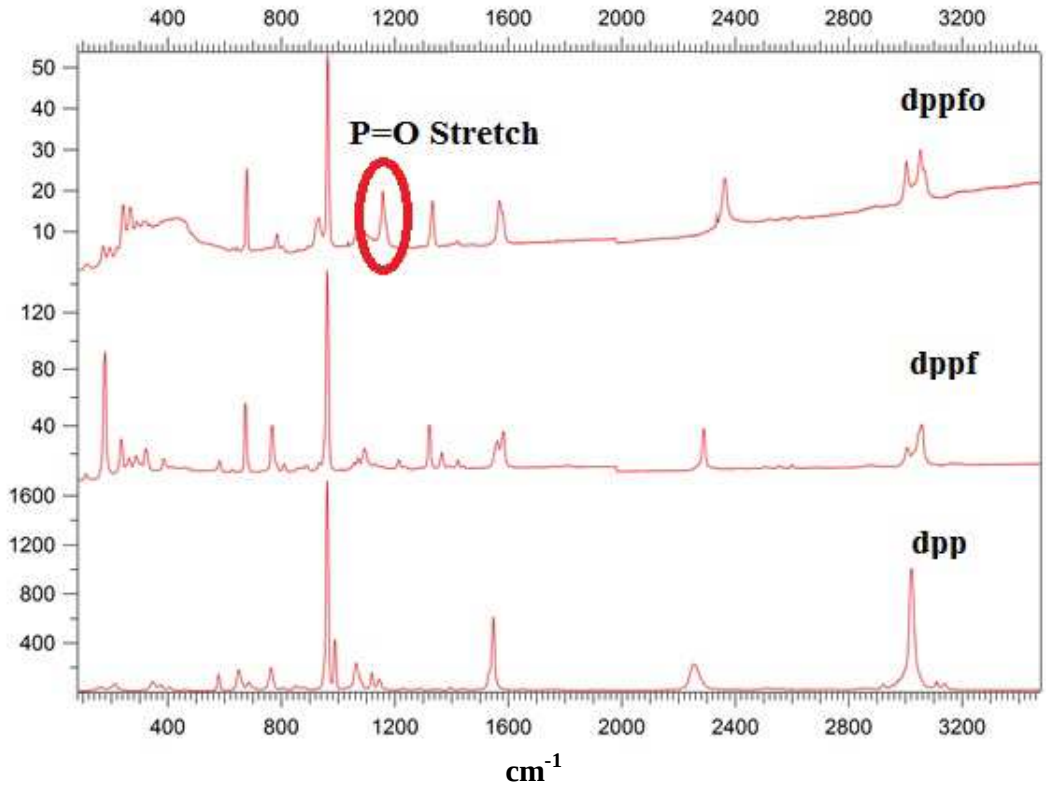

Figure 4.6. Raman spectra comparing the secondary phosphine oxide vs. the secondary phosphines without an oxide. The notable difference is the P=O stretch in the top spectrum at 1156.2.

For the SERS experiment, the phosphines were dissolved into a silver colloidal solution. Methanol and ethanol were used as solvents due to the fact that the phosphines precipitated out of aqueous solutions. It was noted that after several days both dpp and dppf oxidized to phosphine oxides, hence the data taken for these compounds were inconclusive. Future SERS experiments involving these two phosphines will be run in an air-free environment.

Since we could not compare the phosphine oxide to the other secondary phosphines, we decided to run SERS on the secondary phosphine oxide and tertiary phosphines. In the case of tertiary phosphines, only the L-type (lone pair) bonding exists, hence if these bind and dppo does not, it is suggested that phosphines bind to the silver surface via their lone pair. The tertiary phosphines we used included triphenylphosphine (tpp), tris(4-methylphenyl)-phosphine (t4mppp), triphenylphosphine d-15 (tppd15), and tris(4-fluorophenyl)-phosphine (t4fpp) (Table 4.1). These compounds were dissolved into silver colloidal solutions of methanol or ethanol and the SERS spectra were collected. Figure 4.7 shows the spectra of the four tertiary and the one secondary phosphine oxide. From the data, it is suggested that all four tertiary phosphines bind to the silver surface, while the phosphine oxide does not. Although further data must be taken on the secondary phosphines, this data suggests that the phosphines bind to the silver surface via their lone pairs off of the phosphine, which is different from how thiols bind to the silver surface.

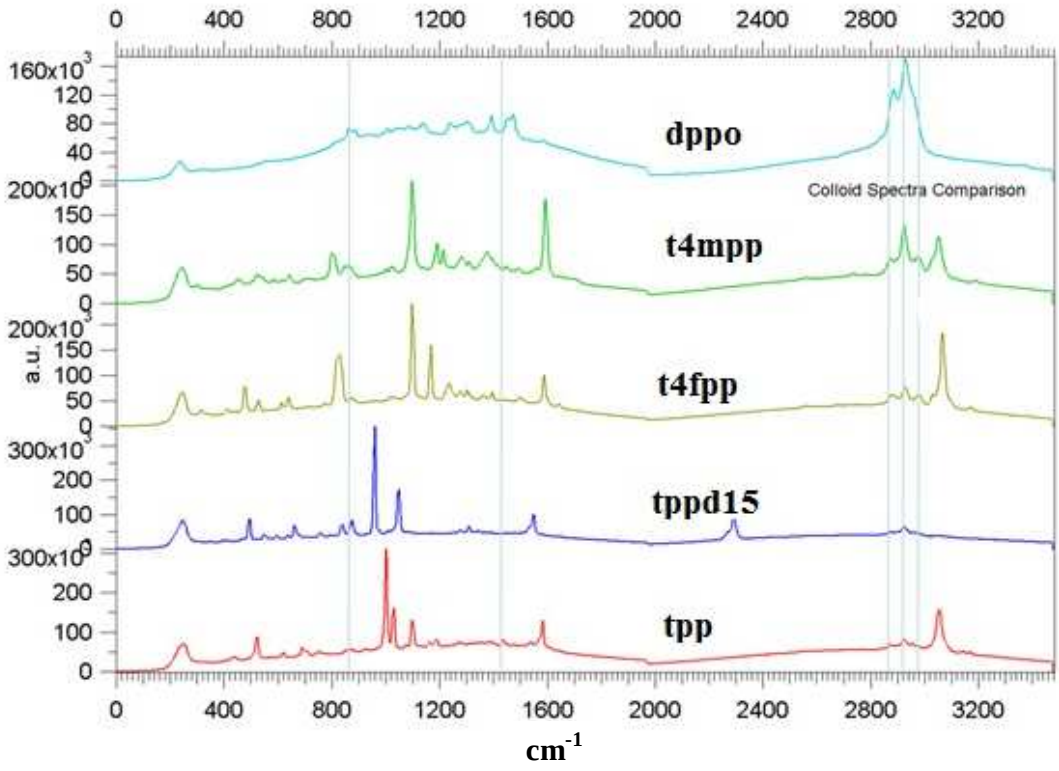

Figure 4.7. SERS spectra of dppo, t4mpp, t4fpp, tppd15, and tpp.

Conclusion on Aryl Phosphines

The bonding mode of aryl thiols to metal surfaces has been thoroughly investigated, while the bonding mode of one of their neighbors, aryl phosphines, has not. We were interested in determining the bonding mode of these phosphines by using SERS. In order to accomplish this, we investigated secondary aryl phosphines, secondary aryl phosphine oxides, and tertiary aryl phosphines. Even though our secondary phosphines oxidized in the presence of air, we were able to investigate tertiary phosphines versus our secondary phosphine oxide. After a series of runs, it was noted that the tertiary phosphines bonded to the silver surface, while the secondary phosphine oxide did not. Seeing how the phosphine oxide has no lone pair on the phosphorus

while the tertiary phosphine does suggests that phosphines bond using their lone pair to the silver surface and not in an X-type fashion as thiols. In order to conclusively confirm that phosphines are bonding through their lone pair, we still need to investigate the secondary phosphines in an air-free environment.

Experimental

Synthesis of 2-octyl-1-(*p*-tolyl)aziridine. *0.1% catalyst loading:* In a 20 mL vial, [(^{Me,Et}TC^{Ph})Co(OTf)](OTf) (0.0010 g, 0.000752 mmol) was added to a solution of 1-decene (approximately 5 mL). The catalyst stirred in the solution for ten minutes at 90 °C, followed by the addition of *p*-tolylazide (0.1000 g, 0.752 mmol). The reaction stirred at 90 °C for 18 hrs after ensuring that all of the azide had reacted as confirmed by GC/MS. The solution was filtered over Celite to get rid of [(^{Me,Et}TC^{Ph})Co(OTf)](OTf). Volatiles were removed under reduced pressure. To isolate the product, a silica column was run using a 9:1 hexanes to ethyl acetate solution as eluent. After removing all of the hexanes and ethyl acetate the pure product remained (0.1552 g, 84.2% yield). ^{1}H NMR ($CDCl_3$, 499.74 MHz): δ 7.03 (d, *J* = 7.5 Hz, 2H), 6.89 (d, *J* = 7.0 Hz, 2H), 2.28 (s, 3H), 2.03 (m, 3H), 1.59 (m, 4H), 1.40 (m, 2H), 1.31 (m, 8H), 0.91 (t, *J* = 6.0 Hz, 3H). ^{13}C NMR ($CDCl_3$, 125.66 MHz): δ 152.77, 131.45, 129.51, 120.65, 40.33, 34.17, 33.41, 32.02, 29.74, 29.69, 29.42, 27.85, 22.80, 20.78, 14.24. GC/MS (*m*/*z*): 245.1. DART/MS (*m*/*z*): $[M+H]^+$ 246.23579 .

Synthesis of bis[3,5-bis(trifluoromethyl)phenyl]phosphine oxide. Under a N_2 atmosphere, a solution of diethylphosphite (0.65 g, 4.7 mmol) in THF (10 mL) was added dropwise to (3,5-bis(trifluoromethyl)phenyl)magnesium bromide (0.5 M solution, 34 mL, 1.7 mmol) in 20 mL of THF. The mixture was heated to 50 °C and stirred for 1 hr. After the hour elapsed, the mixture was cooled to room temperature and hydrolyzed with a saturated ammonium chloride solution (20 mL). The aqueous layer was separated and the product was extracted from the aqueous layer with methylene chloride (3 X 20 mL), which was subsequently dried with magnesium sulfate. The resulting methylene chloride portion was run over a silica

plug then was dried under reduced pressure leaving a light brown solid. To get rid of further impurities, the product was washed with petroleum ether (4 X 4 mL) and dried under reduced pressure leaving the pure, light brown product (0.34 g, 15.5%). ^{1}H NMR ($CDCl_3$, 300.1 MHz): δ 8.31 (d, J_{PH} = 504 Hz, 1H), 8.20 (d, J_{PH} = 13.5 Hz, 4H), 8.16 (s, 2H). ^{19}F NMR ($CDCl_3$, 282.3 MHz): δ -63.0. DART/MS (*m*/*z*): $[M+H]^+$ 475.1.

References

(1) (a) Thibodeaux, C. J.; Chang, W.- C.; Liu, H.- W. *Chem Rev.* **2012**, *112*, 1681. (b) Jenkins, D. M. *Synlett* **2012**, *23*, 1267. (c) Salvati, M. E.; Nguyen, M.; Armstrong, R. W. *J. Am. Chem. Soc.* **1992**, *114*, 3144. (d) Tomasz, M.; Palom, Y. *Pharmacol. Ther.* **1997**, *76*, 73. (e) Takahashi, I.; Takahashi, K.; Ichinura, M.; Morimoto, M.; Asano, K.; Kawamoto, I.; Tomita, F.; Nakano, H. *J. Antibiot.* **1988**, *41*, 1915. (f) Hofle, G.; Bedorf, N.; Steinmetz, H.; Schomburg, D.; Gerth, K.; Reichenbach, H. *Angew. Chem., Int. Ed.* **1996**, *35*, 1567.

(2) (a) Hodgkinson, T. J.; Shipman, M. *Tetrahedron* **2001**, *57*, 4467. (b) Casely-Hayford, M.; Searcey, M. *In DNA and RNA Binders, from Small Molecules to Drugs*; Wiley-VCH: Weinheim, 2002; p 676.

(3) (a) Rajski, S. R.; Williams, R. M. *Chem. Rev.* **1998**, *98*, 2723. (b) Wolkenberg, S. E.; Boger, D. L. *Chem. Rev.* **2002**, *102*, 2477. (c) Tomasz, M.; Lipman, R.; Chowdary, D.; Pawlak, J.; Verdine, G. L.; Nakanishi, K. *Science* **1987**, *235*, 1204.

(4) (a) Solladié-Cavallo, A.; Roje, M.; Giraud-Roux, M.; Chen, Y.; Berova, N.; Sunjic, V. *Chirality* **2004,** *16*, 196-203. (b) Lu, P. *Tetrahedron* **2010**, *66*, 2549. (c) Bauer, J. T.; Hadfield, M. S.; Lee, A.-L. *Chem. Comm.* **2008**, 6405.

(5) (a) Yadav, J. S.; Reddy, B. V. S.; Purnima, K. V.; Nagaiah, K.; Lingaiah, N. *J. Mol. Catal. A: Chem.* **2008,** *285*, 36. (b) Martín, C.; Molina, F.; Alvarez, E.; Belderrain, T. R., *Chem. Eur. J.* **2011,** *17* (52), 14885. (c) Zhang, J.-L.; Che, C.-M. *Org. Letts.* **2002**, *4*, 1911.

(6) (a) Yudin, A.; K., Ed. *Aziridines and Epoxides in Organic Synthesis*; Wiley-VCH: Weinheim, Germany, 2006. (b) Abu-Omar, M. M. *Dalton Trans.* **2011**, *40*, 3435.

(7) (a) Karila, D.; Dood, R. H.; *Curr. Org. Chem.* **2011**, *15*, 1507. (b) Pellissier, H. *Tetrahedron* **2010**, *66*, 1509.

(8) Driver, T. G. *Org. Biolmol. Chem.* **2010**, *8*, 3831.

(9) Fantauzzi, S.; Caselli, A.; Gallo, E. *Dalton Trans.* **2009**, 5434.

(10) Cramer, S. A.; Jenkins, D. M. *J. Am. Chem. Soc.* **2011**, *133*, 1934

(11) Bass, H. M.; Cramer, S. A.; Price, J. L.; Jenkins, D. M. *Organometallics* **2010**, *29*, 3235.

(12) Lu, Z.; Cramer, S. A.; Jenkins, D. M. *Chem. Sci.* **2012**, *3*, 3081.

(13) Daniel, M.; Astruc, D. *Chem. Rev.* **2004**, *104*, 290.

(14) (a) Stewart, A.; Zheng, S.; McCourt, M. R.; Bell, S. E. J. *ACS NANO* **2012**, *6*, 3718. (b) Ma, C.; Harris, J. M. *Langmuir* **2012**, *28*, 2628.

(15) Pailloux, S.; Duesler, E. N.; Smith, K. A.; Paine, R. T.; Klaehn, J. R.; McIlwain, M. E. *Main Group Chem.* **2009**, *8*, 207.

Conclusions

To date, relatively few macrocyclic tetracarbene complexes have been synthesized. Each of the strategies employed to synthesize macrocyclic tetracarbenes previously has an inherent limitation. For instance, the 16-atom ringed variant from Hahn, although an elegant synthesis, is made via a templating reaction, which is not viable for a wide variety of metals.[1] On the other hand, Murphy's 24-atom ringed variant is synthesized by the deprotonation of a tetraimidazolium, which is the preferred approach; however, the bulkiness of the ligand linkers blocks the apical positions, inhibiting reactivity at the metal center.[2] Our group has synthesized a smaller, 18-atom ringed tetraimidazolium, $(^{Me,Et}TC^{H})(OTf)_4$, that can be deprotonated to form a strong σ-donating tetracarbene ligand in complexes such as, $[(^{Me,Et}TC^{H})Pt](OTf)_2$, $[(^{Me,Et}TC^{H})RhH(OTf)_2$, and $[(^{Me,Et}TC^{H})IrH](OTf)_2$.[3] This 18-atom ringed macrocycle is a superior size, allowing for plenty of space at the apical position for reactivity as seen in Cramer's $[(^{Me,Et}TC^{Ph})Fe(NCCH_3)_2](PF_6)_2$, which catalyzed the first examples of tri- and tetrasubstituted alkenes and organic azides in an aziridination reaction.[4]

The second focus of our research was modifying the size, solubility, and reactivity of metal complexes with $(^{Me,Et}TC^{H})(OTf)_4$ by making a structurally similar dianionic ligand. We accomplished this by installing two borate moieties as linking units in our macrocycle. By using borate linking units, we were able to synthesize $(^{BH_2,Me}TC^{Me})(I)_2$ and $(^{BMe_2,Me}TC^{H})(Br)_2$ to make 16-atom ringed tetraimidazoliums. Notably, ESI/MS suggested the formation of highly unstable metal complexes on $(^{BH_2,Me}TC^{Me})(I)_2$ and we were unable to isolate any of these metal complexes to further characterize them. To date, the stability of complexes supported by $(^{BMe_2,Me}TC^{H})(Br)_2$ has not been thoroughly investigated. Since we were unable to make complexes with the 16-atom

ringed variants, we synthesized an 18-atom ringed borate-based macrocycle ($^{BMe_2,Et}TC^{H}$)$(Br)_2$.[5] Using ($^{BMe_2,Et}TC^{H}$)$(Br)_2$, we synthesized neutral, nickel(II) and palladium(II) complexes that were soluble in nonpolar solvents such as toluene.[5] We were also able to synthesize metal complexes featuring manganese(III) and iron(III). The manganese(III) complex, ($^{BMe_2,Et}TC^{H}$)MnI, is the first example of a macrocyclic tetracarbene on this metal. Preliminary results using ($^{BMe_2,Et}TC^{H}$)FeBr, suggests we have made a bridging iron nitride, as well as, potentially other high valent iron complexes.

Since Cramer's [($^{Me,Et}TC^{Ph}$)$Fe(NCCH_3)_2$]$(PF_6)_2$ proved to be a successful catalyst for aziridination reactions we were also interested in testing the reactivity of other metals using ($^{Me,Et}TC^{Ph}$)$(OTf)_4$.[4] In order to test other metal complexes, we synthesized [($^{Me,Et}TC^{Ph}$)Co(OTf)](OTf) as a second potential catalyst.[6] Following the reaction conditions used for [($^{Me,Et}TC^{Ph}$)$Fe(NCCH_3)_2$]$(PF_6)_2$, various alkene and azide combinations were tested. The most effective of these was using 1-decene and tolyl azide for the synthesis of 2-octyl-1-(p-tolyl)aziridine. Yields for both 0.1% and 1.0% catalyst loadings were comparable to those obtained using [($^{Me,Et}TC^{Ph}$)$Fe(NCCH_3)_2$]$(PF_6)_2$. Preliminary testing on cyclopropanations and epoxidations were not successful. Further studies must be obtained in order to understand the breadth of [($^{Me,Et}TC^{Ph}$)Co(OTf)](OTf) as a catalyst.

Lastly, we were interested in the bonding mode of aryl phosphines due to the extensive knowledge of the bonding mode of aryl thiols. The bonding mode was tested through the use of secondary phosphines, a secondary phosphine oxide, and tertiary phosphines, all of which exhibit different bonding modes onto metal surfaces. By using SERS, we were able to see which phosphines bonded to the surface and which phosphines did not. Notably, the secondary phosphines both oxidized, so no conclusion on their bonding could be made. The secondary

phosphine oxide and tertiary phosphines were investigated and it was found that the tertiary phosphines bonded to the silver surface, while the secondary phosphine oxide did not. This evidence suggests that aryl phosphines bond to metal surfaces via the lone pair off of phosphorus.

References

(1) Hahn, F. E.; Langenhahn, V.; Lügger, T.; Pape, T.; Le Van, D. *Angew. Chem., Int. Ed.* **2005**, 44, 3759.

(2) McKie, R.; Murphy, J. A.; Park, S. R.; Spicer, M. D.; Zhou, S. *Angew. Chem., Int. Ed.* **2007**, 46, 6525.

(3) Bass, H. M.; Cramer, S. A.; Price, J. L.; Jenkins, D. M. *Organometallics* **2010**, *29*, 3235.

(4) Cramer, S. A.; Jenkins, D. M. *J. Am. Chem. Soc.* **2011**, *133*, 1934.

(5) Bass, H. M.; Cramer, S. A.; McCullough, A. S.; Bernstein, K. J.; Murdock, C. R.; Jenkins, D. M. *Organometallics* **2013,** *32*, 2160.

(6) Lu, Z.; Cramer, S. A.; Jenkins, D. M. *Chem. Sci.* **2012**, *3*, 3081.

Vita

Heather Marie Bass was born on February 14, 1986 in Spartanburg, SC to Carol R. Bass and Miller G. “Buddy” Bass. She grew up in Knoxville, TN where she ultimately attended college at The University of Tennessee, Knoxville (2004-2007). During her freshman summer at UTK, she visited France for an intensive, three-week study abroad program. She was a member of Phi Beta Kappa and graduated magna cum laude, earning her bachelors of science in chemistry with a minor in French. During a brief six month hiatus after graduating, she worked as a server at Chop House. She applied to and was accepted into the PhD chemistry program at the University of Tennessee, Knoxville (2008-2013). While at UTK as a graduate student, she published two ACS papers, presented two talks at National ACS conferences, and aided in writing the General Chemistry I/II lab manuals. She was also recognized with the C.W. Keenan Outstanding Teaching Award for her excellence in teaching. In August 2013, she received her PhD in chemistry from the University of Tennessee. Recently, she accepted a visiting professor position at Centre College where she will be teaching from 2013 to 2014.